Design and Optimization of a Reconfigurable Vehicle Chassis for Shared Use Application

BY

EDUARDO TERZIDIS
Laurea, Politecnico di Torino, Turin, Italy, 2014

THESIS

Submitted as partial fulfillment of the requirements
for the degree of Master of Science in Mechanical Engineering
in the Graduate College of the
University of Illinois at Chicago, 2016

Chicago, Illinois

Defense Committee:

Carmen Lilley, Chair and Advisor
Lin Li
Stefano Tornincasa, Politecnico di Torino

TABLE OF CONTENTS

TABLE OF CONTENTS (continued)

LIST OF TABLES

LIST OF FIGURES

LIST OF FIGURES (continued)

LIST OF FIGURES (continued)

SUMMARY

The following thesis project outlines the design and analysis of a vehicle chassis for a re-configurable electric car. The project is sponsored by the Partners for the Advancement of Collaborative Engineering Education (PACE). PACE is an organization that promotes students putting into practice what they study during their academic engineering formation as undergraduate and graduate students. The goal of this research is to reduce congestion and pollution in the cities by enabling drivers to optimize the configuration of an electrical vehicle specific to a user's need, for example by allowing the car to be lengthened or shortened to increase or decrease its capacity. The research objectives are to design and perform a structural analysis of a re-configurable car chassis that met design specifications while achieving cost and weight criteria. Existing market solutions will be analyzed to identify design innovations that do not exist in commercial markets

Chapter 1

INTRODUCTION

1.1 What is PACE?

The Reconfigurable Shared-use Mobility System (RSMS) focuses on alternatives to traditional modalities of transportations by substituting leased or owned cars with shared access vehicles. Students from global institutions in Partners for the Advancement of Collaborative Engineering Education (PACE) bring their expertise in industrial design, engineering and manufacturing design to formulate new, innovative and transformative societal solutions that address RSMS needs. Nine global teams have been created, each one composed by sub-teams of different nationalities. Each team is tasked to design a system of vehicle components or modules that can be combined into a variety of transportation configurations to fulfill a flexible means of mobility. Modules must combine to on demand customer needs. The design criteria for the RSMS project (which may be found at pacepartners.org) and the main vehicles requirements are the following [1]:

- *Reconfigurability* – The designed vehicle has to be made up of different modules and give the user ease of use for switching and combining units (such as cargo unit or additional seats).
- *Modularity* – User's needs have to be associated to quantifiable metrics to establish module criteria.
- *Integrability* – The ability to integrate modules rapidly and correctly by a set of mechanical systems and control interfaces for a user-friendly system.
- *Diagnostic capability*– The ability to automatically read the state of the system and identify errors or failure in the chassis.
- *Scalability* – The ability to easily change the internal carrying capacity by quickly and

- easily combining the different available modules.
- *Convertibility* – The ability to easily change the functionality of the vehicle by re-arranging the vehicle modules.
- *Customization* – The ability to adapt, within a family of similar products, each vehicle to its user's needs and enabling a fully personalized vehicle.

1.2 Research goals and objectives

The research goal is to design a vehicle that can be easily and quickly modified for on demand customer requirements, such as number of passengers or cargo delivery needs. The main objective is to interpret "re-configurability" concepts to design a vehicle that meets a variety of on demand commuter needs using design consideration of:

- A predictable flow of commuter movement (mainly during morning and late evening commutes)
- On demand need for cargo transportation, and random trips with multiple passengers (up to 5).

The research presented in this thesis will be focused on the design and analysis of the vehicle chassis for a reconfigurable electric vehicle. The discussion in Chapter 2 will outline the background research on reconfigurable vehicles. Design constraints relevant to local government policies and economic factors are identified and discussed. The pros and cons of several solutions adopted through the years are discussed to identify opportunities to achieve better solutions for sustainable mobility. From the above research, design objectives and criteria were established and are discussed in Chapter 3. A preliminary design of the vehicle chassis is presented in Chapter 4, still partially focused on the understanding and analysis of selected existing solutions. In Chapter 5 and 6, the chassis design modifications were made and analyzed in order to optimize mechanical performance and

manufacturability while achieving weight requirements. Chapter 7 includes the conclusions of the design research outlines future work to improve the current design research

Chapter 2

PRELIMINARY RESEARCH

Today's citizens intensively use individually owned or leased cars as mobility solutions; and reversing this dependency is a difficult challenge. Due to a wide set of individual consumer needs (i.e. personnel needs, number of riders, economic status, etc.), new solutions are needed to solve environmental pollution and traffic congestion problems around the globe. In the last decades, the proper management of transportation regarding both cargo and commuters systems allowed improvements to everyday quality of life. Examples include the introduction of innovative transportation systems (including public and private ones) and incentives to increase use of non-internal combustion engines. In the particular case of midsized towns (up to half a million inhabitants), governmental institutions, such as the World Bank, have emphasized the importance of new models for transportation systems [2]. A good example is the Bus Rapid Transit (BRT). The BRT does not require costly infrastructural investments to improve services for urban commuter mobility for people who need to travel small distance within a city. BRT is a project that focuses on the improvement of the existing public transportation systems through the improvement of busses and trains schedules and optimization of the vehicles.

The definition of mobility is strongly related to the local environment in which it is being defined. This requires identifying the transportation need of commuters at localized urban settings as clearly state by Ericson in the quote "People power will drive urban development" [3]. Thus, the proper interpretation and management of citizen's mobility needs and requirements is necessary and has had positive effects to the global problem of mobility.

A review in the urban transportation projects funded between 1999 and 2009 has shown that only 2 of the 55 projects of the last decade had effectively addressed problem of mobility [18]. According to the World Bank published reports, pedestrian and mobility infrastructure improvements are essential to change transportation concept, by encouraging users to switch from an individual mobile transportation system to a sustainable shared mobility model. Jose Viegas, General Secretary of the International Forum of Transports of the Organization for Economic Co-operation and Development (OECD), predicts that vehicles powered by standard combustion engines will significantly decrease in number [5].

2.1 Target city analysis

Two cities, New York and Mexico City, have been identified as target cities for the proposed tailored shared use vehicles. The main factors in selecting these cities were trying to find a location where the technology could be implemented and where there would be a strong consumer market due to demand for mobility solutions.

2.1.1 Mexico City

Due to the local geography and high population density, Mexico City is one of the most polluted cities of the world [6]. It is located in a geological depression surrounded by mountains, which does not allow for air circulation and promotes air pollution stagnation. There are more than 3.5 million circulating vehicles [6] in the city every day; the pollution created by this factor is in addition to the local industrial pollution [6]. In addition, a large percentage of these vehicles are EUR 2 or less. In Europe, a car's emissions are rated through a scale going from 0 to higher numbers. EUR 0 cars are the most pollutant, while higher numbers (EUR 6, EUR 7…) are created to comply with lower emission requirements. Thus, EUR 2 cars are nowadays among the most pollutant [7]. Moreover, as an economically emerging country, the number of vehicles is increasing exponentially [8]. Thus, the combination of these conditions results in high air pollution and will worsen unless new mobility solutions can be found and adopted by the population.

Figure 1. Mexico city pollution

In recent years, the federal government of Mexico has tried to halve the environmental impact from CO_2 emissions. The service and metropolitan transportation system has been improved by adopting electric vehicles. In 2010, the government approved a plan of eco-sustainable development to convert to an electric taxi service using Nissan electric vehicles. Charging zones, located in different districts, will be equipped in the Mexican capital. While at the national level, there will is planned construction of electric charging points along the 90 km that separate Mexico City from Cuernavaca, in the south of the country [9]. As can be seen, the government is building the infrastructure that can result in adoption of electric vehicles for a larger population. This makes Mexico City a strong candidate for innovative mobility solutions using electric vehicles.

Figure 2. Typical traffic congestion in Mexico city

2.1.2 New York

New York city also has a very high population density and has been moving towards new mobility solutions [17]. The mayor, Bill de Blasio, recently approved development plans for sustainability to cut down air pollution, reduce smog and greenhouse effects [10]. The main objective for the development plans is to prevent commuters from using private cars and increase use of taxicabs and shared use vehicle solutions. As part of this policy, the adoption of electric vehicles is being promoted as their purchase prices decrease. For example, the Ford Focus I costs went decreased $4000 to a price of $35200 [11] and GM has also cut the prices for the Volt [12]. Car sharing services, such as CarTwoGo or ZipCar, also have obtained widespread development and success in the USA [13]. These factors could lead to a dramatic increase in the number of families that do not have a privately owned or leased vehicle in the future.

2.2 Analysis of Existing Configurable Vehicles

Modern vehicles already include elements of re-configurability, although they are typically limited to passenger compartments or the bodywork. Some examples are adjustable seats, steering wheels and back mirrors that allow people of different heights to

customize their driving conditions. These types of re-configurations are focused on making the driving experience more comfortable rather than solving mobility problems discussed above. The aim of this research is to create a vehicle able to suit custom driving and transportation needs, such as the need for more passengers or cargo space in a dense urban setting. In the following section, an overview of existing or proposed re-configurable vehicles is discussed.

2.2.1 Urban Tabby by OSVehicle

One of the most interesting reconfigurable vehicles is the "Urban Tabby by OSVehicle" [14]. OSVehicle is a partial acronym for Open Source Vehicle. Tabby is based on a platform where anyone can assemble their own car. Several different options are possible, ranging from two to four seats, and a hybrid, standard or electric engine. This allows the user to fully customize their car to fit their lifestyle. Moreover, this vehicle has been designed as 100% configurable; meaning, tailored engineering changes can be done on vehicle components. It is in fact possible to download the CAD file of the original design and make personal changes. However, re-configuration of this vehicle after manufacturing is not possible. Thus, there can be no on demand user customization.

2.2.2 Mercedes Benz TET city car

The TET city by Mercedes Benz car has many different dimensions and is reconfigurable; it can in fact be transformed into a bus and can even be used as a small living space (Fig. 3 illustrates how a bed can be obtained from the seats) [15]. Different configurations can also be obtained through the opening and closing of the vehicle top. This innovative design is still not in production, and is still in the concept phase.

2.2.3 Mono EV

The Mono EV vehicle [Reference] allows tailored cargo capacity and internal space adjustment by increasing its width. By enabling contraction of the width, large advantages

are obtained in terms of mobility and parking in a dense urban setting. For example, the space for parking would be much lower compared to current vehicles. In this case, investments for parking infrastructures could be devoted to the development of new mobility solutions. This project is still in the development phase.

Chapter 3

DESIGN OBJECTIVES AND CONSTRAINTS

The research goal is to design a vehicle chassis that can be lengthened and shortened, to accommodate two to five seated passengers. In addition, cargo modularity is an objective too; the vehicle will in fact be also able to be re-configured to obtain more cargo space. The objective was then find a safe and efficient way to allow lengthening or shortening of the; after this, the structural design analysis was done to ensure mechanical operation since the lengthening mechanism will significantly affect the stiffness of the entire system.

From the above review, it is evident that the ability to reconfigure after a vehicle is manufactured would lead to greater adoption of shared electrical vehicle by enabling on demand customer satisfaction while reducing pollution. A modular system has been chosen for the proposed shared use vehicle system. The vehicle will consist of a main module and several different sub-modules. The main module is the vehicle itself, which can be lengthened in order to accommodate additional sub-modules. Four different kinds of sub-modules will be available: (1) a *Passenger module* (when more passenger seats are needed), (2) the *Luggage module* (when big cargos have to be transported), (3) an *Additional power module* (when a trip is made and no charging stations will be available for a long time), (4) and a *module compliant for people with disabilities*.

The main focus of this thesis research is on the vehicle chassis that can be modified in length to accommodate the vehicle sub-modules. In Reference [22] it can be found that

safety factors for cars chassis are usually around 1.5 or 2, while in Reference [23] safety factors up to 6 appear. Thus, the design criteria for the chassis are:

- The vehicle chassis must therefore have a safety factor of 4.5 for all parts of the system.
- The chassis must support a maximum mass of 1200 kg or weight of roughly 12000 N.
- The chassis length must have a minimum size of 1.8m and a maximum length of 2.7m.
- The width of the chassis must be 1.3 based on the SmartCar vehicle [29].
- The chassis should be manufactured with readily available stocked sheet metal, see [35] for available stock dimensions to be considered..
- Ease of manufacturing and assembly should be considered in the design. For this criteria, the design should leverage bending of sheet metal to form beams and welding of parts as much as possible.

Chapter 4

PRELIMINARY DESIGN

Before the chassis could be designed, some considerations had to be made on how to integrate the sub-modules to the main module. The aim of this chapter is to outline what the design factors to be considered. Two main design criteria were identified during the preliminary design phase: (i) the vehicle must be able to climb a steep hill or remain in control in a steep downhill and (ii) have a small turn radius. For example, while approaching a steep uphill, the chassis suffers high bending moments. This especially happens when the two front wheels already are on the hill while the rear ones are not. If the integration of the sub-module onto the main one is not properly designed, the vehicle in the extended configuration will experience bending moments, and could experience yield stress or fatigue stress failure. When considering a small turn radius, on the other hand, the vehicle must not tip or experience any mechanical instability.

A modular system has been chosen for the proposed shared use vehicle system. The system is made of two main components: vehicles and stations. The vehicle will be composed of a main module and several different sub-modules. The main module is the vehicle itself, which can be lengthened in order to accommodate additional sub-modules. Four different kinds of sub-modules will be available: (1) a *Passenger module* (when more passenger seats are needed), (2) the *Luggage module* (when big cargos have to be transported), (3) an *Additional power module* (when a trip is made and no charging stations will be available for a long time), (4) and a *module compliant for people with disabilities*.

Figure 3. Truck trailer example

A possible solution to the module design can be found in truck trailers, which are integrated with the main module via a linkage system. In this case, the cabs are designed to attach to several different kinds of sub-modules (trailers) and meets the concept's target of re-configurability through modular design.

A preliminary design using the cab and trailer concept was realized and studied. Figure 4 is a CAD model that illustrates the preliminary chassis design based on a latching system. The lower disk is fixed onto the chassis, and it functions as a guide to let upper disk rotate when in open configuration. While in closed configuration, the upper disk is fixed and not able to rotate. To allow the sub- module to be hooked onto it, the upper disk is unlocked and slides backwards coming out of the bodywork.

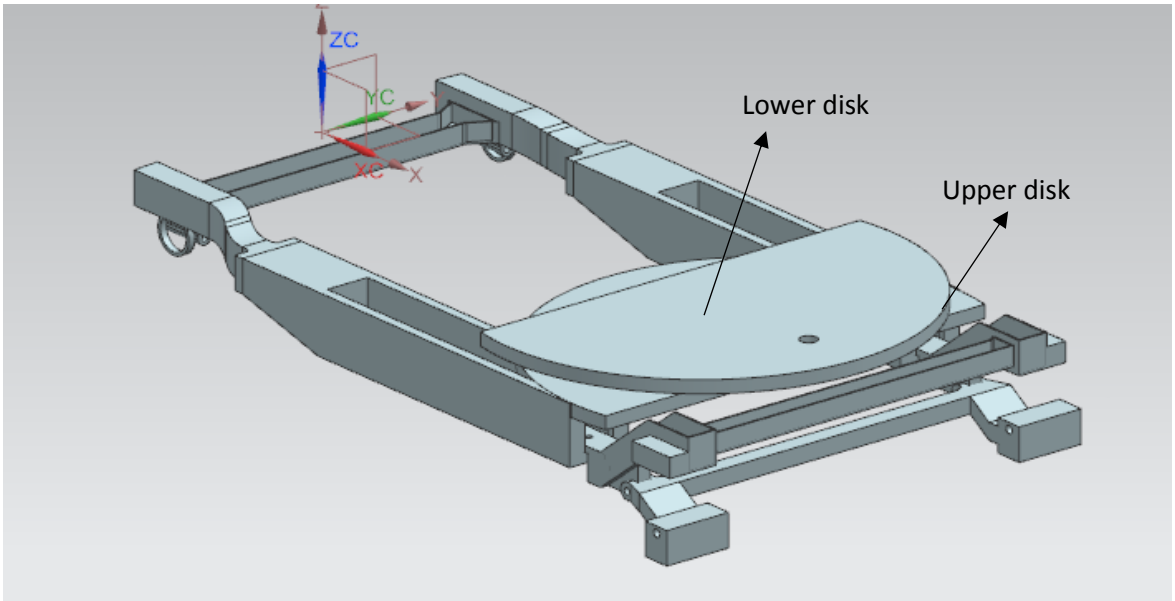

Figure 4. Preliminary model, closed configuration

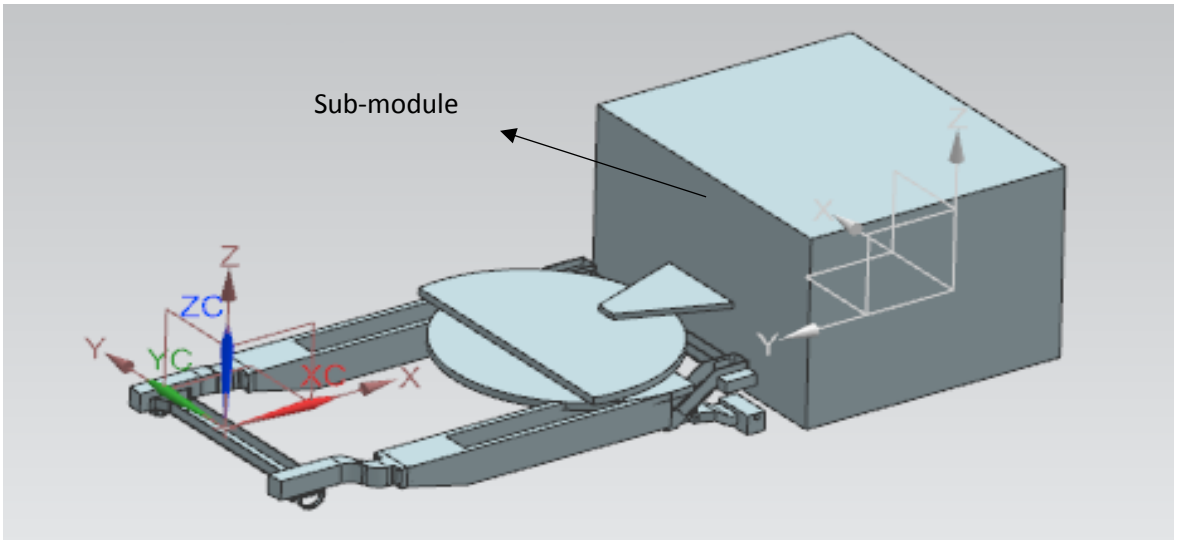

Figure 5. Preliminary model, open configuration

In this last figure, upper disk is unlocked, able to rotate. It also will slide backwards to allow free movement of the sub-module. However, the design has several disadvantages. The small radius curve at high velocity could result dangerous since the sub-module is attached to the main one through a hook, which may be unstable at high velocities. This solution would also create two different volumes for the passengers and the drivers, thus

creating low comfort. Figure 5 shows how the main module and the sub-module are two independent volumes, and communication between passengers and driver cannot happen. With a sliding mechanism, the sub-module is attached to the vehicle on the chassis and part of the sub-module would slide into the main module based on the selected configuration. Additional seats and other devices to be used in the sub-module would have to be folded when in the closed position (when the vehicle is in the two-seated configuration). Thus, this configuration would dramatically reduce the available internal space as well as the flexibility of the system. Moreover, available space in the car would be significantly reduced, due to the sub-module occupying part of the main module's internal space when in closed configuration.

Therefore, the preliminary design integrates the advantages of a trailer design's ease of re-configurability with the more mechanically robust sliding mechanism. To this aim, no hooks have been used. However, the sub-module will still be designed as an independent system, to be added and locked onto the car chassis after the chassis has been lengthened to accommodate the sub-module, see Figure 6.

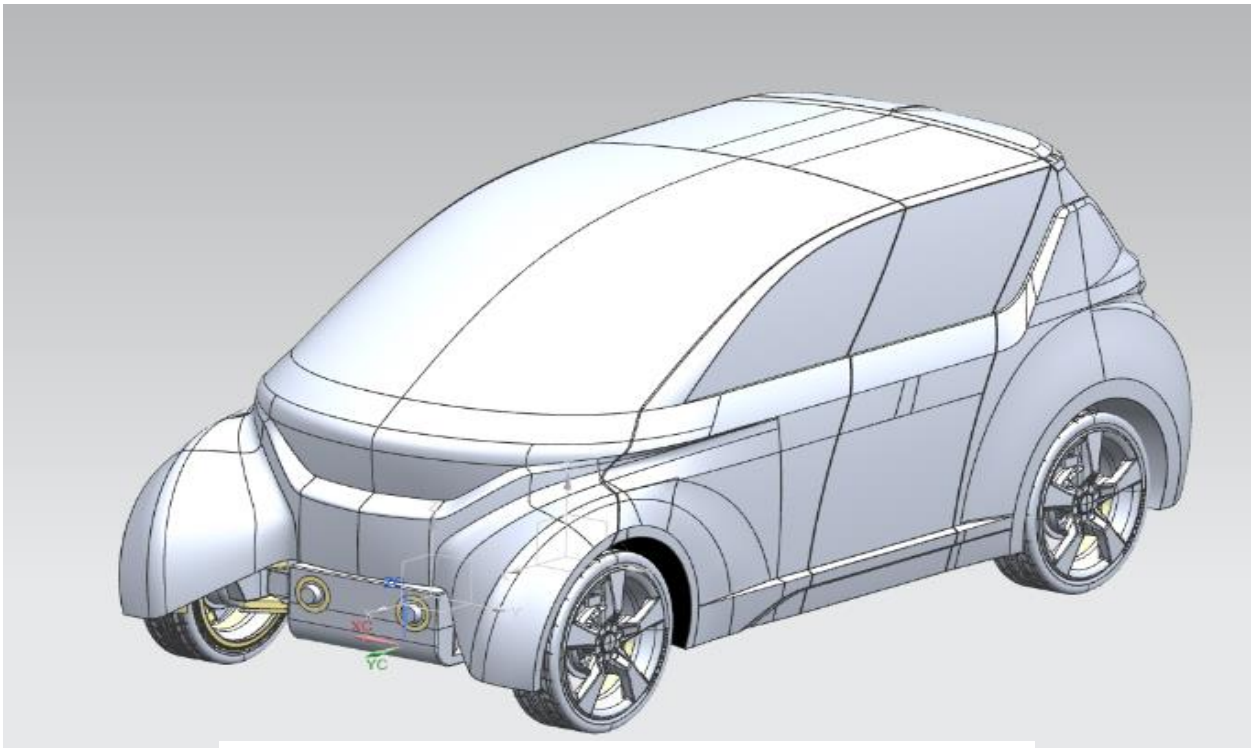

Figure 6. Concept model

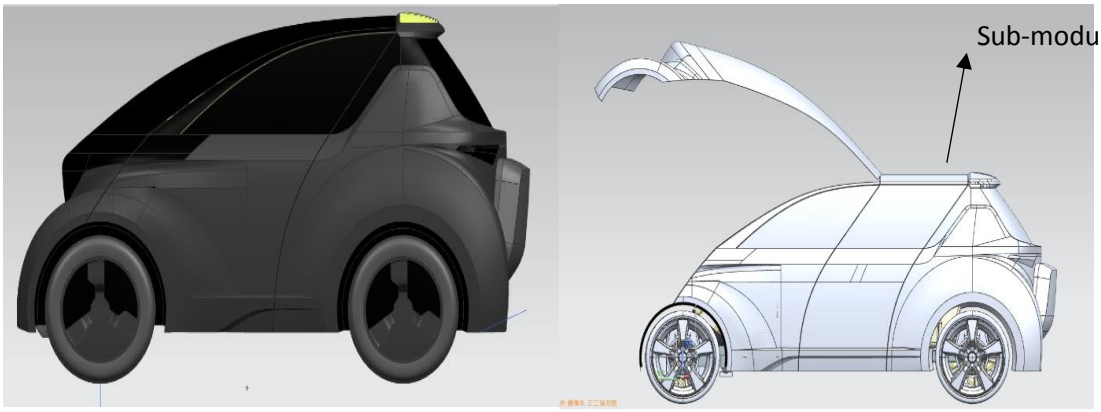

Figure 7. Concept model, short version on the up and long version on the bottom.

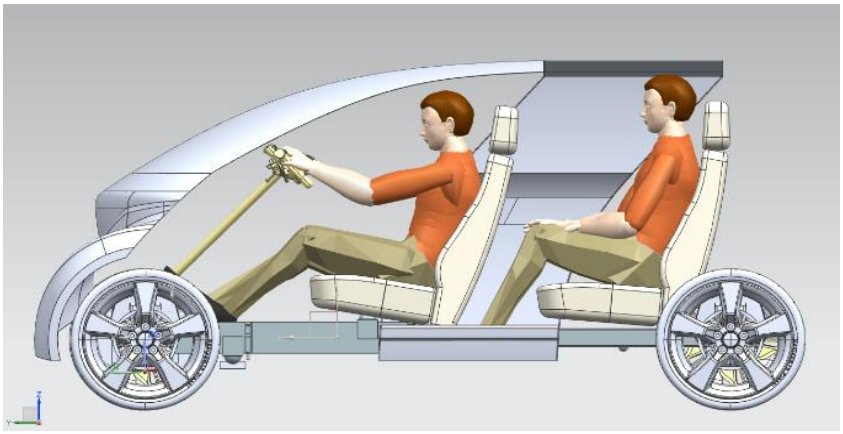

Figure 8. Concept, long configuration

4.1 Main Module Design

To design the main module, dimensions of the Smart Car [29] were considered as the desired dimensions due to its popular use as a two-seated city vehicle. The Smart Car's available internal vehicle space and volume were established as the minimum design criteria for a driver of the proposed reconfigurable system. A 1.90 meter tall human model, was used as the reference adult that would operate the vehicle. This height has been chosen since the average height is usually around 1.75 meters, and people above the average wanted to be satisfied [16]. Originally, the PACE teams considered integrating a Segway as the driving mechanism for the main module, see Figure 14. However, this would have reduced the available space of the driver. Figure 10 is a model that was created to explore the impact of using a Segway module for the main module and show the results of the initial concept and ergonomics study. For this design, the front part of the car is integrated so that the two wheels of the Segway work as the front wheels of the car itself. When parked, the car offers the possibility to detach the Segway and use it for small distances in the city. Figure 9 shows a detailed representation of the design. Stations would offer both main modules and sub-modules and be distributed around a city, where people would pick up and return both main modules and sub-modules at any station.

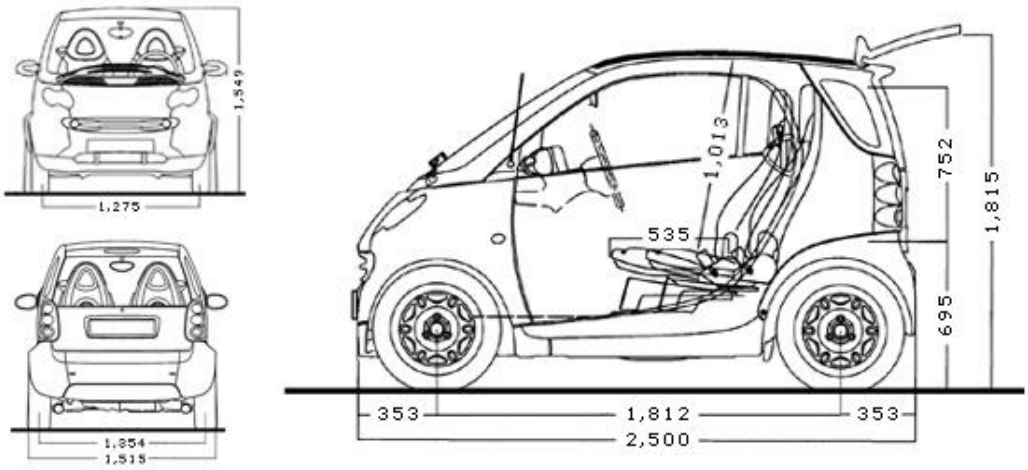

Figure 9. Smart car dimensions

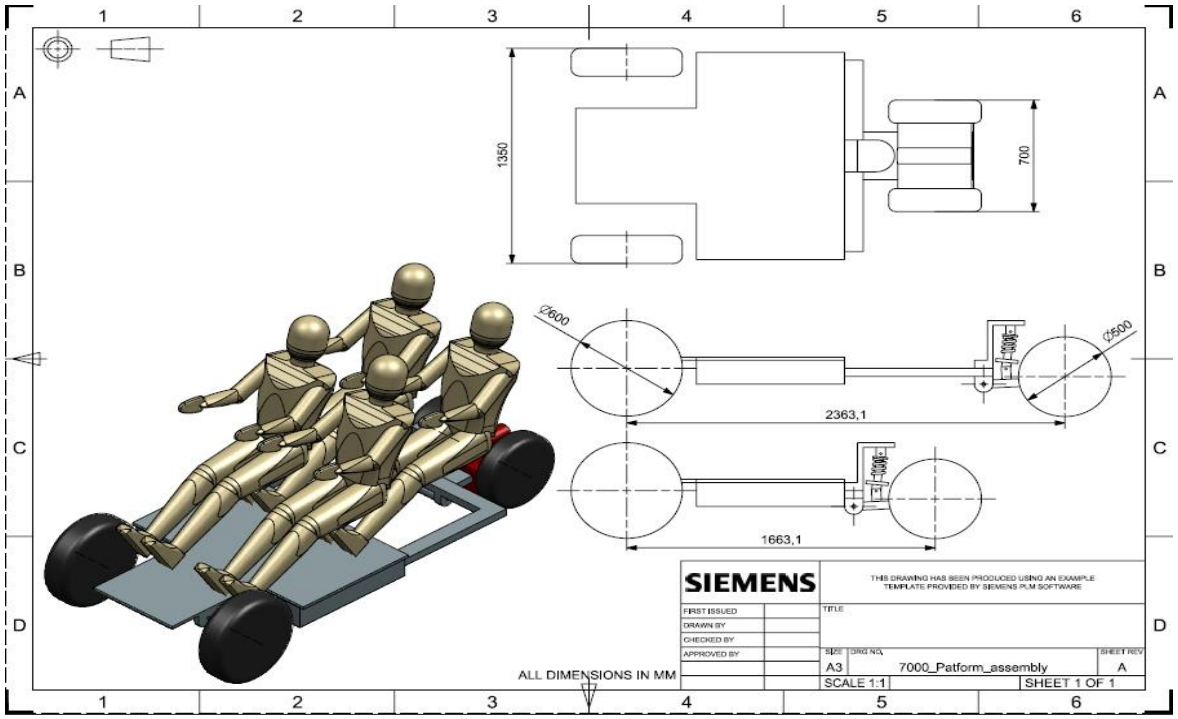

Figure 10. Basic chassis dimensioning

Figure 11. Concept

A second preliminary model was considered that ignored the reduction of volume due to the Segway module. In this model, the sidewalls were also included in the model to determine the approximate height of the car.

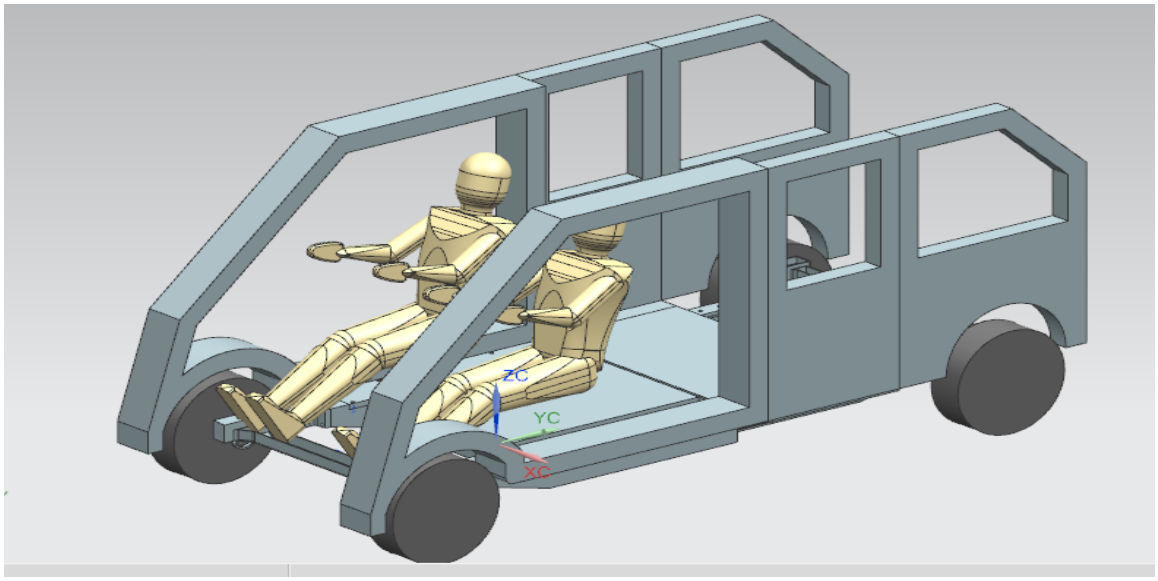

Figure 12. Ergonomics study

After having found an approximate estimate of the dimensions, the sliding mechanism was designed and then integrated into the vehicle chassis. The reason why this sequence in the design process was chosen is because it was expected that the chosen sliding mechanism would affect the overall stiffness and rigidity of the chassis. It was then necessary to design the structure to properly balance the eventual loss of stiffness given by the lengthening mechanism. The concept applied was that of creating a telescopic system composed by two parts: a “female”, which interacts with a “male” sliding in and out of it during the chassis lengthening and shortening process. To this aim, the first step was to engineer an efficient sliding mechanism.

4.2 Design of the Vehicle Sliding Mechanism

Figure 13 illustrates the initial sliding mechanism design. The male and female system mentioned above was realized by having both the male and the female sliding parts be “U” shaped beams and one sliding over the other. A “T” shaped cover was used as a guide to position the motion of the male sliding mechanism. Figure 14 illustrates the open (or long) configuration of the chassis. A gap between the end of the male sliding mechanism and the rear part of the chassis can be seen (see red lines in Fig.21). This gap will accommodate the sub-module, which will be locked onto the main vehicle chassis by using a proper locking system.

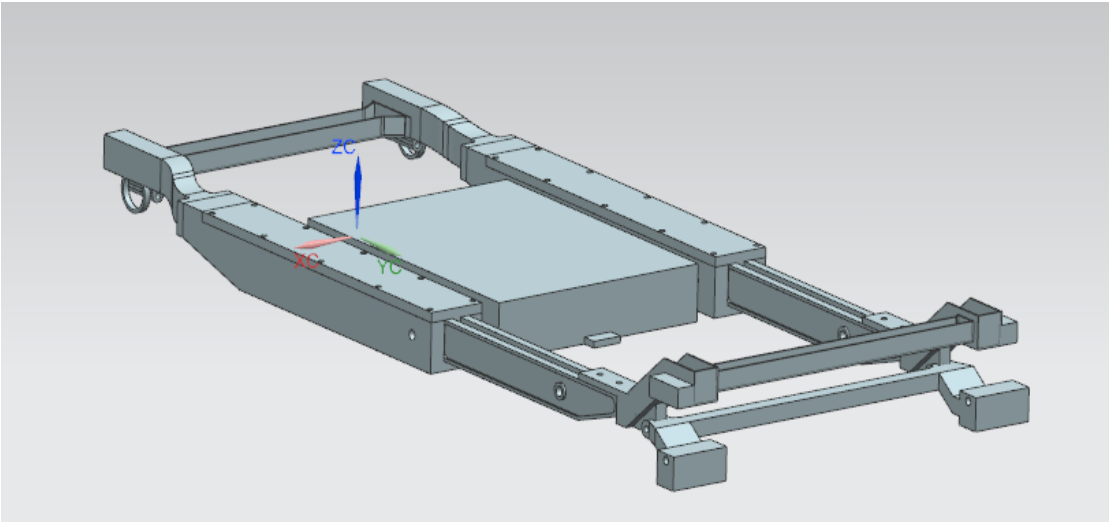

Figure 13. Chassis platform, long configuration

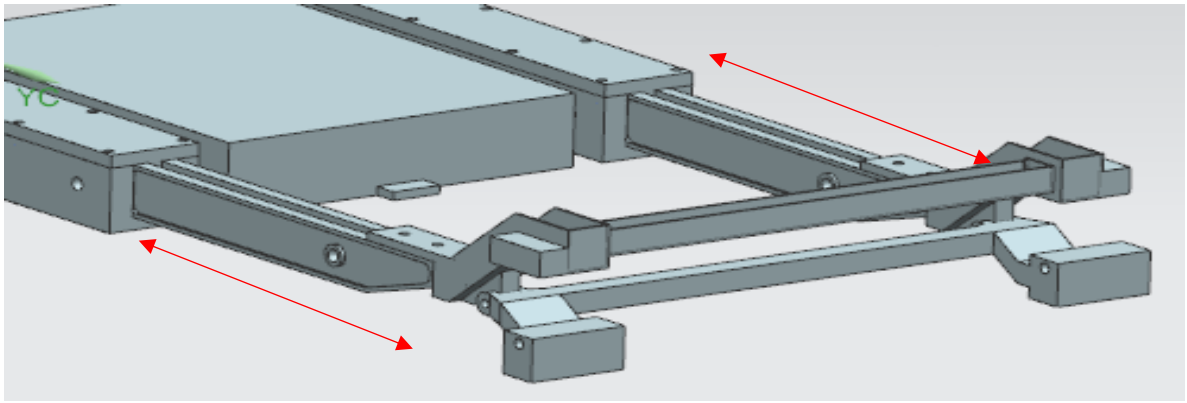

Figure 14. Space for sub-module

Figure 15. Male and female with guides

A linear bearing system was considered for the sliding mechanism so by using a bearing system, sliding could occur with little friction between the mating parts as shown in Figure 15. The sliding guides are rectangular cross-section. The bearings are integrated into linear cage to ensure proper sliding of the male and female guides. The cage would be fixed with welded spots on the male guide to allow for ease of disassembly, maintenance and repair or replacement since the welds can be removed and re-made when necessary. Despite the design achieving the desired sliding motion, there are several design disadvantages. A system like this requires accurate dimensioning (i.e. high tolerance), which results in high manufacturing costs and potentially undesired stresses concentration effects that could

cause premature mechanical failure if not aligned properly. Moreover, as the female goes in and out of the male, dust is brought onto the rolling elements, which would cause high wear and an increase of friction.

Due to the fact that sliding or a vehicle chassis would not occur at high rates and cycles, the sliding elements themselves do not require a high life for service hours. In fact, wearing of the various mechanical and electrical components will not be significant for the track lengthening or shortening operations which results in more flexibility in the bearing design. Thus, it is proposed that Teflon sheets be used between the sliding elements. Teflon has a low coefficient of friction [19] and interposing Teflon sheets between the two sliding elements would efficiently reduce friction while allowing the necessary sliding. Compared to the linear bearing design, the reduction of friction for the two sliding parts with Teflon is lower. However, there are significant advantages. First, it removes the restrictions for high machine tolerance in the manufacturing and assembly, which significantly reduces costs. Second, is simplifies the ease of maintenance and assembling of the chassis system. The Teflon sheets can be easily attached to either the male or the female by glue mounting or other attachment systems, thus allowing a fast way to change the sheets in cases of wear or damage. Thus, this simple design was integrated onto the chassis to reduce sliding friction.

Chapter 5

STRUCTURAL DESIGN

5.1 Final Design

After the sliding mechanism was designed, the chassis system was redesigned to simplify the manufacturing and assembly of the chassis system. Fig. 16 shows the updated version of the chassis, and a detailed description is provided below.

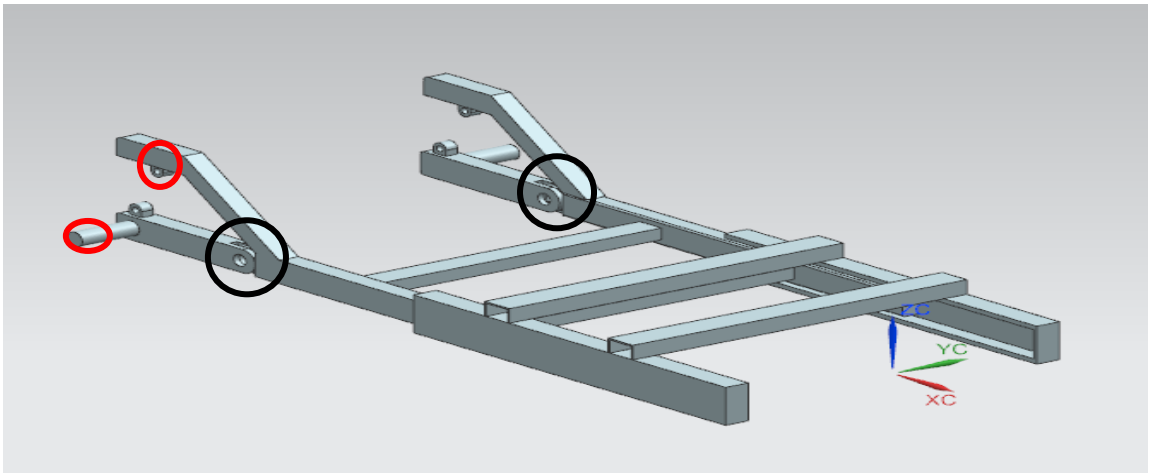

Figure 16. Updated chassis

Both the male and the female have been transformed into C-channel beams (refer to [34]), due to ease of availability for materials and manufacturability. The upper and lower surfaces of both the male and the female are flat, thus, sheets of Teflon can be readily attached to reduce friction between the two components. Attention has been put on designing the new chassis in such a way to guarantee high stiffness against bending moments acting along each possible direction.

In fact, C-channel beams offer a high moment of inertia against bending moments about the Y-axis (see Figure 16). The two sides of the chassis are connected through four

reinforcing elements (two for the male and two for the female), constituted by U-channel beams, which will be welded onto the male and the female. Again, U-channel beams have been preferred to circular tubes, given their higher moment of inertia acting against bending moments about the X-axis (see Figure 16).

Analytical calculations have been done to test the chosen dimensions for the male and the female track components. For the evaluation of the stresses acting on the platform, its long configuration has been considered since would be the configuration where largest bending moments would act on the chassis.

The loading bearing of 1200 kg the car corresponds to a distributed 12 kN acting on the platform as shown in Figure 46. As sheen in Figure 17, since the chassis and loads are symmetric, only half the system is modeled. The load *qL,* represents the total load acting on the system, which is given by the distributed load q times the length L.

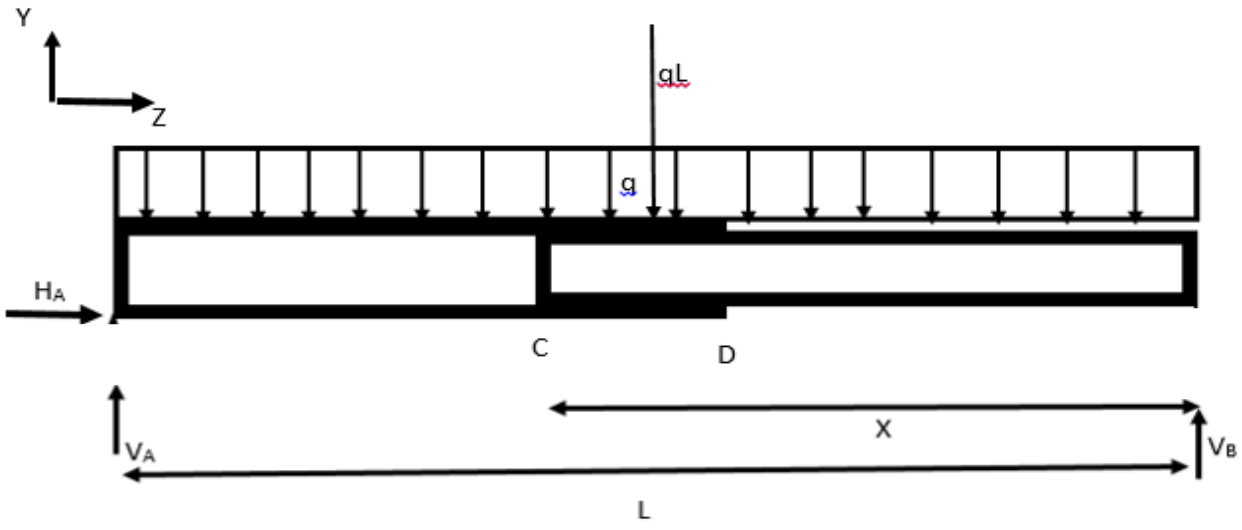

Figure 17. Load scheme

Here, the length L has be chosen to be equal to 2 meters which is the maximum chassis length for the vehicle design.

Considering the free body diagram in figure 17, hereafter a set of equilibrium equations is provided:

- $H_A = 0;$
- $V_A = qL/2;$
- $V_B = qL/2;$

From these equations, applying De Saint Venant's principle [24], the behavior of the bending moment can be determined as:

$$M(z) = \frac{q}{2}\, z\, (l - z) \quad (1)$$

From point C to point D as seen in Figure 18, the load bearing on the system results in coupled the bending moments is approximately constant in this zone.

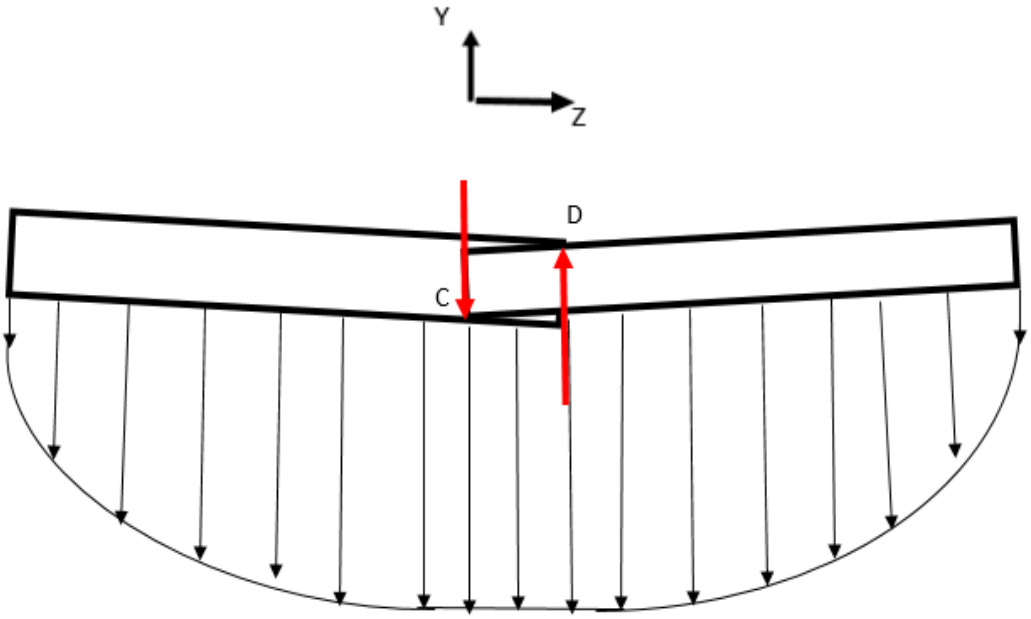

Figure 18. Moment behavior. Constant between C and D due to couple of forces generated

When under a load, the system undergoes a deformation that causes the male to touch the female at points C and D. These contact points result in bending forces acting on the chassis, as shown in Figure 18. Due to this considerations, the most critical section is the one belonging to the male, in correspondence of point D. In this section, not only the bending moment is at its maximum, but also the resisting cross sectional area is the smallest under the conservative hypothesis that only the male is receiving all the load. It can be in fact seen from formula (1), that the bending moment has a parabolic behavior with respect to z, which would reach its maximum for z = l/2. This result can be obtained by differentiating M(z) with respect to z and finding the maximum of function M(z) :

$$\frac{\delta(M(z))}{\delta z} = 0$$

The value of the bending moment at point D has been evaluated and is equal to 3960 Nm. The selected available sheet metal is AISI 1020 steel with the following properties [25]:

- Young's modulus E = 210000 N/mm^2
- Yield stress σ_{yield} = 235 N/mm^{2t}
- Failure stress $\sigma_{failure}$ = 360 N/mm^2

The cross-sectional image of the male C-channel is shown in Figure 19 and the principle stress in the z direction [26] are also shown.

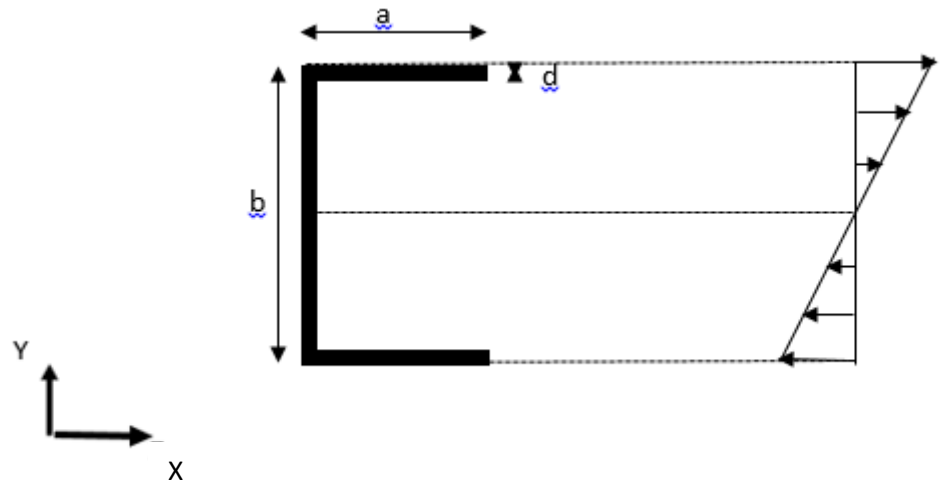

Figure 19. Cross sectional area and stress distribution

Referring to the just mentioned figure and to [35]:

- a = 10 cm;
- b = 20 cm;
- d = 0.6 cm;
- Moment of inertia I = 5175456 mm^4;

As seen in Figure 19, the stresses reach their maximum at the two extremities of the C shaped beam as calculate.

$$\sigma(\max) = \frac{M(\max)}{I}\frac{b}{2}.$$

The maximum normal stress was calculated as 76.51 MPa, which is lower than 235 MPa (yield strength of the chosen material) with a safety factor of 3. Therefore, this material selection and dimensions were kept for further analysis. For the female track, the same material dimensions and shape was used. This choice was based on the assembly of the tracks and uniformity in dimensions to prevent interference in sliding of the track parts.

Once this preliminary model was completed, the chassis was analyzed to ensure ease of manufacturability of each component before the final failure analysis. Figure 20 shows a detail of reinforcements to reduce deformation and connect the tracks to the chassis.

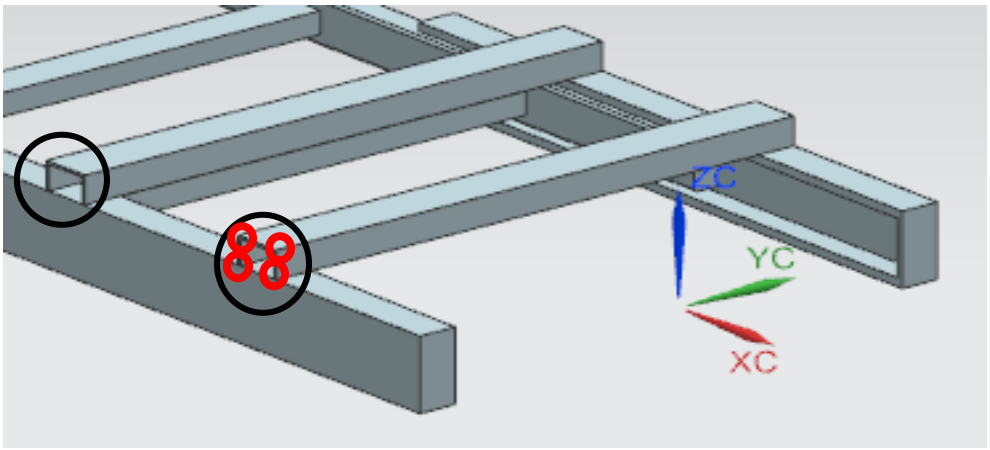

Figure 20. Current reinforcements

The two regions highlighted by black circles in Figure 20 show where the beam supports have small areas (approximately 4 cm^2) to secure with weld. Therefore, this small contact region could potentially result in welding failure. Moreover, the actual shape of each reinforcement could cause concentration of stresses due to presence of sharp edges, see red circles in Figure 23, and create localized regions of yeild strength failure. [28] Therefore, a new cross bar to connect the tracks to form the chassis was designed. The section has the

same moment of inertia, but allows for a larger welding surface as well as a lower number of sharp edges. To clearly understand how the reinforcement has been modified, Figure 21 provides a comparison between the two design solutions.

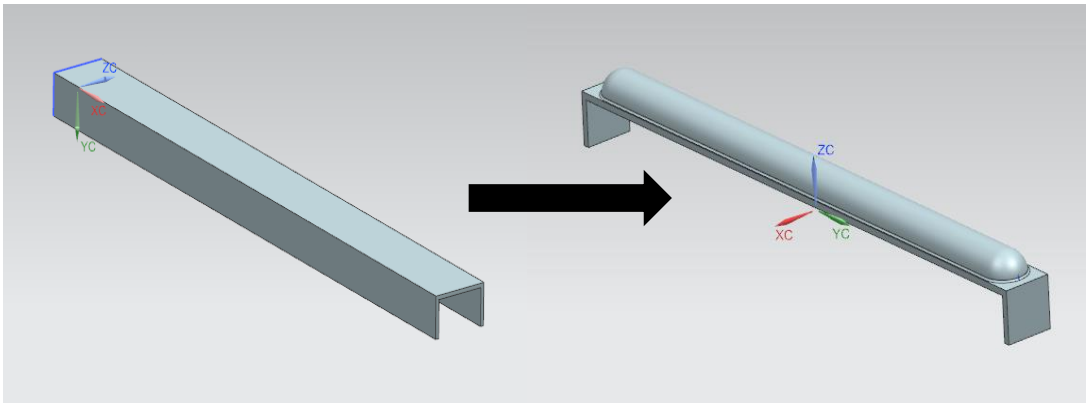

Figure 21. Old and actual reinforcement comparison

This new reinforcement can be obtained by bending and punching a simple sheet of metal at its far ends, as indicated by the black ellipse in Figure 22, thus allowing it to create a bigger contact area for welding on the male or the female track components. The deformation given by the punching procedure would give the component a higher stiffness against bending moments. Moreover, as Figure 22 shows, welding will also happen on the sides of the male or female, thus offering more resistance during bending moment application.

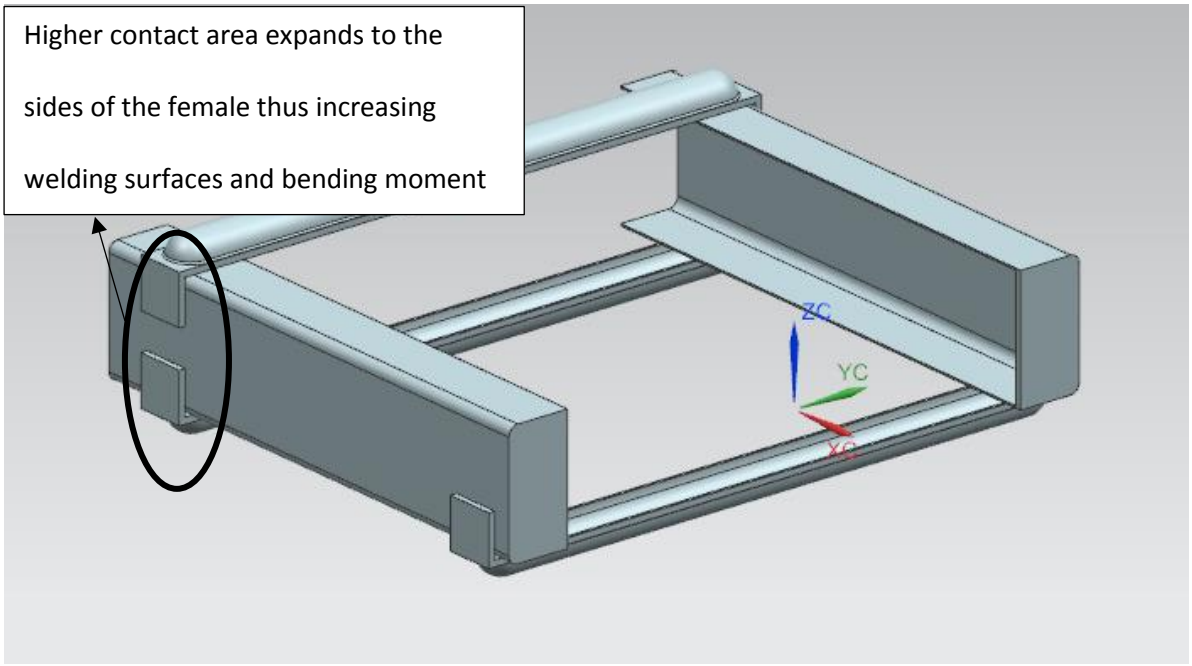

Figure 22. New reinforcement mounting

Before finalizing the model, the suspension mechanism had to be specified to design the front and the rear chassis connections. Existing vehicles were considered for the model suspension system. Since the Smart [20] car has been used as a reference, its suspension system was considered at first. This model, however, cannot be used. The appendix, is an illusration of the entire rear chassis for a 1998 Smart car [20]. This part is connected to the front one through a central joint, indicated by a black-circled in the sketch. The reason why

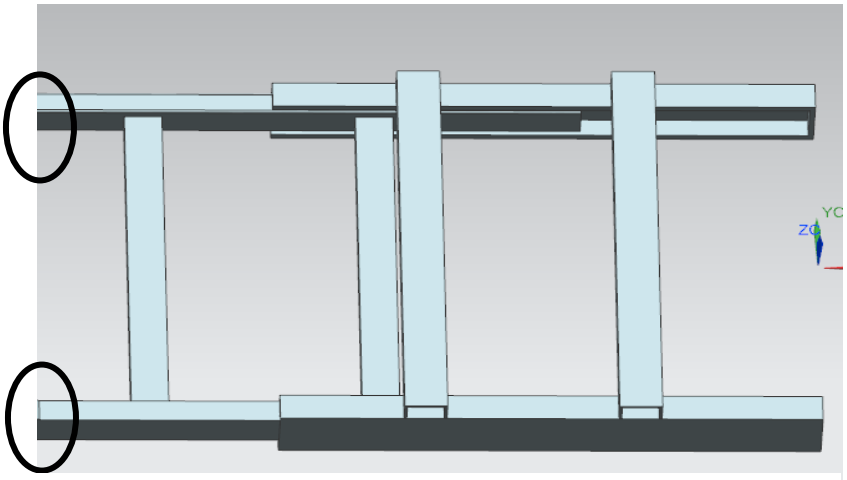

Figure 23. Male ends

this kind of system cannot be used is because it would require the front part of the chassis to end with a unique trasversal beam (red line in the figure). The current version of the chassis, on the other hand, ends with the two circled points which are indipendent and not connected, as shown in figure 23.

Even though this problem could simply be adressed by designing a transverse beam connecting the two ends, the total weight of the system would increase.

For this reason, another model has been considered, belonging to a 1974 Volkswagen Golf [20]. This model matches the needs of the current concept and this is why it has been chosen and the suspension solution shown in Figure 24.

The second sketch in the appendix reproduces this suspension system and clearly shows how even in this case, two independent and non-connected points are at the end of the chassis. Inspired by this last model, a suspension was chosen and the corresponding suspension mounting system was designed.

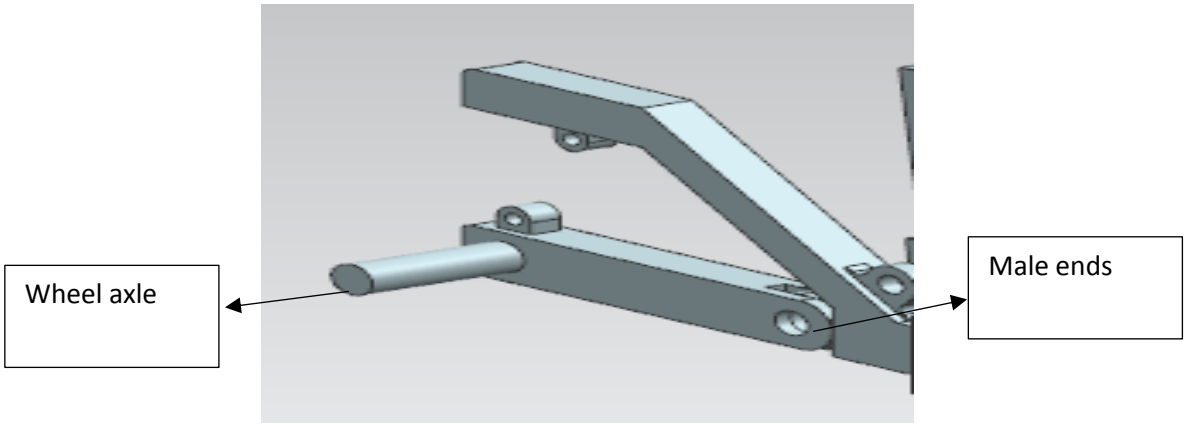

Figure 24. Suspension mechanism 3D model

Once the suspension design was selected, this system was adopted for both the front and the rear wheels. The rear part of the chassis was updated to allow to properly accommodate the chosen suspension system as shown in Figure 26. Transverse reinforcements have also been added to the rear chassis, in order to improve its rigidity. A locking mechanism also had to be designed and integrated to keep the chassis in a closed or open position. A welded folded metal sheet, see Figure 27, was added to the internal side of the male to provide a hole where the pin will be inserted. The pin is attached to the external side of the female and is retracted during the lengthening/shortening procedures.

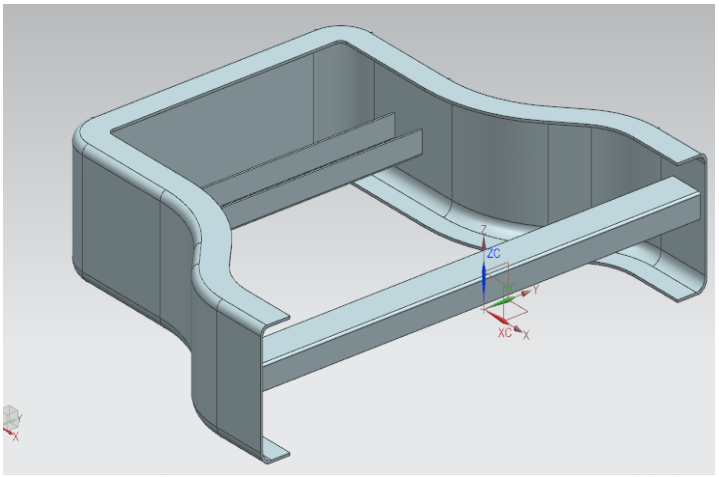

Figure 25. Improved rear part of the platform

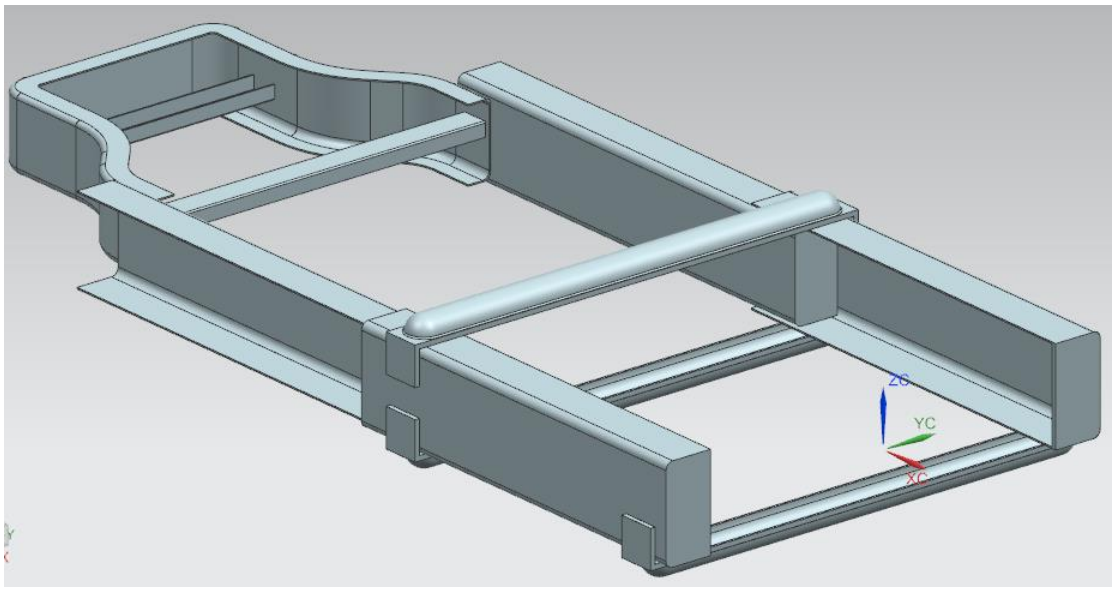

Figure 26. Platform with all the improvements applied

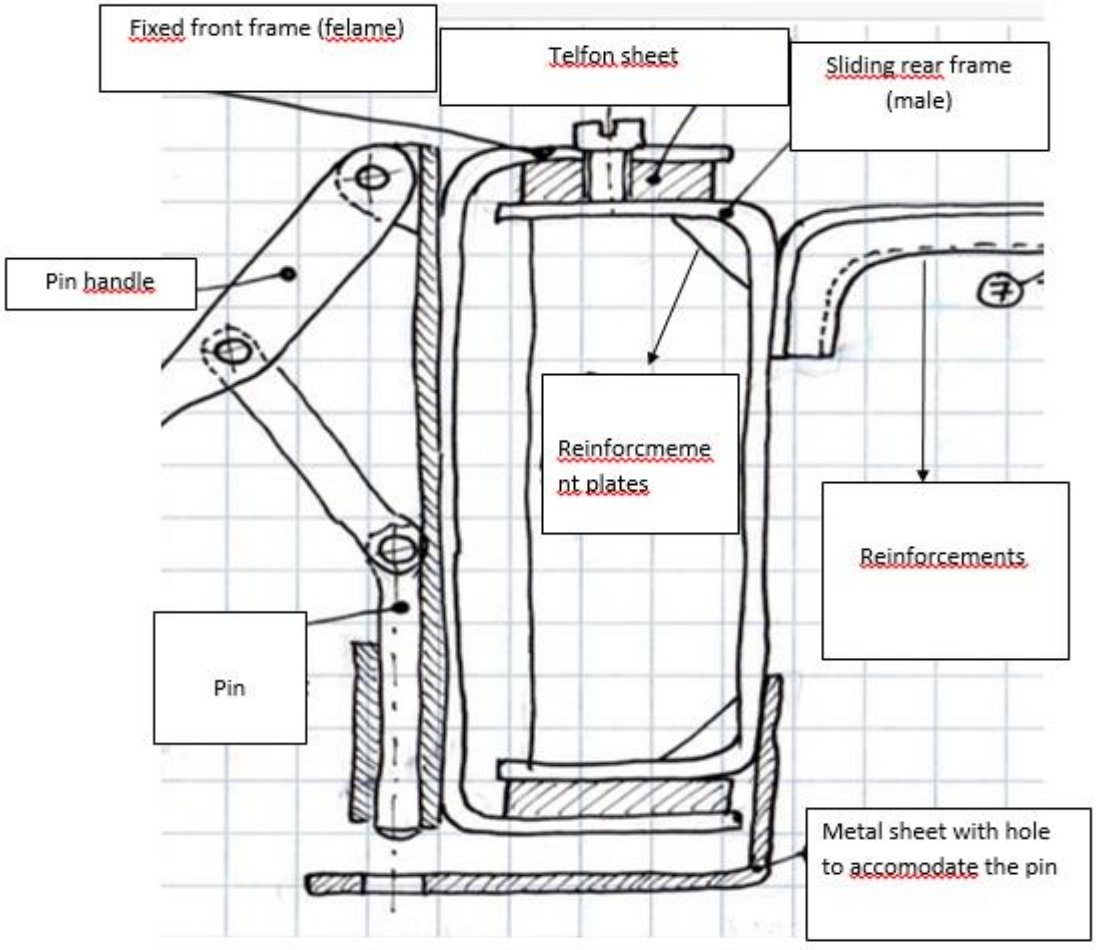

Figure 27. Pin sketch

A pin handle, see Figure 28, was integrated to the bodywork to safely and easily disengage the pin. By integrating a spring in the system, this would push the pin downward so that engagement into the next hole will happen automatically. Figure 29 illustrates the assembly where the locking mechanism has been integrated, this time mounted in the inside of the female.

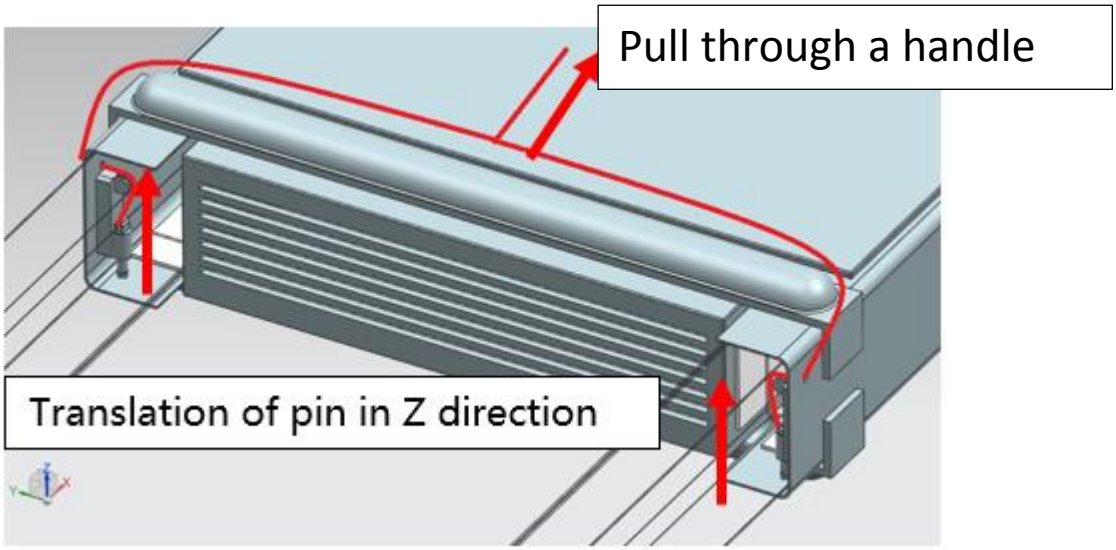

Figure 28. Locking system, preliminary models

After having performed the lengthening of the vehicle through the shown mechanisms, the sub-module will have to be added by an external machine and is outside the scope of this research project. In order to minimize the weight to be lifted by the machine while adding the sub-module to the main module, the first design concept was to try to let as many components as possible stay on the main module to lighten how much

each sub-module weighs. To this purpose, a foldable system for chassis lengthening and shortening was integrated to the main module, as shown in Figure 29.

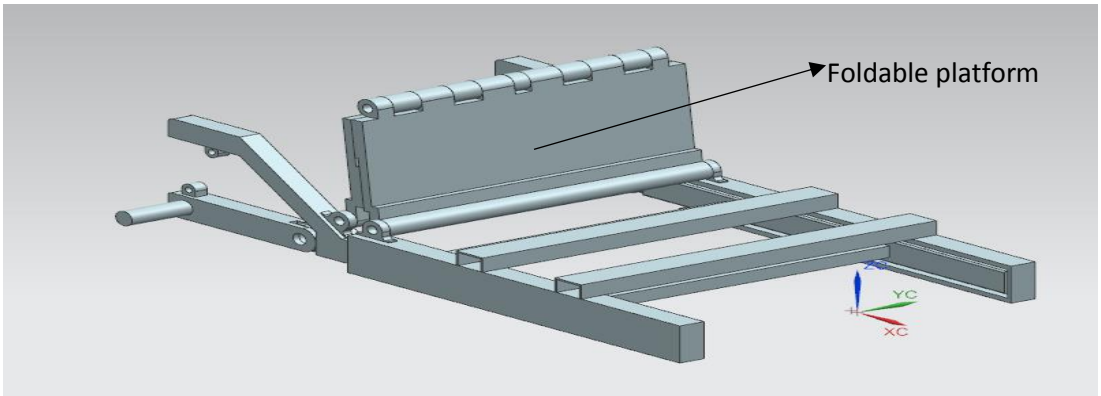

Figure 29. Integration of foldable platform onto main module

As one can infer from the picture, the folded platform would flatten during the lengthening of the main module, thus requiring the sub-module structure to only be composed of sides and a roof. However, due to the already scarce room available for cargo in the closed configuration and significant increase of weight with a foldable platform, this idea was abandoned. The final choice for the sub-module is then letting it be a completely independent structural and ergonomic system. Another solution is to keep the sub-module's seats attached to the main module and in some way fold them when in a short configuration. However, the same issues with high weight and loss of cargo space led to dismissing this idea. This last solution would also dramatically decrease the flexibility of the vehicle. For example, a single vehicle could be re-configured only to obtain more passenger or more cargo space. Since the objective was to obtain a vehicle capable of offering both two solutions, an independent sub-modular system was selected to achieve the greatest flexibility.

To integrate and provide a way to mount this element to the chassis, design of the upper part of the chassis was undertaken by a separate team (reference who), taking into account limits and requirements of the bodywork shown in Figure 31. The first design consideration to the sub-module was the manufacturing process to be adopted. To avoid use of CNC machining as a method of production, because of high manufacturing time and cost, sheet metal folding was selected as the preferred manufacturing method of beams with square or rectangular cross-sections. For the wheelhouse, folded sheets of metal have been used as seen in Figure 33.

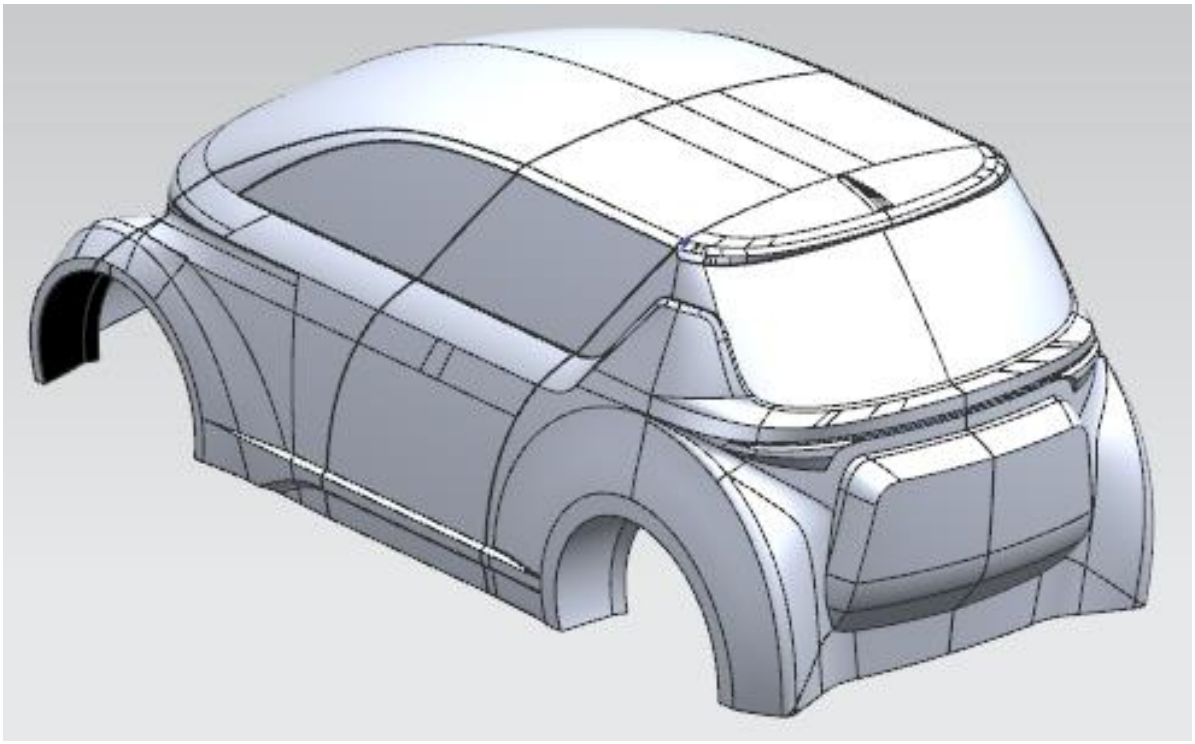

Figure 30. Design study

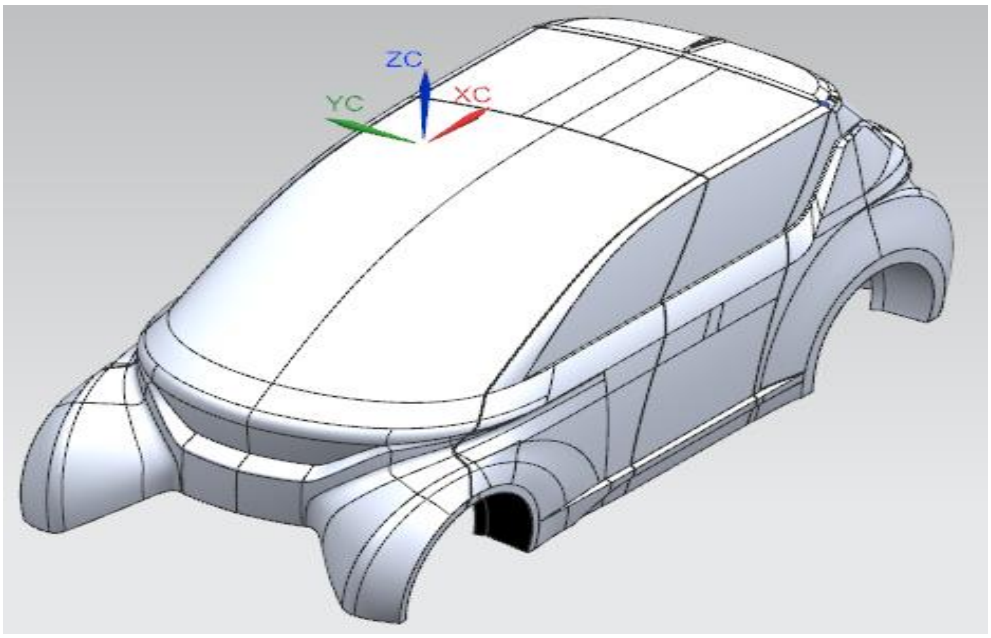

Figure 31. Design study

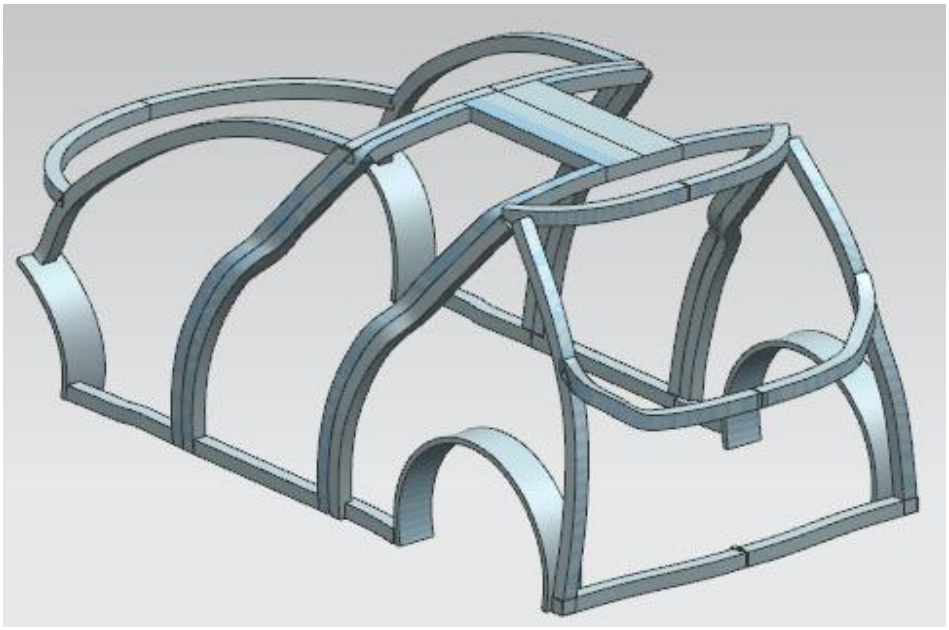

Figure 32. Body work integration

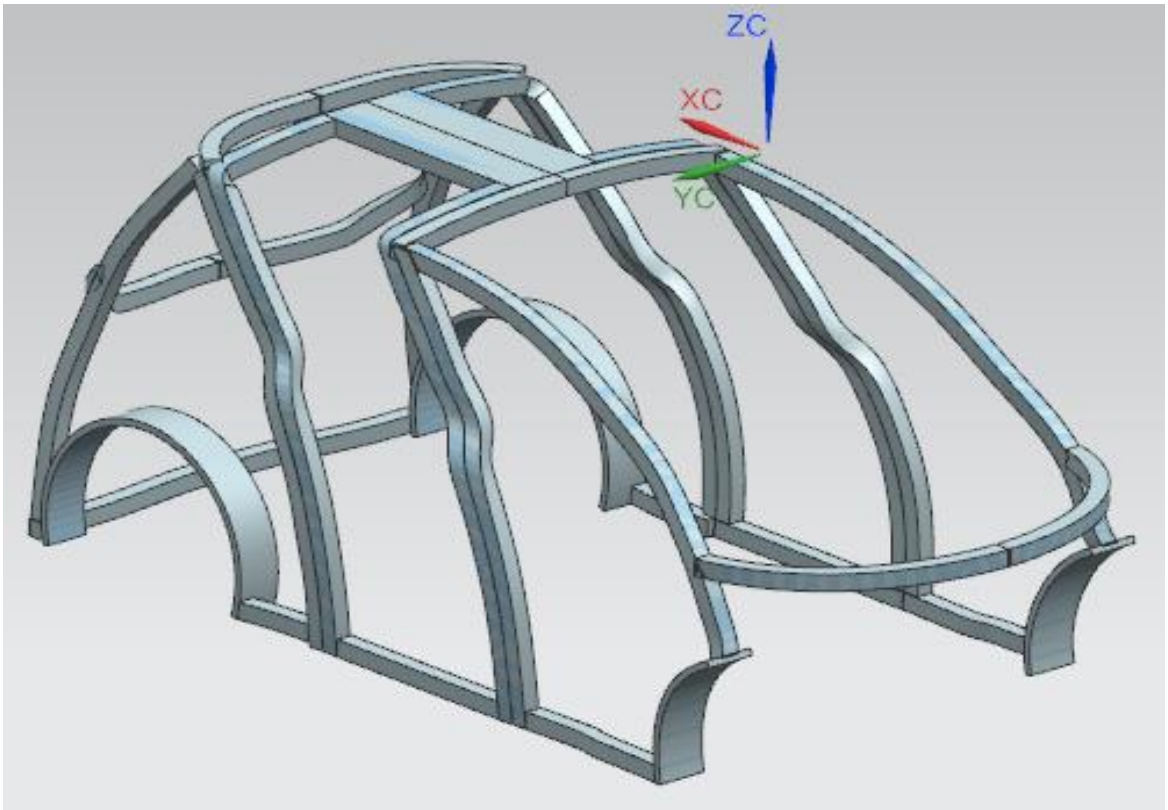

Figure 33. Body work integration

Since the design was focused on folding and welding procedures, this structure will be very effective both in terms of cost and production time. Moreover, once the final prototype is built, if structural testing results in mechanical failure, simple and quick modifications can be made and integrated without requiring a new prototype to be built anew. The rectangular channels selected for the prototype are 2x3 cm cross-section beam with a 1.5 mm wall thickness of steel. These dimensions have been chosen because of high availability in the market. However, validation of the vehicle body was outside the scope of this research.

5.2 Preliminary stress analysis

Before building a scaled, non-functioning model, a stress analysis was performed to understand whether or not the so far adopted dimensioning met the design safety criteria.

Only the chassis platform was analyzed as this was the focus of the research for this these. The boundary conditions used in the analysis are described next. There were two loading conditions that were studied for mechanical failure of the chassis. The car encountering a street curb or pothole with (i) the rear wheels, see Figure 46 and (ii) the front wheels, see Figure 48. The weight of the car was 1600 kg, based using the Smart car weight with 4 seats [29]. The long chassis configuration was selected since this is the condition where the chassis experiences the highest bending moments. Hereafter, parameters characterizing the analysis are described:

- Type of analysis: Static, structural analysis.
- Used program for the analysis: Siemens NX Nastran 9.0.
- Material: Steel.
- Meshing elements: CTetra10 elements. (WHY these elements)...Explain the modeling more on decisions for elements mesh and testing them both to ensure accurate modeling.
- Nominal dimension of the meshing elements: 12 mm.

Under the above mentioned load hypothesis, failure analysis due to material yield has been conducted. The reason why yield has been chosen as a test method is because ductile materials (like steel), experience yield before complete failure [33]. When a ductile material experiences yield, it permanently experiences change in shape deformation [33]. Thus when the load is released, only the elastic deformation is recovered [33] and there is a permanent change to the material system. For the designed system, such an operating condition is not acceptable since it would not allow a proper functioning of the assembly. Moreover, when a ductile material experiences yield, its mechanical properties change permanently and it becomes more fragile and more prone to experience failure without significant increases in deformation [34].

5.1.1 Rear chassis collisions

A rear chassis collision with a curb or pothole was simulated on the rear wheels using a reaction force of 10000 N acting as a distributed load onto the lower part of the rear chassis, see Figure 37. This load has been chosen by making the hypothesis that 80% of the total car's weight is transferred from the collision to the car to the rear chassis. The overall weight of the vehicle was applied as a distributed load acting on the top of the whole chassis system as shown in Figure 37. To fully constrain the system, the front of the chassis has been fixed. The, maximum displacement shown as red areas in Figure 38 has been found to be equal to approximately 11.3 mm, while the blue regions are area of zero displacement. Here, the maximum Von Mises stress is 20 MPa, while the yield stress for steel is 235 MPa [25]. As can be seen, the chassis has a safety factor of SF=11.75 when considering failure from yield stress.

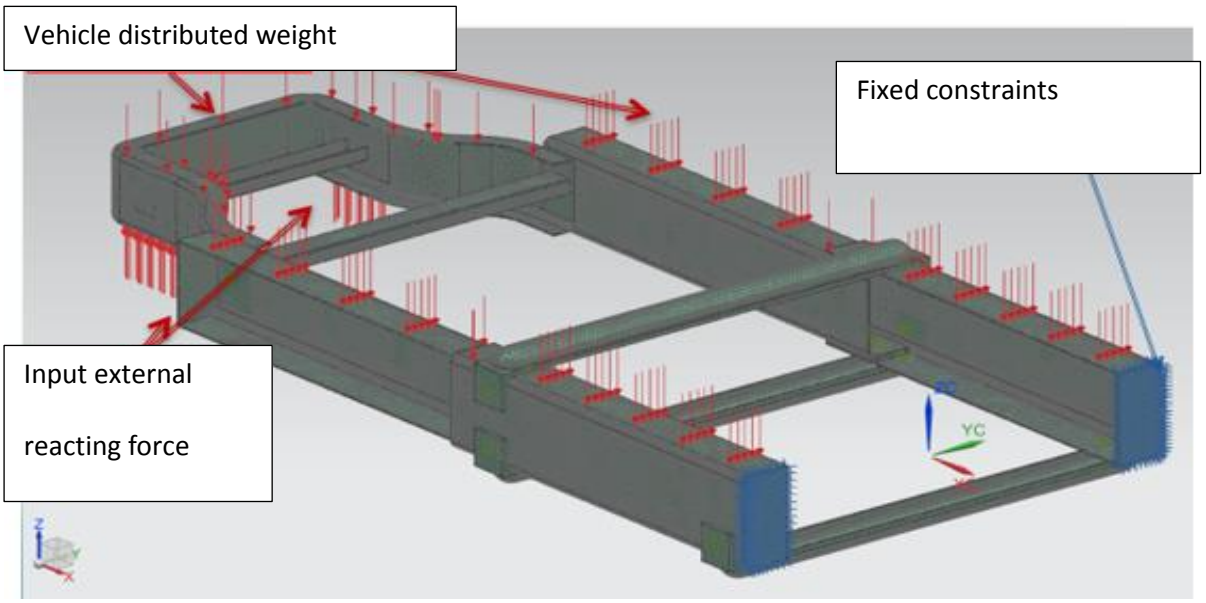

Figure 34. Boundary conditions scheme a)

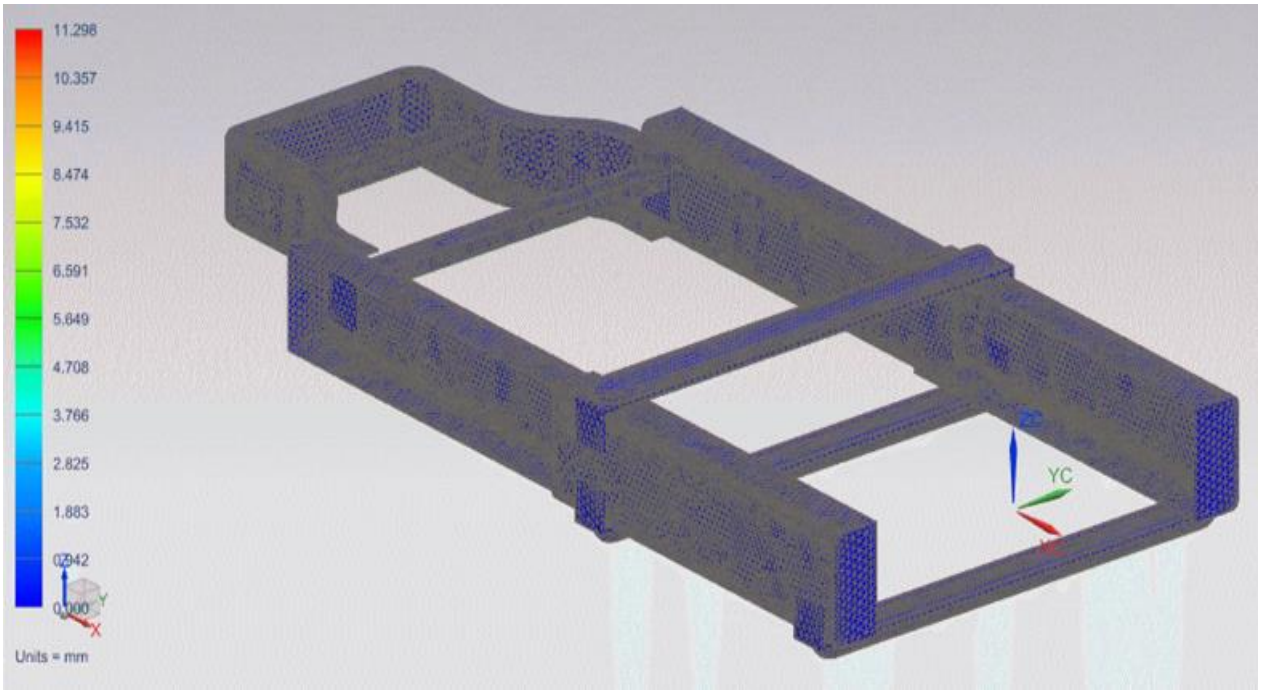

Figure 35. *Results a) Displacement*

5.1.2 Front curb

Similar to the above discussion, the collision force for a curb or pothole was simulated as a distributed load acting on the front part of the chassis, see Figure 39. Similar to the previous model, the front end of the chassis has now been fixed to fully constrain displacement. The car's weight and distribution remained the same; in this case, the maximum displacement, shown as red regions in Figure 40, is approximately 7 mm, while the zones with zero displacement are blue. The maximum Von Mises stresses is again approximately 20 MPa and so the safety factor is SF=11.75.

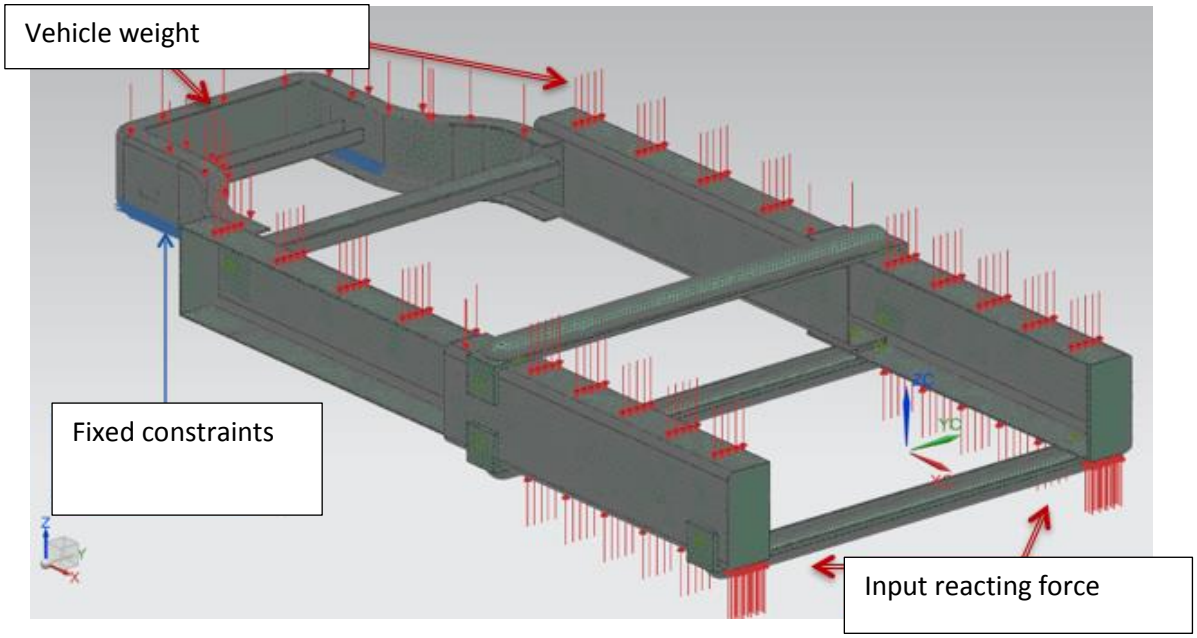

Figure 36. Boundary conditions scheme b)

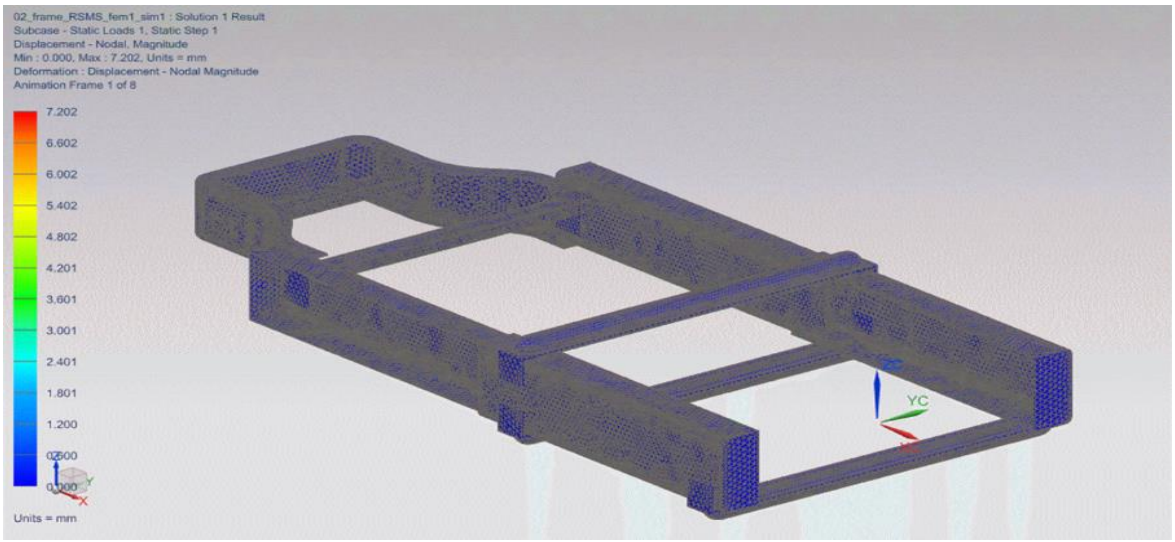

Figure 37. Results b) Displacement

5.1.4 Conclusions

From the above stress analysis, it was found that the preliminary chassis design had high safety factors and the system could be lightened. Some lightening holes could be made onto the male and the female part to reduce the overall weight, and a further analysis could

be carried out to see whether the safety factor would decrease to non-acceptable values. However, this procedure would bring an important increase in the cost of the manufacturing processes. The choice was made to begin building the 3D non-functioning scaled prototype and to troubleshoot manufacturing issues as well as test the designed lengthening mechanism.

CHAPTER 6

BUILDING A PROTOTYPE

6.1 Choice of prototype typology

A scaled prototype was built and is shown in Figure 53. The aim for building a prototype was to perform design study and to validate the dimensioning of the entire system. Moreover, a prototype would allow identifying possible inefficiencies to the design. In general, there are four prototypes used in industry [36]. A brief description of each is outlined below:

- *Conceptual prototype*: for evaluation of general shapes, verifying assemblies, verifying possible technological issues.
- *Functional prototypes*: for evaluation of performances with functional tests, optimization of the product for its function. Devices being tested in this phase must be similar to the final design, while the manufacturing process is still not considered.
- *Technical prototypes*: for evaluation of both the performances of the product and of the manufacturing process. Devices must be very similar to the final product design and the manufacturing process must be quite similar to the one used to build the final device.
- *Pre-series prototypes:* where a final evaluation of the product is performed and minimal marginal changes are allowed. Both the material used and the manufacturing process must be the ones used during the final production of the series.

For the proof of concept testing, a conceptual prototype was built and can be seen in Figure 53. Here, the research aim was to verify the assemblies as well as the lengthening mechanism. The prototype included the lengthening and shortening procedure of the chassis with the main objective to understand how the tracks would work together as well as test the efficiency of the chosen re-configurability.

6.2 Choice of manufacturing technology

3D printing technology was chosen to manufacture the external bodywork and the chassis platform. 3D printing technology was chosen because of its simplicity, ease of manufacturing, and much lower cost compared to other manufacturing processes (e.g. molding). The part of the chassis holding the bodywork was not fabricated at this time since building the whole internal chassis via 3D printing technology would have required a great amount of supports to be created during the process itself. Thus, the whole chassis was not manufactured to save both time and material in the 3D printing process. The parts built with 3D printed technology were: the main module, the added sub-module and the wheels, see Figure 44. For the Female track component, a W-shaped beam was used. On the other side, as a male, a U-shaped beam was used and no sliding elements were placed between the two. Reinforcements were also added and very simple bars have been used for them. The front chassis was manufactured through waterjet cutting methods of a plain metal sheet. Detailed pictures are shown in Figure 44 to allow better understanding of the system being described. Waterjet cutting was chosen for this last application due to ease of manufacturing and high accuracies for the needed purpose. The bodywork was manufactured using a wall thickness to be self-supporting (4mm) and joints were added to the chassis platform in order to fix the bodywork onto it.

No dynamic analysis was performed on the prototype, and this is why wheels were attached in a very simple way. Four pins were designed to come out of the chassis to correspond with the wheel positions, and holes of the same dimension were designed on

the wheels. By inserting the pins into the wheels, they will stay in position in a sufficiently accurate way to allow testing of the lengthening mechanism. Lengthening and shortening of the chassis was performed through a very simple system, see Figure 38. A radio-controlled electric motor, with its wires and controls, was taken from a radio-controlled toy. A screw was then attached to it, such that the motor's rotation would cause the screw to rotate with the same angular speed. Both the screw and the motor are attached to the front part of the car, while a nut has been attached to the rear of the vehicle, allowing, during the rotation of the screw, forward or backward movement of the front part with respect to the rear part. The original controller of the machine allows the motor to rotate in both directions and performs the opening and closing procedures. As seen in Figure 39, the red line shows the space created through the lengthening procedure, in which the sub-module will be placed. The main module is in the fully open configuration, with the male being at its extreme position out of the female. This creates a gap, which will be filled by placing the sub-module onto the main one.

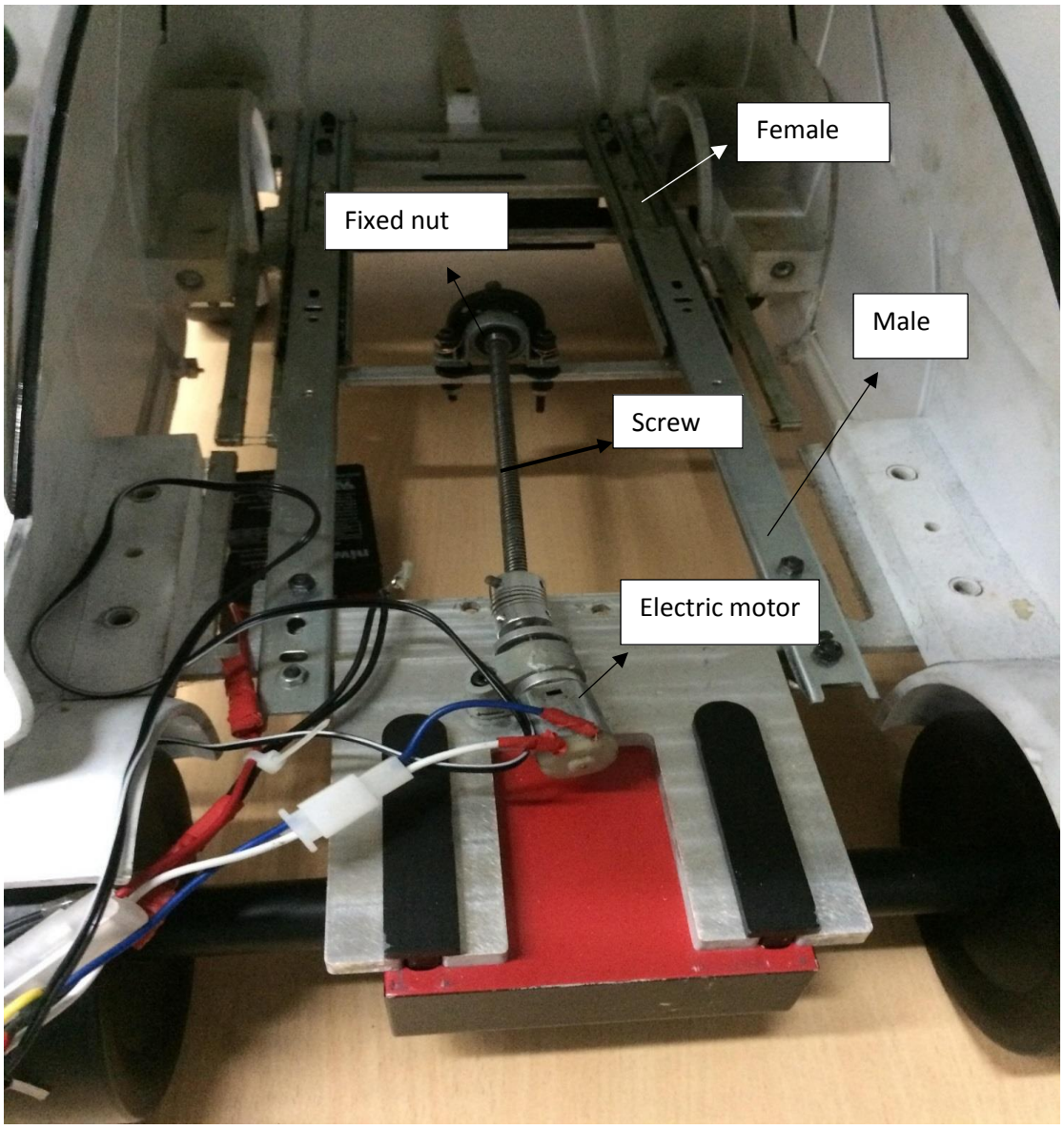

Figure 38. Prototype's lengthening mechanism

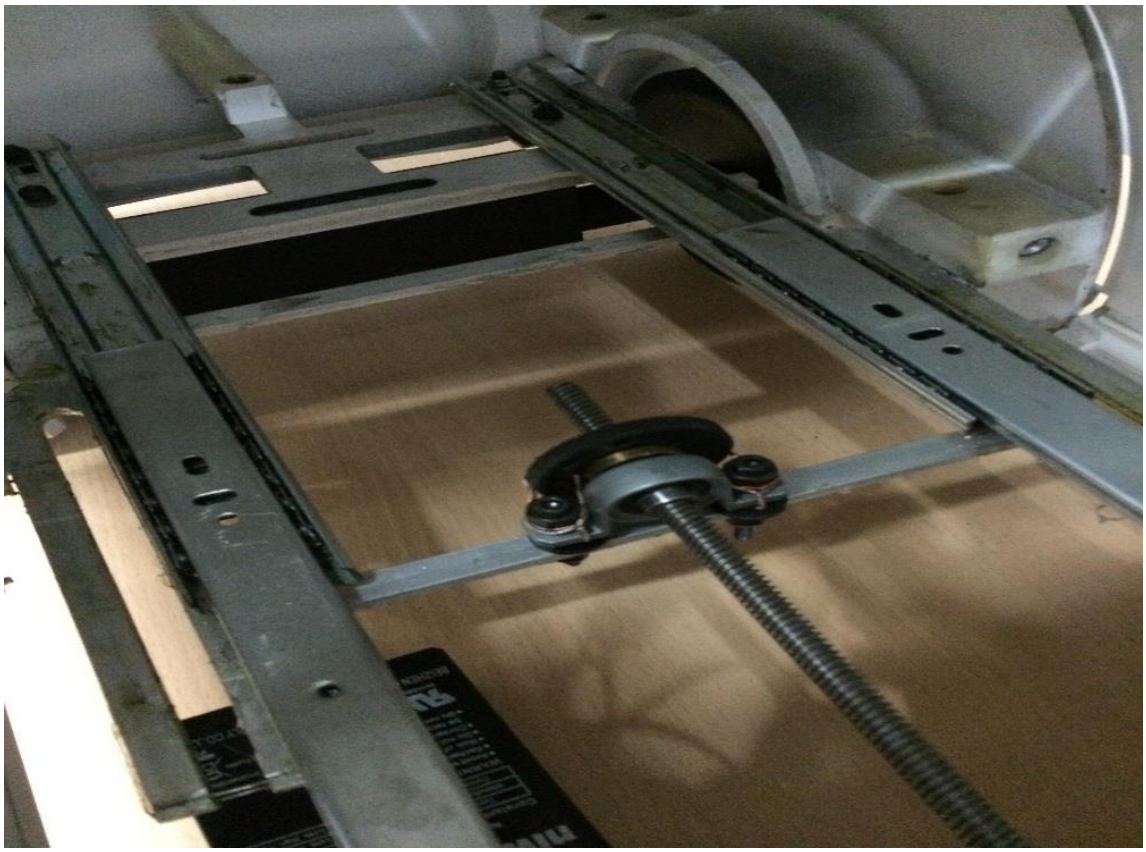

Figure 39. Prototype's nut detail

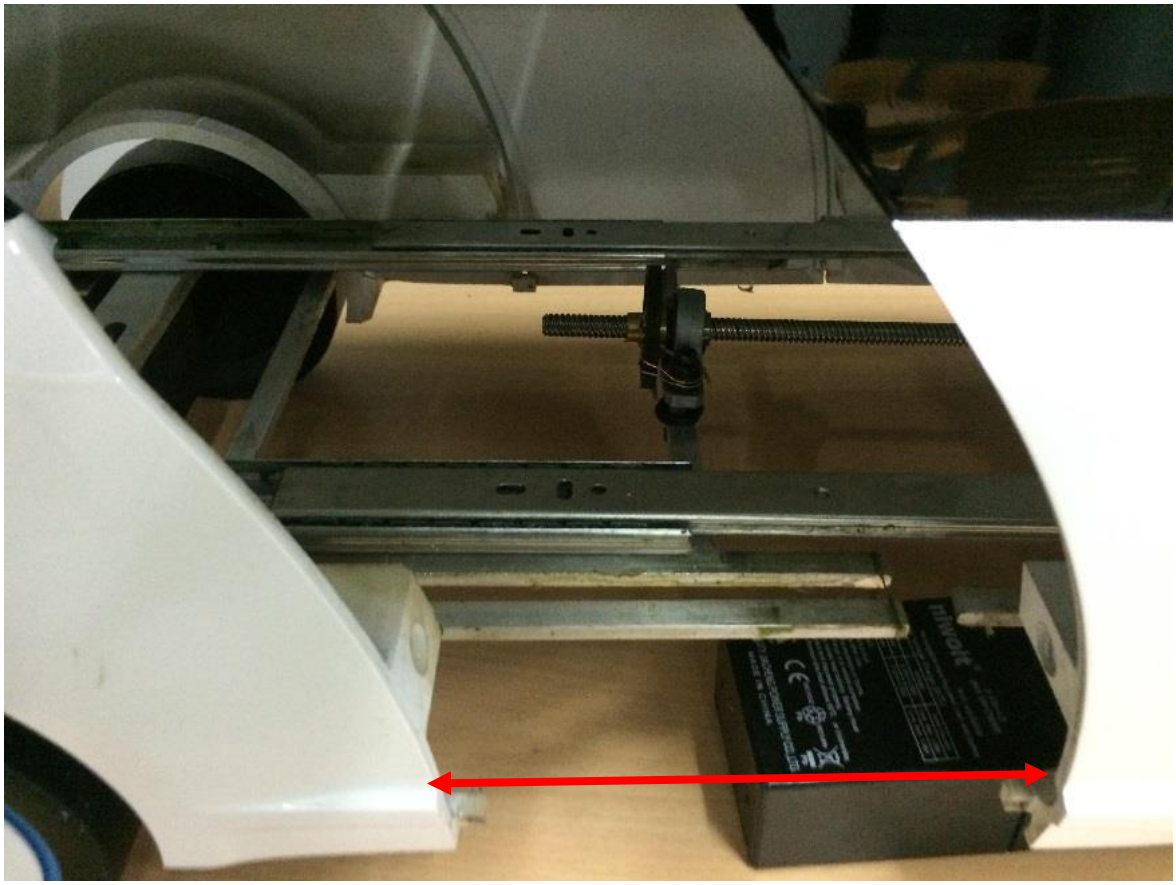

Figure 40. Prototype's lengthening mechanism, side view

Hereafter, a detailed set of pictures of the prototype is shown, to allow the reader to have a deeper idea of what the concept looks like at this step. All the reported pictures show the prototype in its long configuration, with the sub-module attached on the main one.

Figure 41. Prototype

Figure 42. Prototype, front and side views

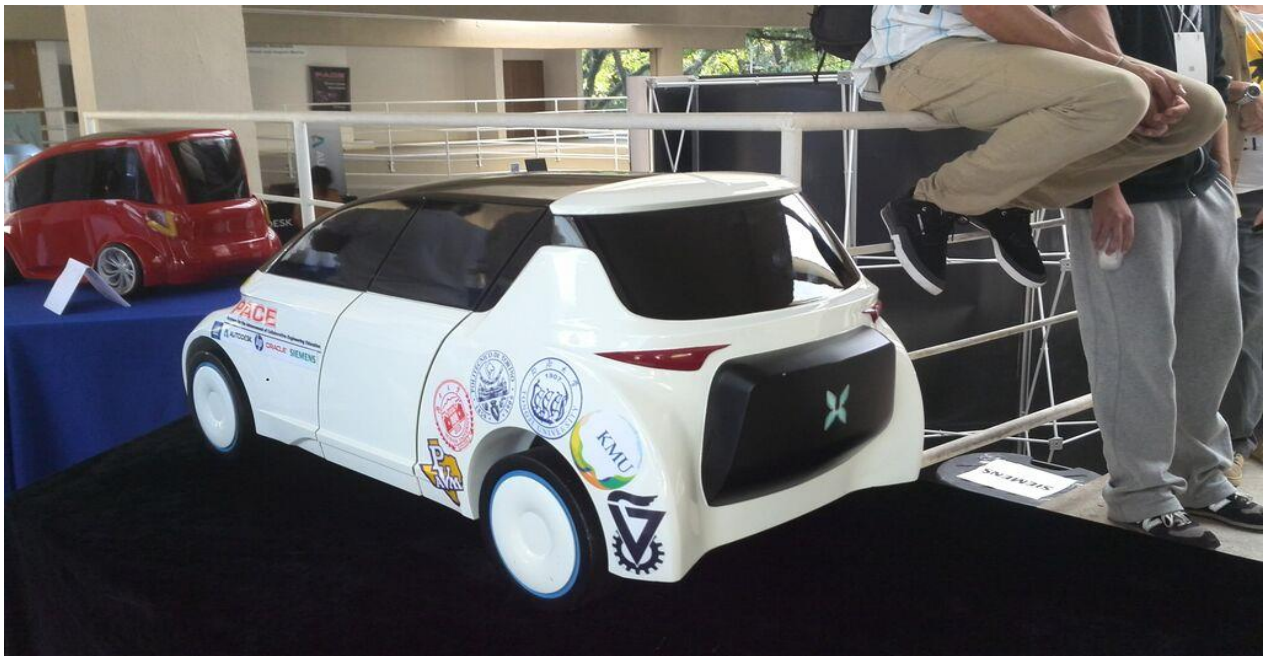

Figure 43. Rear and side views

Figure 44. Prototype sub-module's doors opening

Figure 45. Prototype front door opening

6.3 Prototype Analysis and Conclusions

After building and testing the prototype, some engineering and safety issues were identified and were addressed during the second phase of the project. A detailed list of each design issues are discussed below.

- The front door solution appears to have safety problems. When the vehicle is in the short configuration, the front door is the only possible way to exit the vehicle. In the unfortunate case of a frontal impact damaging the front door system, a driver would not be able to exit the car. For this reasons, side doors will be considered in substitution of the front door in the second phase of the project.
- The Segway module was maybe the most revolutionary and innovative solution. However, many engineering issues were identified during the design and prototype testing phases. Integrating safety and effective integration of the Segway was identified as a very difficult task. It was determined that a detailed analysis of the Segway design was needed to decide whether or not it could succeed, see below.
- The sub-module is designed to be added by using an external device. This solution, despite the high provided flexibility, can result in a user having to bring the vehicle to a car station every time he or she wants to re-configure it. To address this problem, a second version of the car allowing lengthening and shortening without the usage of an external device will be designed in the future.

Figure 46. Segway module concept

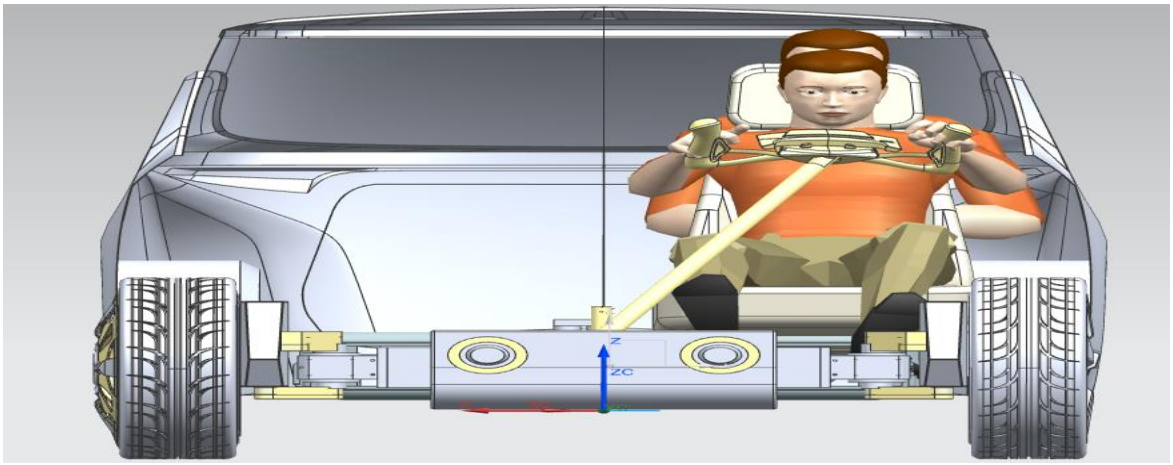

Figure 47. Segway and driving system

The initial design concept was to integrate a Segway onto the vehicle. Segway's wheels would function as the vehicle's front wheels during normal use, with the possibility of being disassembled and used independently as a normal Segway. The first design problem is that the car's width is much bigger compared to the one of a standard Segway. A system to make the two wheels come closer to one another when the Segway is needed had then to be

designed. Moreover, since the Segway is attached to the front part of the car, a system to guarantee a proper steering had to be carefully designed as well. To this purpose, a standard steering system would have not been possible since Segway does not allow its wheels to freely rotate to turn. Instead, Segway use a system that allows turning through the difference in angular speed of the two wheels. To help the reader understand how the steering system would have ideally worked, Figure 62 illustrates the steering concept. As can be seen, the Segway handle is used as steering wheel during normal driving to input steering information to the Segway. The handle bar of the Segway must be folded into the car and towards the driver's seat when the Segway is attached to the vehicle. Since this is project is not the main topic of this thesis, no further explanation will be provided on how to implement the steering design. Construction of the prototype highlighted many design issues using the Segway and this solution was abandoned for the second phase of the project.

Since earlier designs used front wheels from the Segway, the front wheels and suspension system components now had to be designed and integrated onto the car's chassis. The main task is to provide a link to both front wheels and allow a proper suspension mechanism to be used. Since the suspension mechanism had already been chosen for the rear wheels, the choice was to keep the same mechanism for the front ones. Given this decision, the front beam should provide a proper support onto which the two suspension links could be attached. Designing the front beam was iterated twice and each iteration will be discussed below. It should be noted that no calculations were made for the dimensioning at this stage.

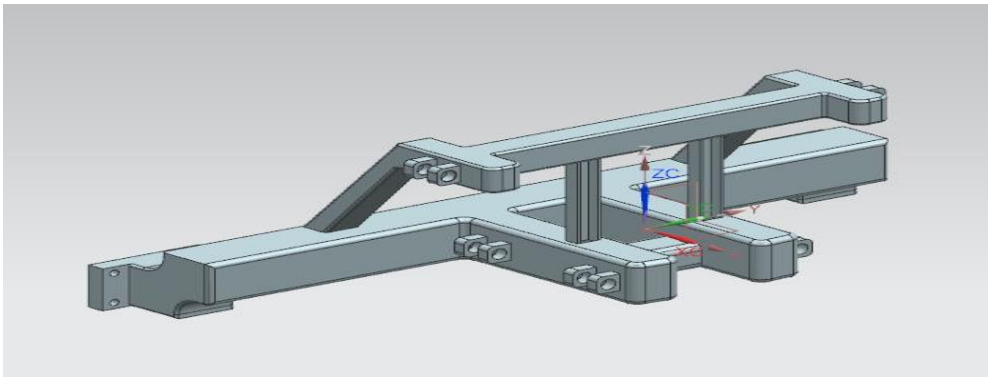

Figure 48. First front beam design

The front beam was originally designed as a single part without any welding. It would be attached to the chassis through four bolted joints, see Figure 49. Upon analyzing the design, it was found that the manufacturing process of such a component would require it to be machined by a CNC machine. Thus, manufacturing of the part could be cost prohibative. Also, since the suspension links are integrated onto the front beam, any suspension modifications would require a re-design of the beam itself which would also increase future manufacturing or repair costs. Figure 50 shows the second and final choice for the front chassis design.

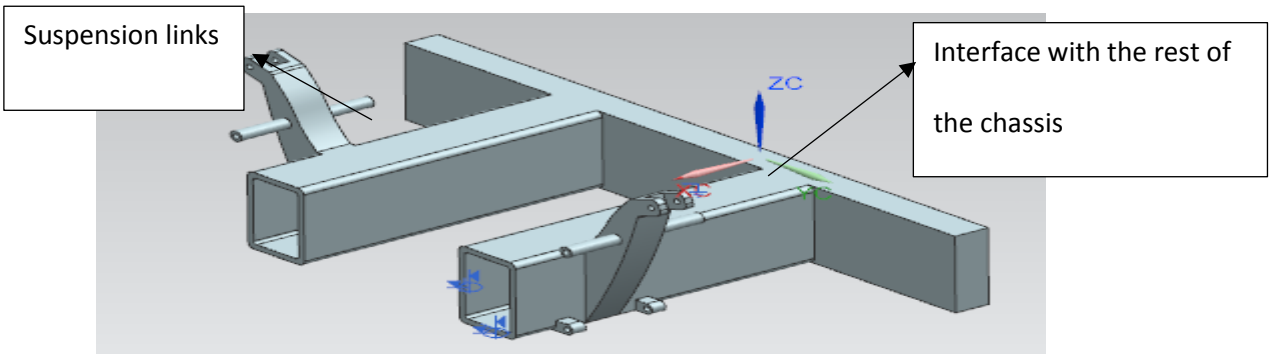

Figure 49. Second and final front beam design

Since the design of the suspension system was outside the scope of this research, an existing suspension design was selected to design the connections from the chassis to the suspension, see Figure 50. The connections to the suspension system are simple to fabricate and thus reduce manufacturing cost and time of manufacturing procedures. The suspension links are composed of two hollow rectangular beams welded to a transverse rectangular beam. The transverse beam will be in turn welded to the front part of the female track. The dimensioning of all the chosen beams were chosen from readily available stock. As can be seen from the above figure, the front beam is composed of several components welded together. All the components will be manufactured using simple machining cutting procedures, and the only components that still have to be machined are the suspension links. However, any changes to the suspension links will not affect the shape of the remaining chassis since they are independently manufactured.

Chapter 7

STRESS ANALYSIS AND DESIGN VALIDATION

A detailed failure analysis of the chassis design was performed to optimize and validate the final chassis design. As discussed above, the material, mesh parameters and applied loads were the same as in the preliminary design work. As discussed in the preliminary analysis, there is the possibility of lightening the structure due to safety factors exceeding 2. Thus, the first step was to analyze the chassis in the same configuration used for the preliminary analysis, but optimizing the design to lighten the weight, while considering manufacturing costs. In the next sections, applied modifications and results are shown.

7.1 Lightening of chassis weight

The first applied modification was to reduce the weight of both the male and the female tracks by removal of material as shown in Figure 51. The chosen shape for the holes was to cut triangular plates from the tracks. The triangles were chosen due to their high moment of inertia, producing high resistance to bending moments.[30], As seen in Figure 52, regions where the Von Misses stress resulted in safety factors above 3 (referring to the preliminary stress analysis) were targeted for material removal. Therefore, the goal was to leave enough material in regions where there were high stress concentrations, as shown in Figure 51 and in zones where parts would be welded to join them together.

In Figure 52, the meshed chassis assembly with lightening is shown. The red circled areas were left without cutouts, since they are areas in which welding will be done and require higher strength. Figures 52 to 55, show the dimensions of the applied lightening triangles.

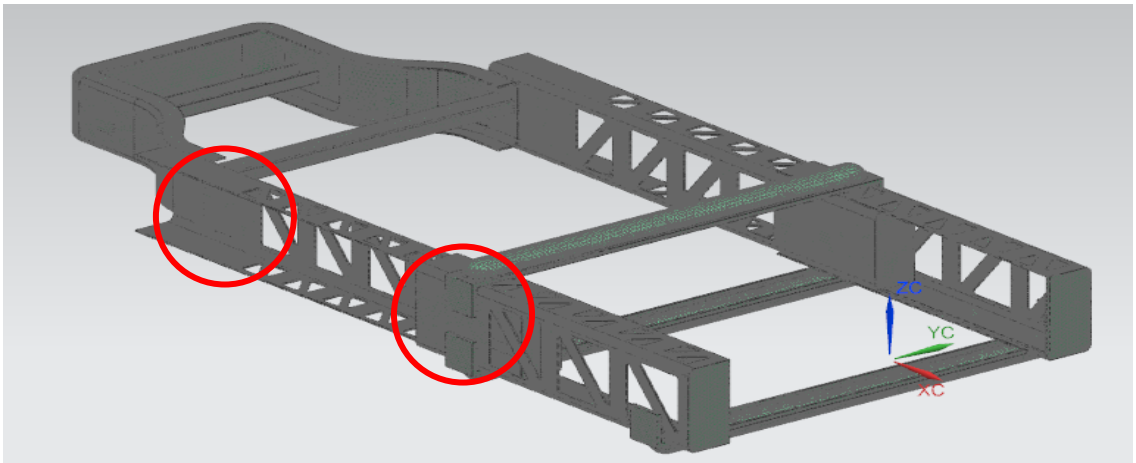

Figure 50. Lightened chassis (through all holes)

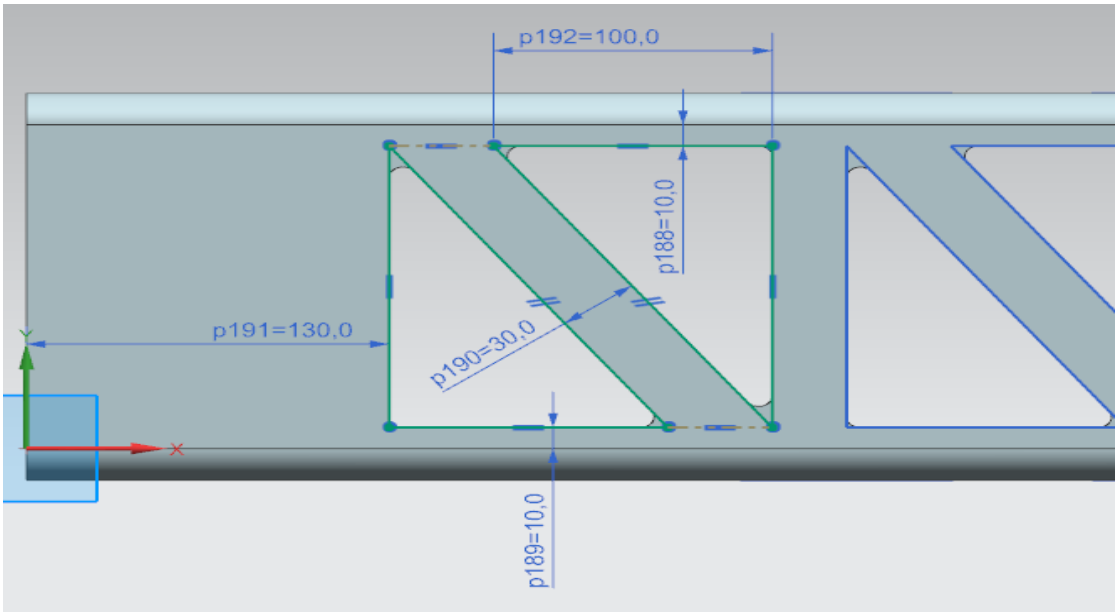

Figure 51. Lightening dimensions, side view (male)

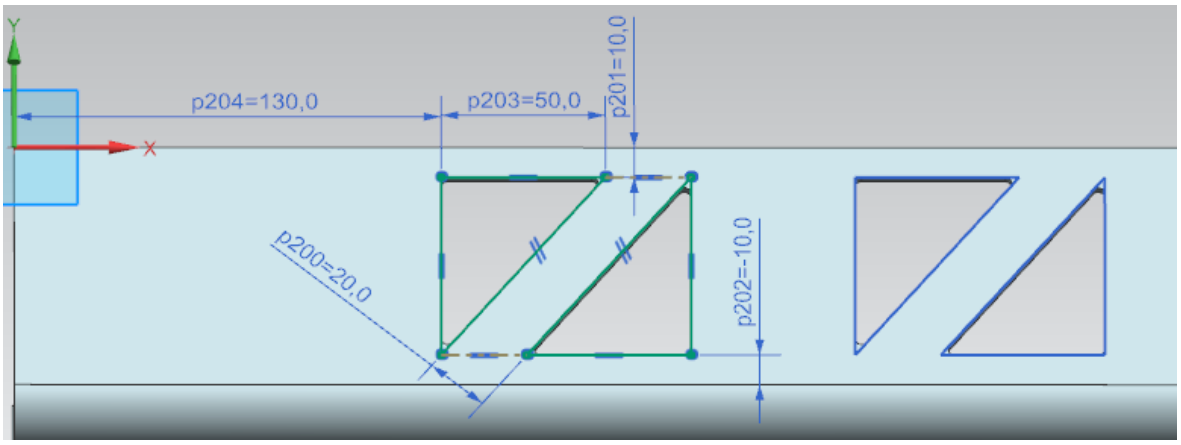

Figure 52. Lightening top and bottom view

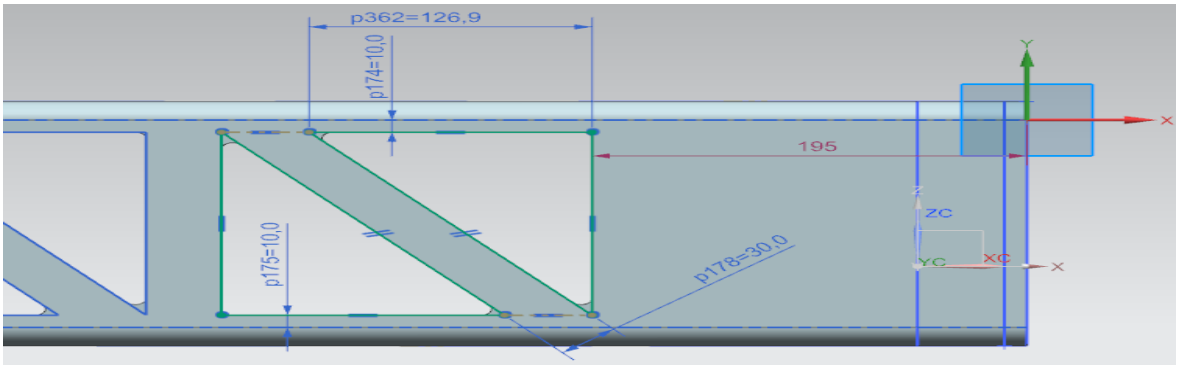

Figure 53. Lightening, side view (female)

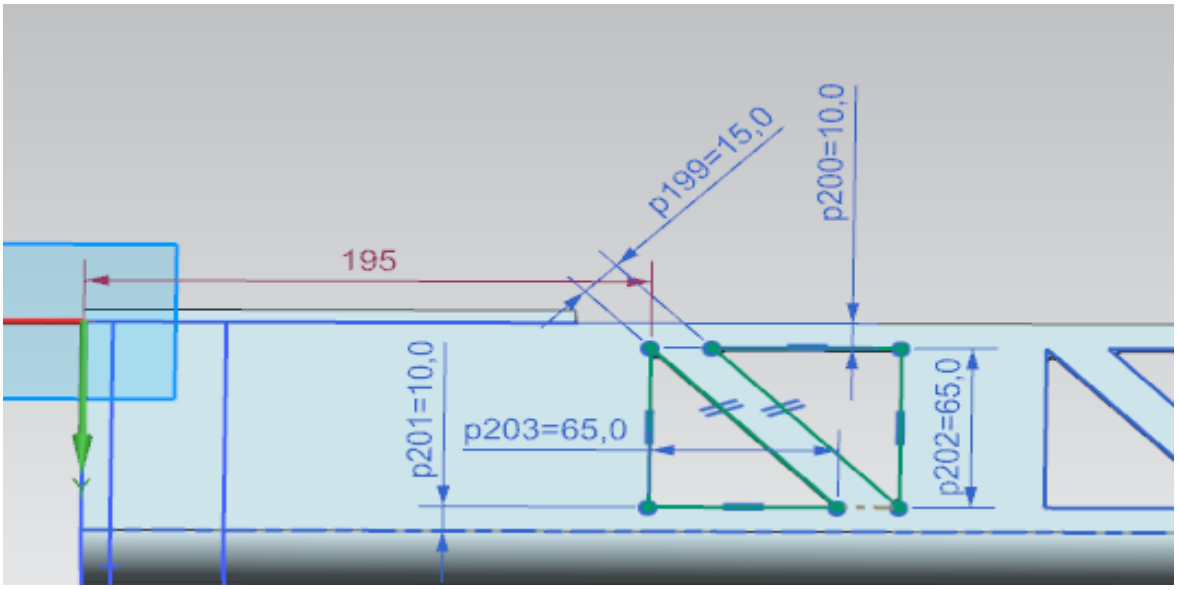

Figure 54. Lightening, top and bottom view (female)

7.1.1 Rear curb impact analysis

Similar to the preliminary stress analysis, an analysis simulating impact between the rear wheels and a curb or pothole was done. Figure 55 shows the applied loads and boundary conditions and are the same as used for the preliminary stress analysis as briefly summarized here as:

- A distributed load of 1200 kg.
- A load simulating the impact of 10000 N with 80% load transfer to the chassis.
- Fixed displacements of the front chassis.

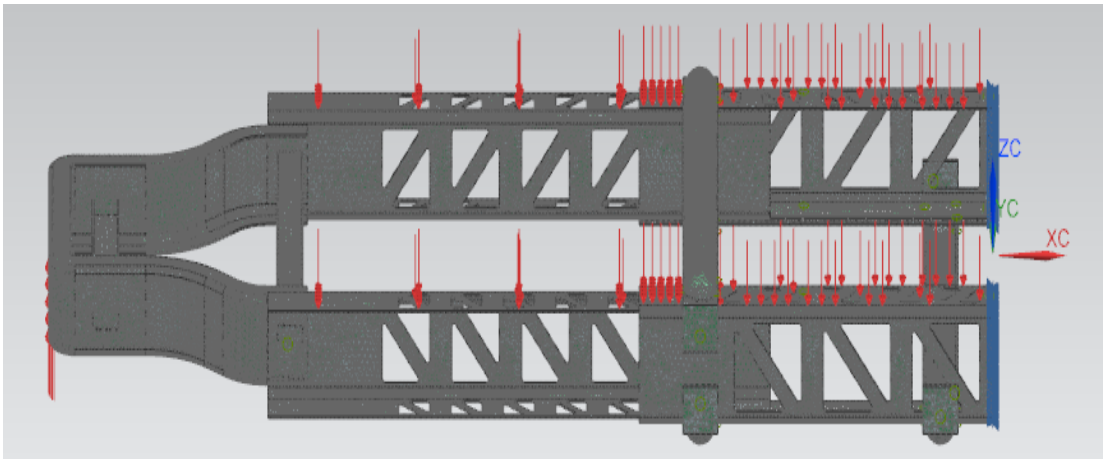

Figure 55. Applied loads, rear bump

For this case, the maximum stresses are above the yield limit (235 MPa) as seen in Figure 55. These yield zone are mainly in the rear part of the chassis, highlighted by red spots in Figure 55. This is a result of the reduced stiffness to both the male and the female tracks. In addition to increased manufacturing costs, the weight savings from the cut outs was only 15 Kg. From these results, it was determined that the weight savings to increased manufacturing costs was not beneficial and no further weight reductions from the vehicle chassis was pursued.

Table 1 shows a comparison between the results obtained in the preliminary analysis and the last obtained ones.

TABLE I: STRESS ANALYSIS RESULTS COMPARISON

	Max Displacement (mm)	Max Von Mises stress (MPa)
Last analysis	20	300
Previous analysis	11.3	20

The following section describes the same lightening solution tested against impact on the front wheels.

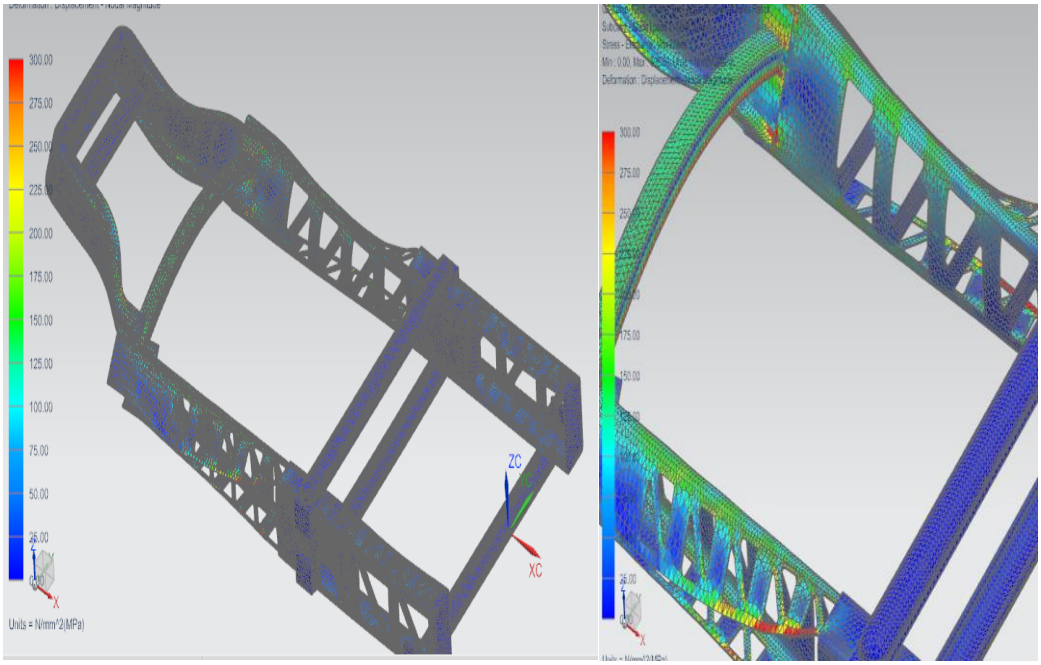

Figure 56. Stress results

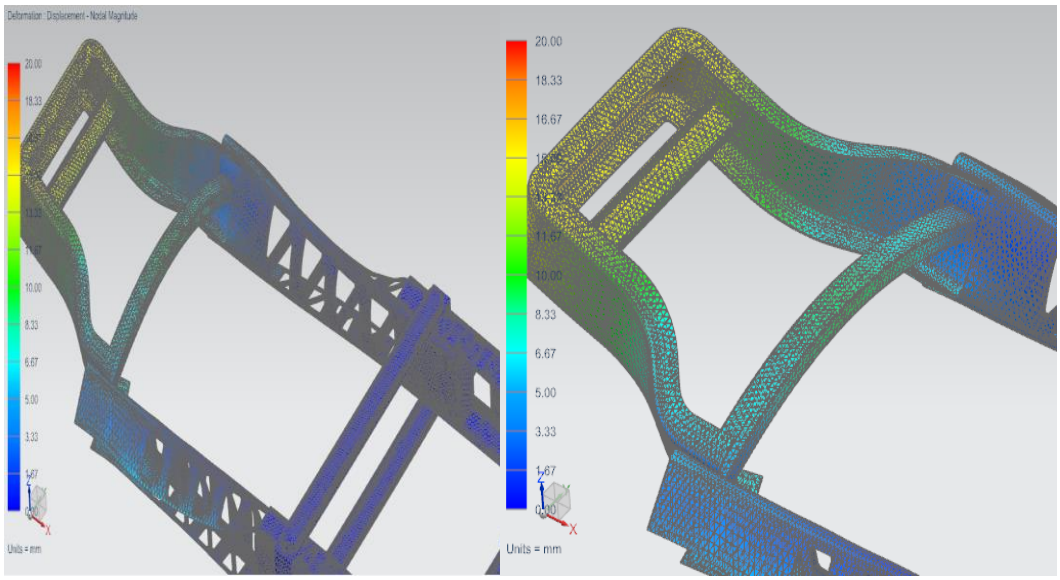

Figure 57. Displacement results

7.1.2 Front curb impact

A front collision with a carb was also conducted to understand the effects of the reduced stiffness to the performance of the front part of the chassis. The goal was to study whether lightening could be performed on the front part of the chassis to reduce weight. Since, as already mentioned, safety factor for car chassis is usually between 3 and 6, the target safety factor has been chosen to be equal to 4.5. From now on, red in the stress result's color scale will correspond to 50MPa. This value has been chosen as an upper limit because with this as a maximum value a safety factor of 4.5 is obtained against yield. So if red zoned will appear in the results images, this means that resulting stresses are equal or higher than 50MPa, thus not acceptable for this analysis. For what concerns the displacement color scale, this will still show maximum (red) and minimum (blue) results.

Figure 58 shows the load condition for this case. Again, a distributed load of 1200 kg is applied, a 10000 N force is applied to the front part of the chassis while the rear part is fixed.

From figure 58, it can again be seen how the resulting stresses exceed the yield limit. Hence, also this analysis points out that this lightening did not bring any advantage.

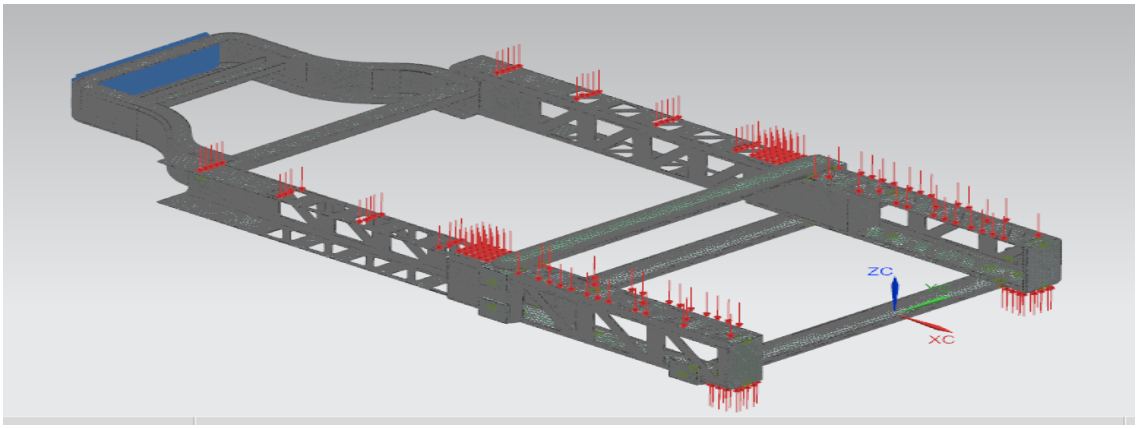

Figure 58. Applied loads, front bump

Obtained results in both terms of displacement and Von Mises stresses are hereafter shown and table two shows a comparison between the previous and the actual results

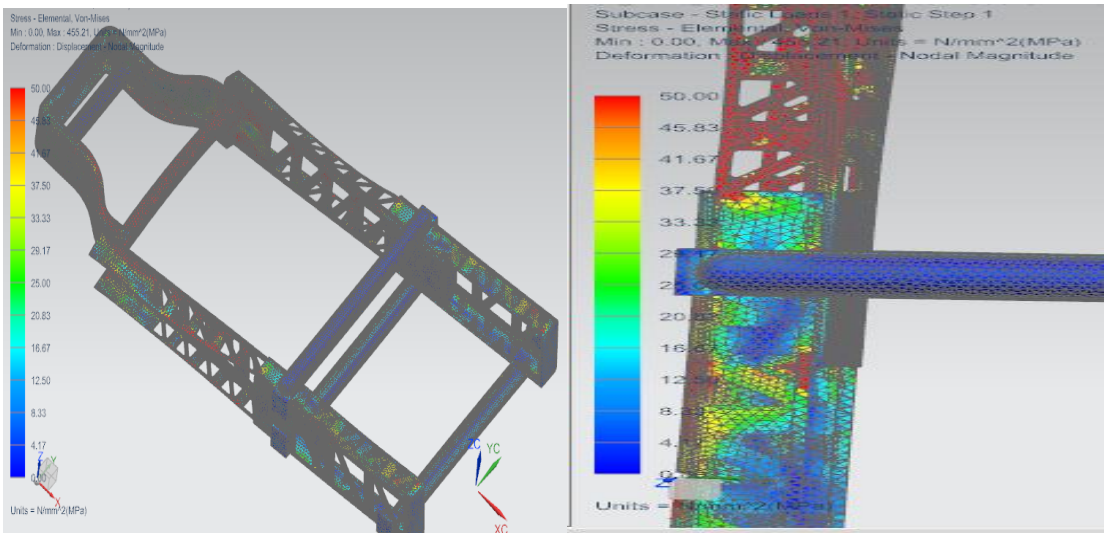

Figure 59. Stress results

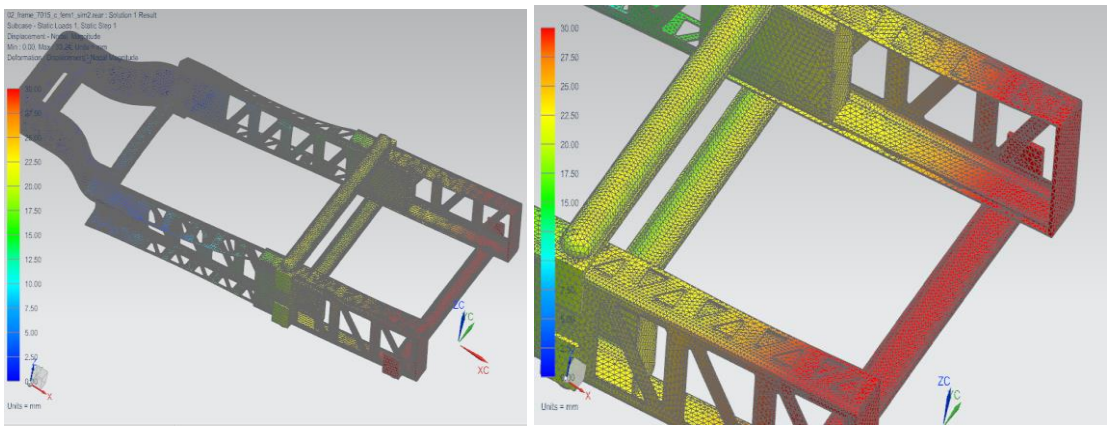

Figure 60. Displacement results

TABLE II: STRESS ANALYSIS RESULTS COMPARISON

	Max Displacement (mm)	Max Von Mises stress (MPa)
Last analysis	30	300
Previous analysis	3	15

7.3 Full Chassis Analysis

For this next analysis, the front beam has been added in order to test the chassis with all its components. The previous analyses used approximation of the load conditions. However, since the front beam was missing, the 10000 N load simulating a front bump could not be applied to the front wheels. This resulted in a lower bending moment acting on the whole chassis do to the missing front section. The same loading conditions will used again on the complete chassis for design verification.

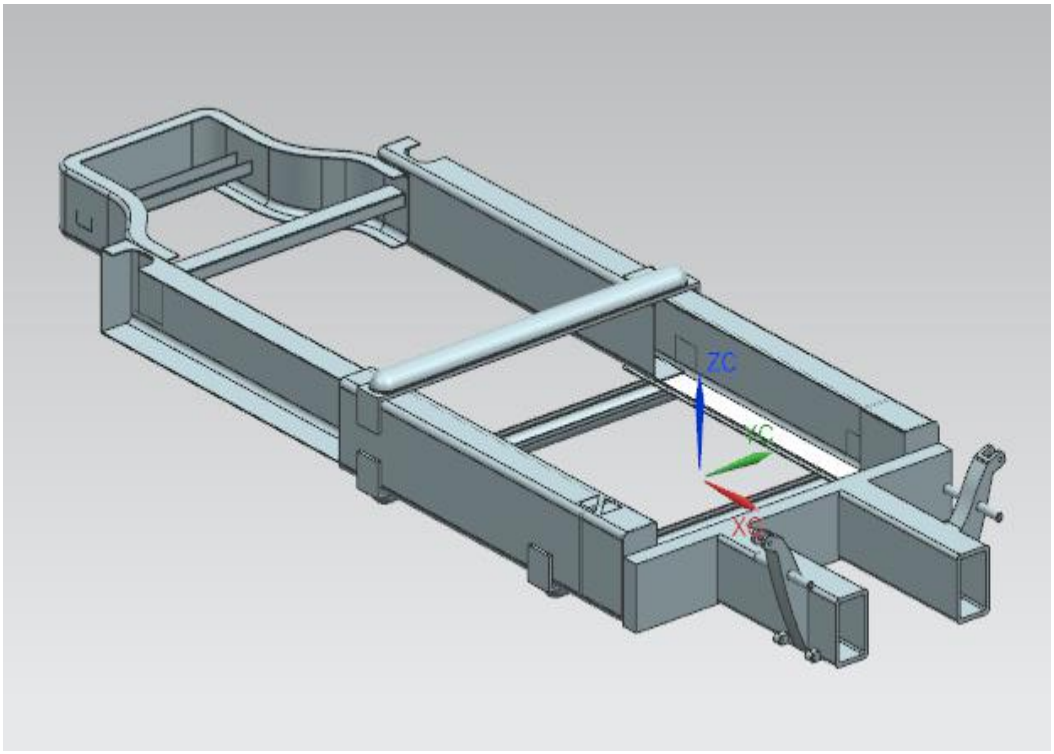

Figure 61. Complete platform to be tested

7.3.1 Front curb impact

The resulting stresses in this case appeared to be much higher with respect to the first made stress analysis. Stresses of well above the yield limit appeared (see Figure 62), and stiffening of the structure is at this point required.

As can be seen, the total bending moment is significantly increased results in increased Von Mises stresses on the whole rear part of the chassis. Additional reinforcements are therefore required to eliminate this yield failure.

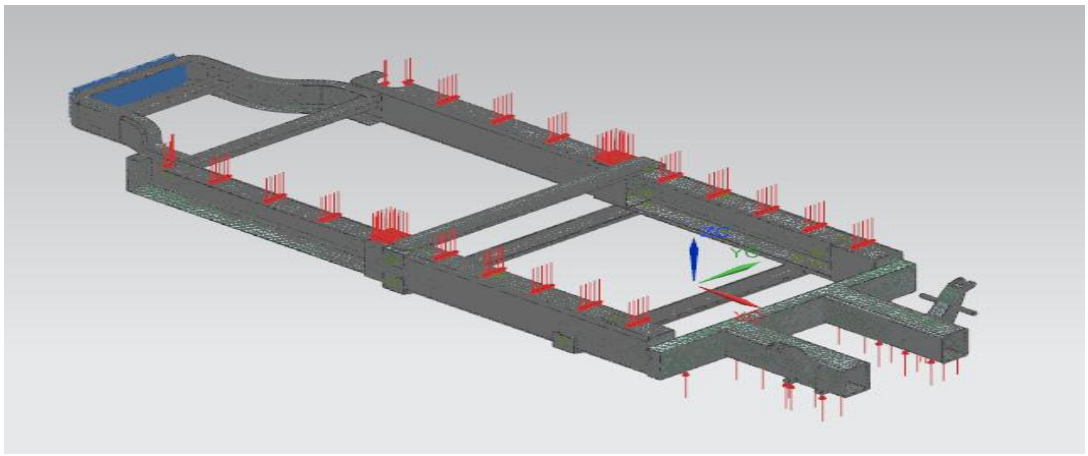

Figure 62. Load condition

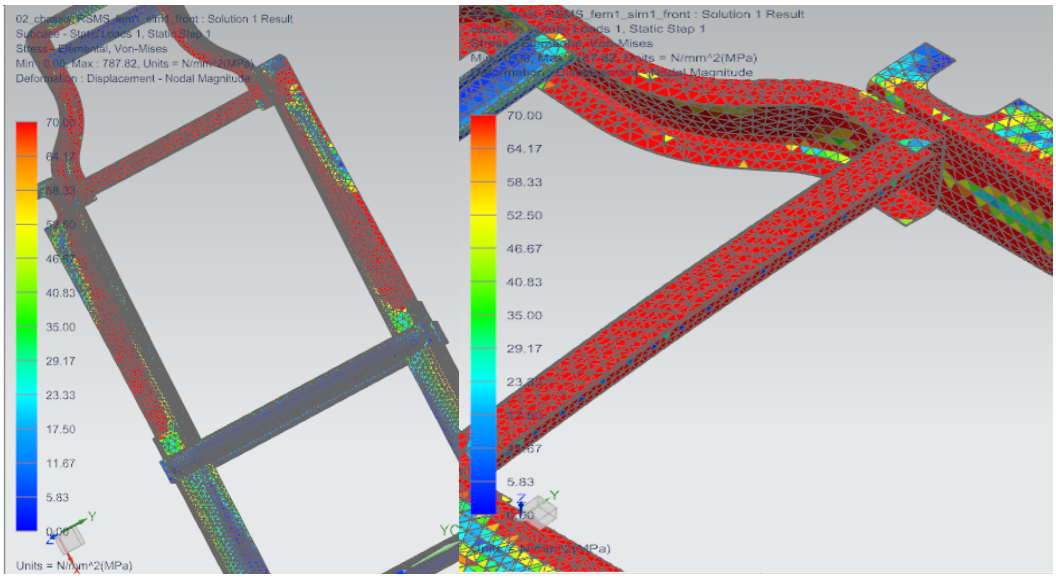

Figure 63. Stress results

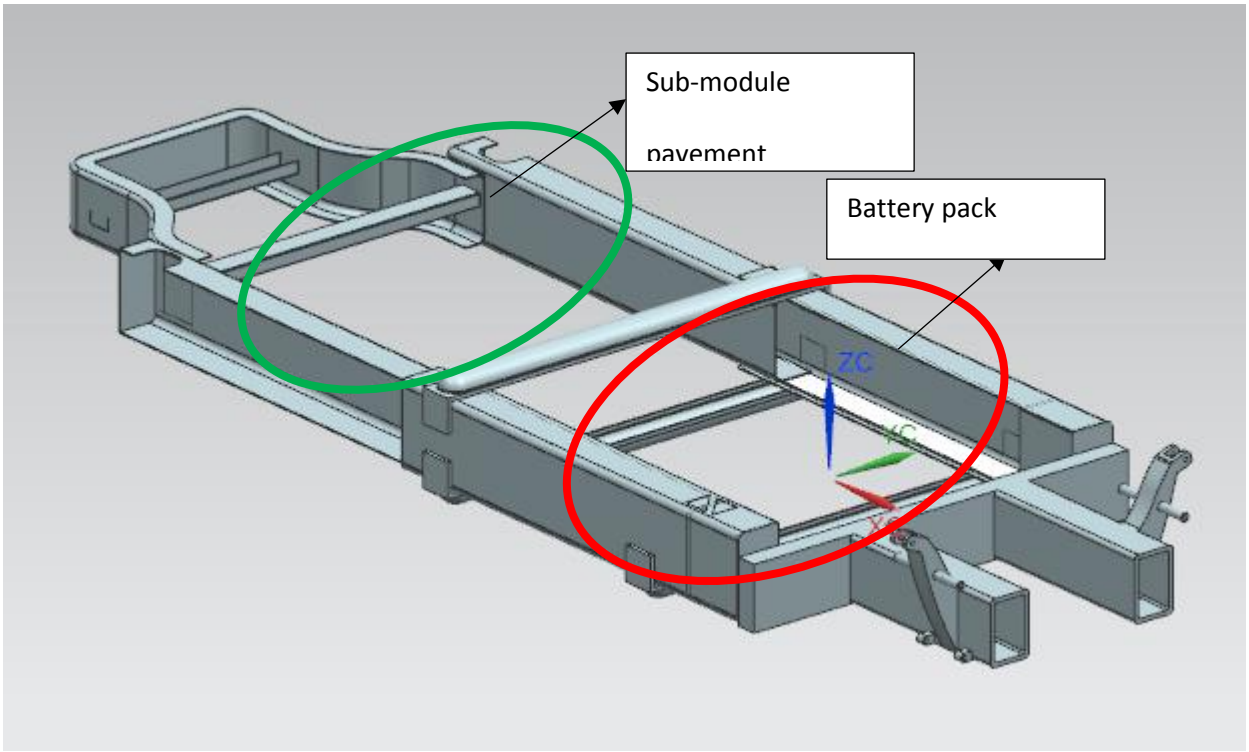

Figure 64. Sketch of additional components

Since the design of the driving mechanism for the vehicle changed, it was decided to include the battery pack on the design since it is directly mounted to the chassis. This in effect would result in changing the bending behavior of the chassis and the load distributions acting on the system. A battery pack was mounted to the front part of the chassis (red circle in figure 64). The choice was made to use the battery packing as a structural element as well by constructing it of steel and welding it to the chassis, see Figure 65.

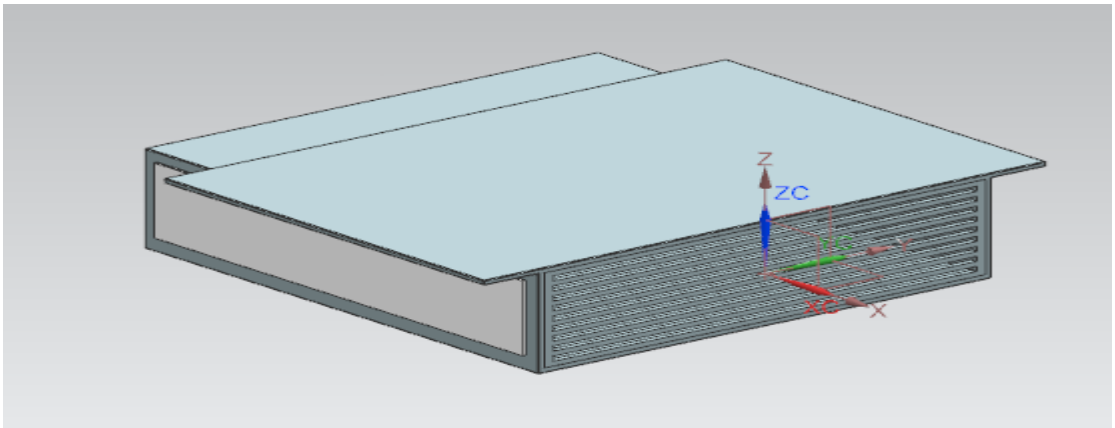

Figure 65. Battery pack

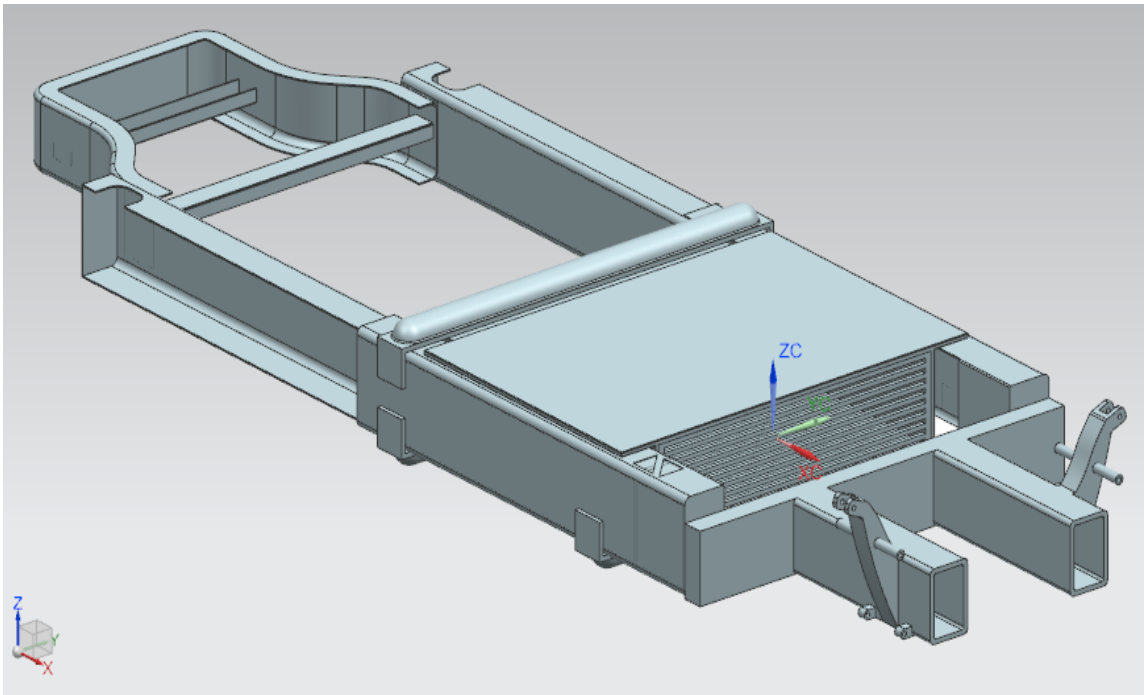

Figure 66. Mounted battery pack

As seen in Figure 68, the upper layer of the pack has been designed so that it will offer a wide surface to be welded onto the female upper faces. In addition, since the fully lengthened chassis was chosen as the critical operation, the sub-module will be present. The impact of the sub-module on the mechanical behavior of the chassis was also included in the

mechanical analysis. The sub-module will be placed onto the male (green circle in figure 64) and will act as a structural component.

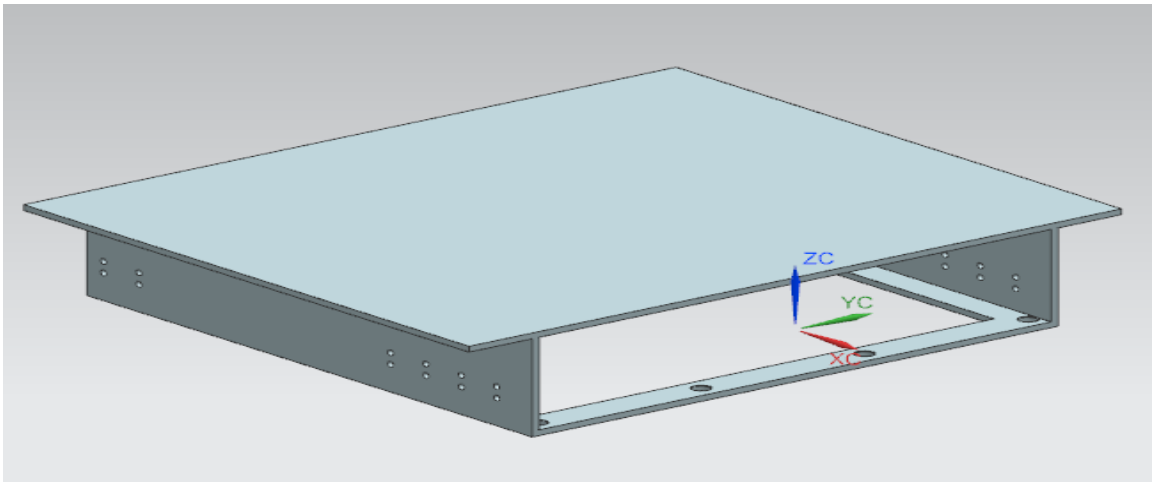

Figure 67. Sub-module pavement and battery pack

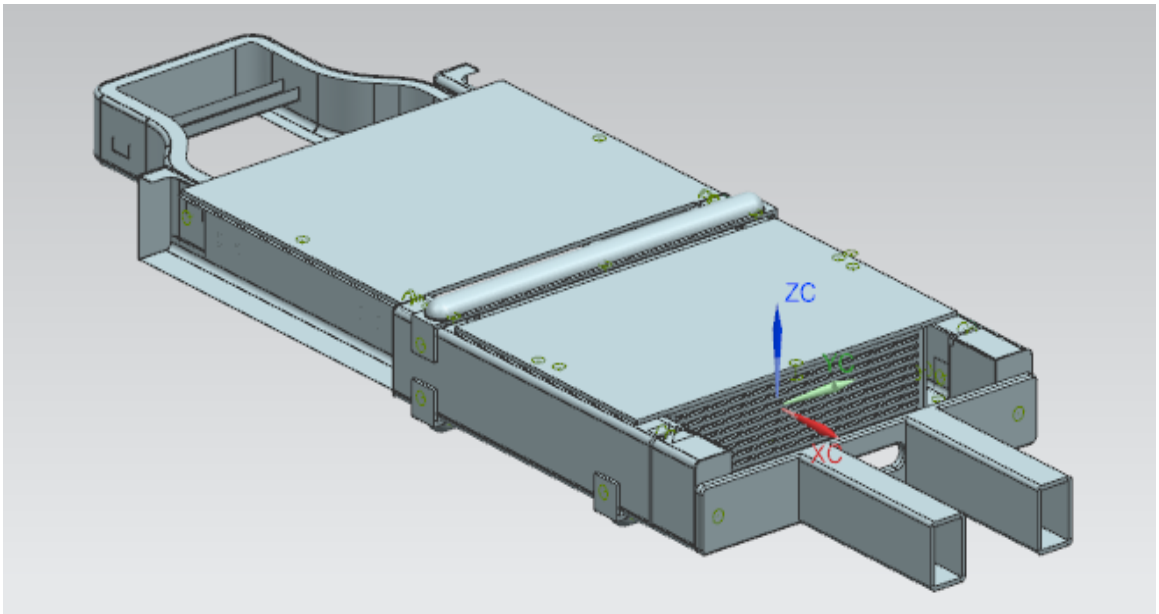

Figure 68. Chassis with both battery pack and sub-module pavement

Thus, the system was modified to include transverse I-beam as reinforcements to the rear part of the chassis to accommodate the added loads for the battery and sub-module (see figure 68). Since only few dimensions are available in the market for I shaped

beams that are not too big for to be mounted on the structure (in [31] only two fit our model), it has been chosen to test one of the available dimensions and see if this would have brought any relief in the stresses. In this case, refinement could have been done by choosing different available dimensions. Dimensions of the chosen beam are shown in Figure 69

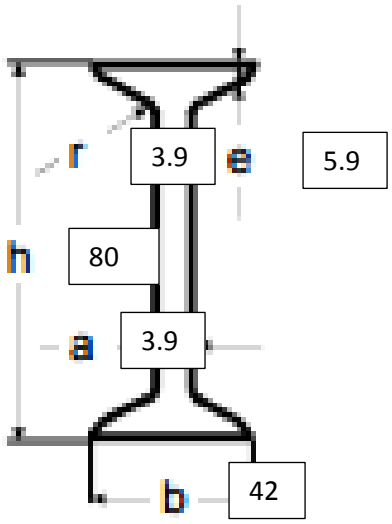

Figure 69. "I" shaped beam dimensions. All dimensions are in mm

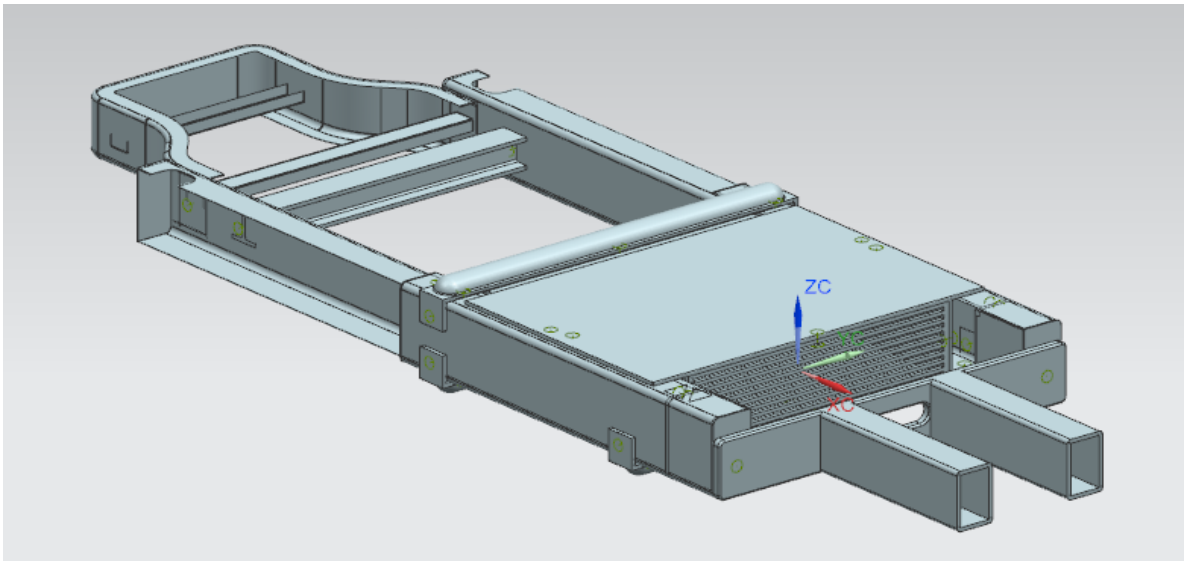

Figure 70. Chassis with battery pack and rear "I" reinforcement

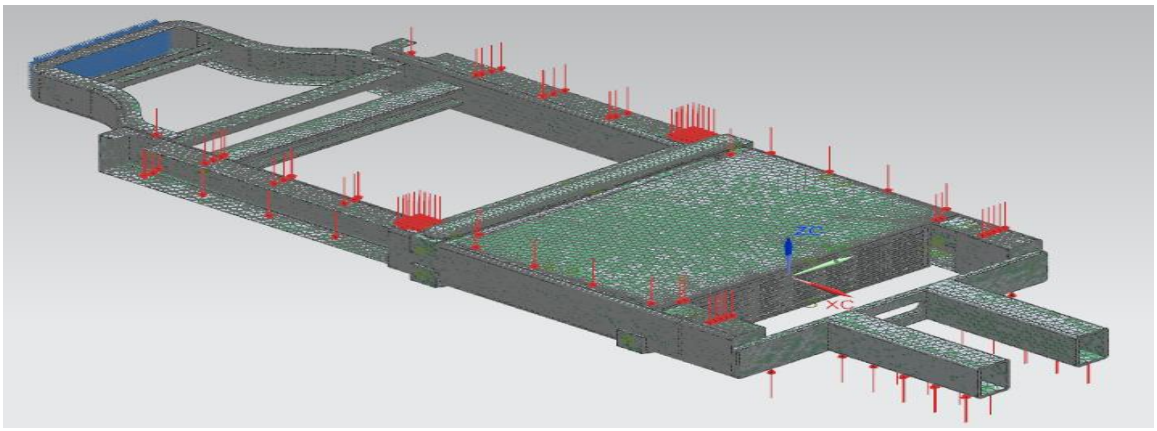

Figure 71. Rear reinforcement load condition

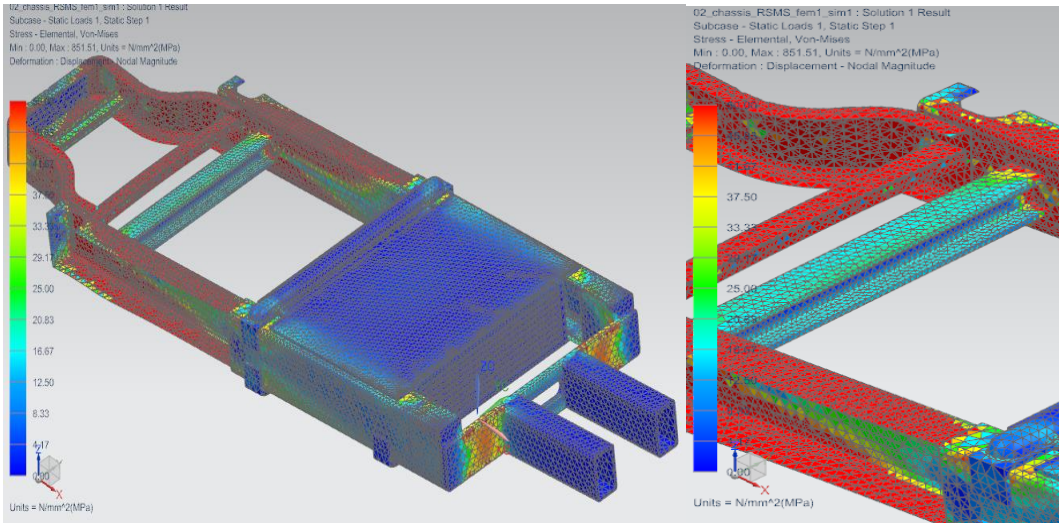

Figure 72. Rear reinforcement stress results

The two analysis have been performed and the obtained results are now shown. Tables still compare stresses to the preliminary analysis results.

Figure 72, shows how the mounting of the “I” shaped beam did not bring any benefit. Stresses are in fact still above the yield limit (red zones still are visible in figure 72). It can be noticed how this solution is not a proper one.

TABLE III: STRESS ANALYSIS RESULTS COMPARISON

	Max Von Mises stress (MPa)
Last analysis	150
Previous analysis	170

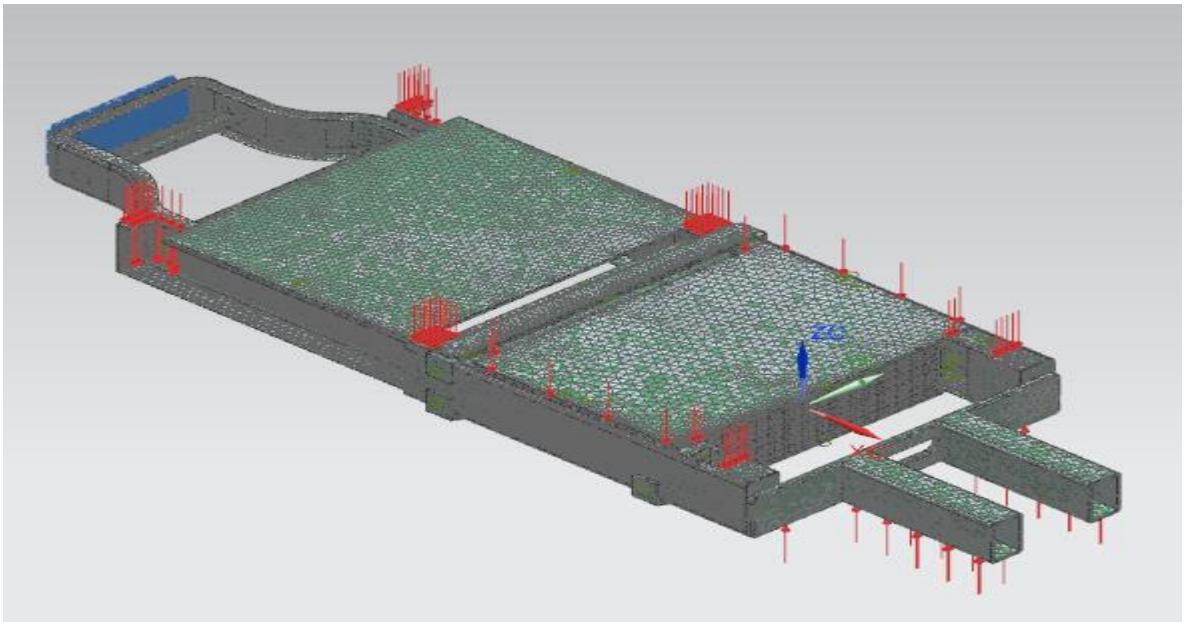

Figure 73. Sub-module pavement load condition

With the presence of the two new components (battery pack and sub-module structure), the distributed load simulating the weight of the car, is now concentrated mainly on the rear, central and front part of the chassis. For this reason, an analysis was performed with the distributed load of the car acting over the two new components (battery pack and sub-module structure) instead of directly over the chassis to analyze changes in stress distributions and deformation.

Figure 74 shows the results for this last analysis. Red zoned, corresponding to zones where resulting stresses went above the yield limit, are smaller in number and extension with

respect to last analysis (Figure 74). Moreover, the maximum obtained stress is of 100 MPa, which is lower than the 150 MPa obtained in Figure 74. This means that, even though the solution is still not the final one, some benefits have been brought by the new components.

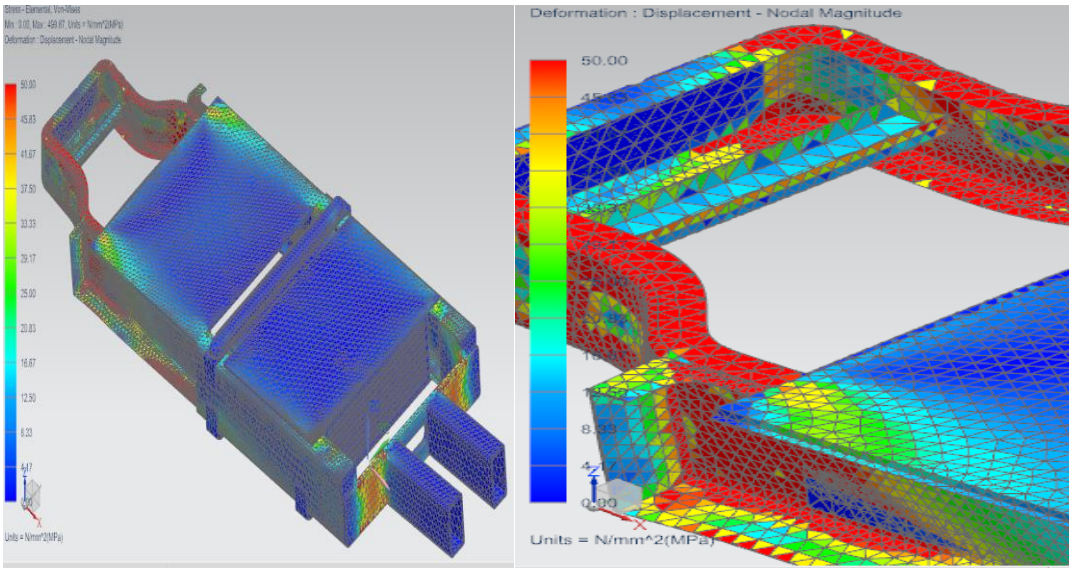

Figure 74. Sub-module pavement stress results

TABLE IV: STRESS ANALYSIS RESULTS COMPARISON

	Max Von Mises stress (MPa)
Last analysis	100
Previous analysis	150

As discussed above, the presence of the sub-module on the chassis affects the load distribution on the chassis. It results in reduced localize stresses, see Figure 76. However, as can be seen, there are regions with Von Mises stress of 100 MPa and greater which results in yield stress failure. Therefore, structural components were added to increase resistance to

bending moment. Two I-beam, which can be welded, have been used to reinforce the rear part of the chassis and the design is showed in Figure 75.

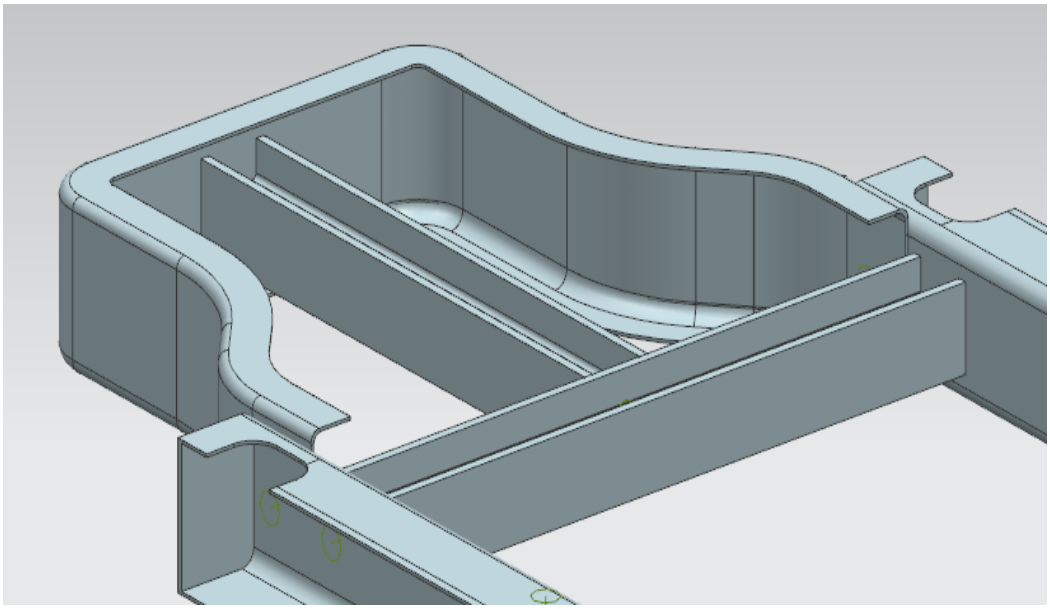

Figure 75. I shaped beams

This solution has then been analyzed, this time distributing the weight in a different way as already mentioned.

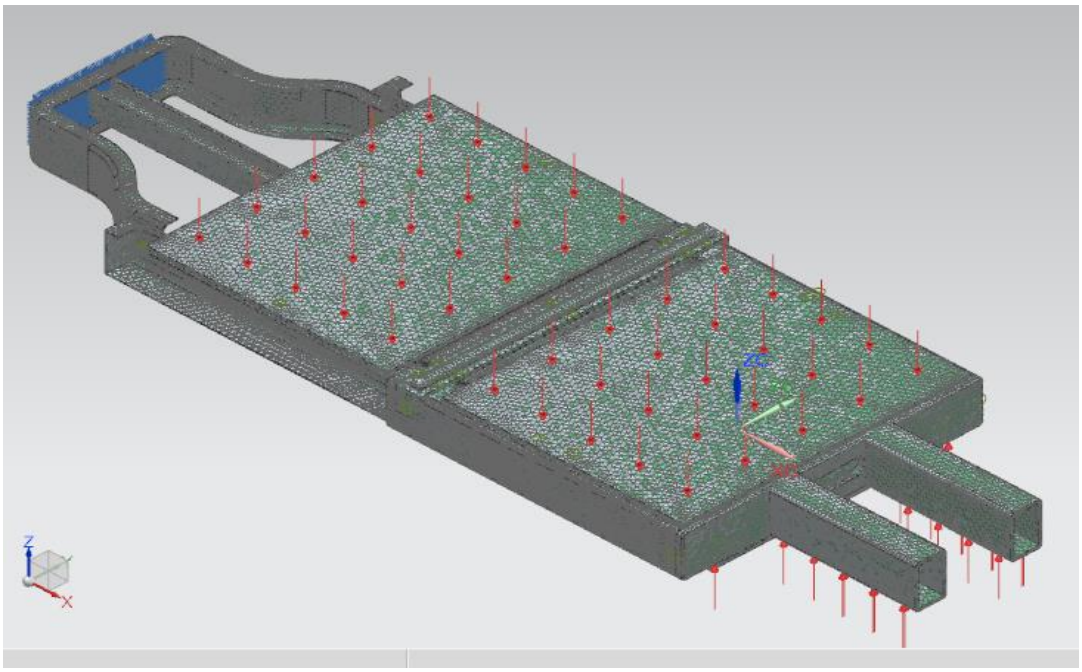

Figure 76. New weight distribution

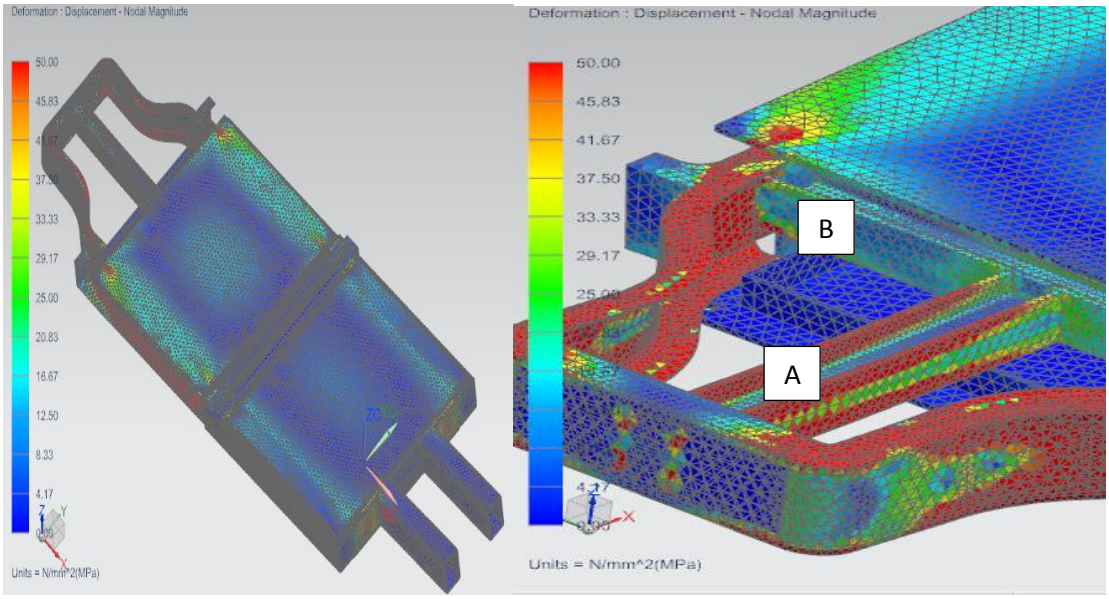

Figure 77. I shaped beam reinforcements

TABLE V: STRESS ANALYSIS RESULTS COMPARISON

	Max Von Mises stress (MPa)
Last analysis	90
Previous analysis	150

As can be seen in Figure 77, the transverse beam, labeled as B, is completely unloaded (the beam is almost everywhere blue, which corresponds to the lowest possible stress), while beam A reaches the yield limit of 50 MPa. To solve this problem, an effort has been put on reducing the length of beam A as well as making beam B closer to the red critical zones appearing on the back of the chassis. The new obtained configuration is shown in Figure 80 and the stress analysis follows in the next section.

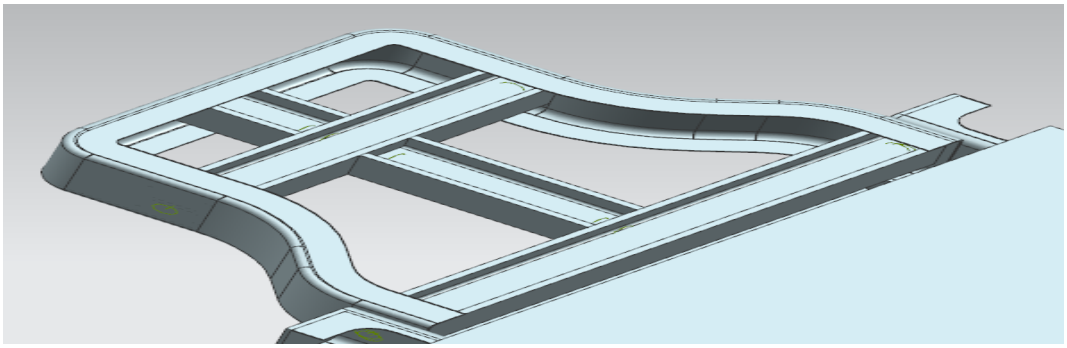

Figure 78. Modified beams

As seen, the beam A was replaced with two smaller beams, while a second transverse beam has been added as shown in Figure 79. Beam B has been moved towards the back of the chassis. The drawback to these modifications is that the overall chassis weight has increased significantly (20 kg more with respect to the original weight).The stress analysis was repeated using the same load conditions as previously explained.

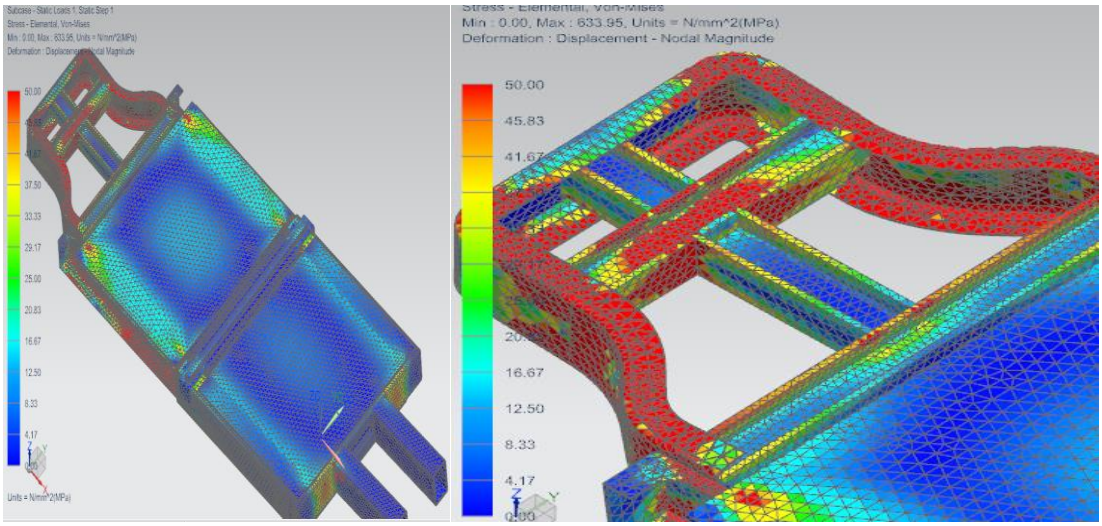

Figure 79. Stress results

TABLE VI: STRESS ANALYSIS RESULTS COMPARISON

	Max Von Mises stress (MPa)
Last analysis	85
Previous analysis	90

Some benefit has been brought by this new solution, although still not enough for it to be the final design. Adding another reinforcing beam made the weight be too high; this is why a totally different solution had to be adopted. Since the aim was to increase the stiffness against bending moment, the idea was then to make the whole rear part of the chassis a closed box. Still following what is said in [32], it is known that a metal sheet offers high resistance to bending moments if it is put in vertical position rather than flat. Hence two vertical metal sheets have been added, each one being 10 mm thick (see figure 92). The

presence of these two elements has the purpose of strongly acting against external bending moments. Moreover, the final structure is lighter than the previous design (almost 5 kg are saved). Also, it was decided to reduce the safety factor target. Originally, the aim was to have a safety factor of 4.5. It was decided that the safety factor was too conservative and the safety factor was then set to 3.5 which is still a conservative value and found in the auto industry [22, 23]. This results in a yield stress limit stress of 70 MPa for the Von Mises calculations.

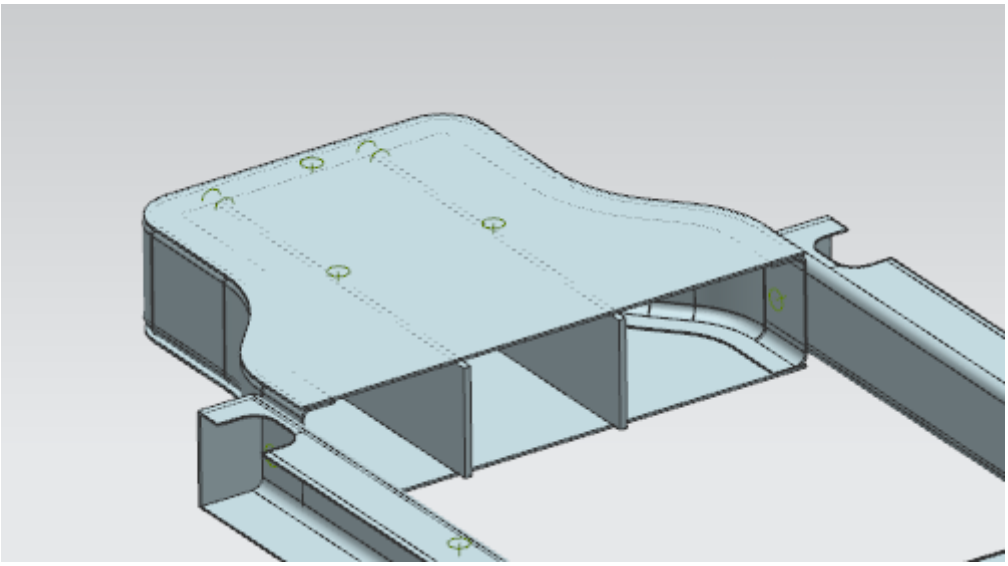

Figure 80. Rear part of the chassis closed with two vertical reinforcements

Results from this solution are now shown.

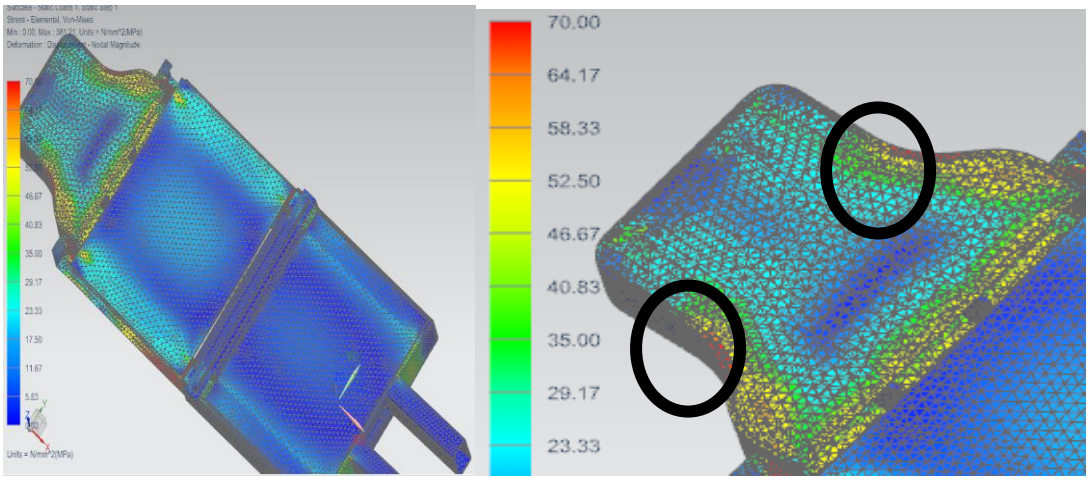

Figure 81. Stress results

TABLE VII: STRESS ANALYSIS RESULTS COMPARISON

	Max Von Mises stress (MPa)
Last analysis	65
Previous analysis	85

In this case, by moving the upper limit for the stresses to 70 MPa, the obtained results are acceptable. As can be seen in Figure 81, maximum Von Mises stress in the final chassis design is 65 MPa (see circles in figure 81). Thus, the design meets the desired safety factor of 3.5. Moreover, figure 82 shows the results concerning displacements, and the same maximum displacement obtained in the preliminary stress analysis (20 mm) has been obtained.

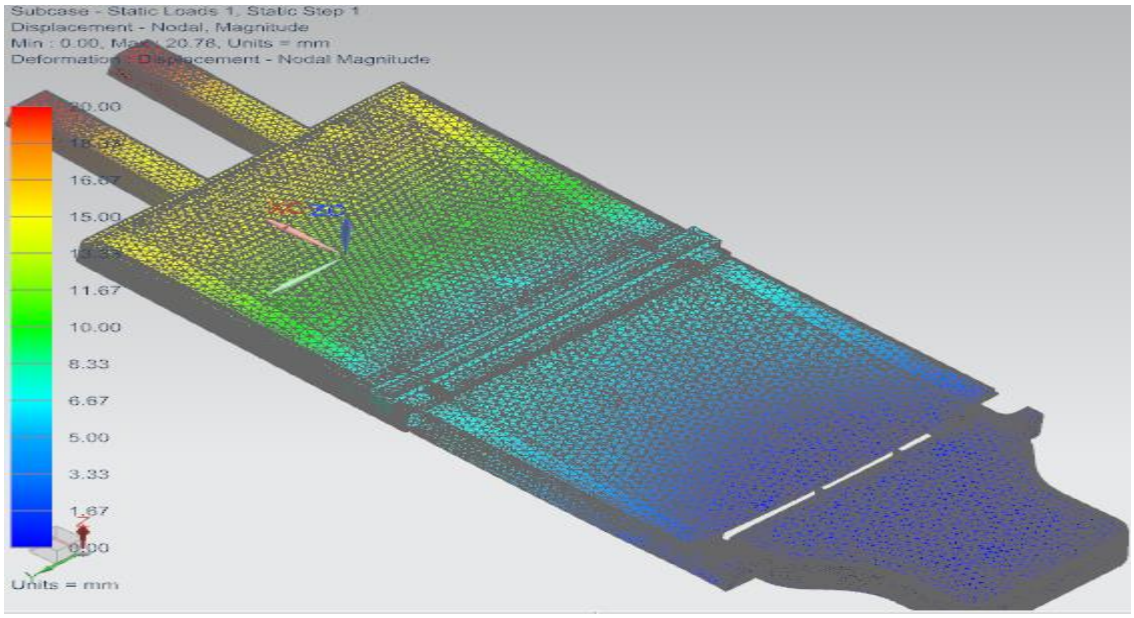

Figure 82. Displacement results

Since this design solution was satisfactory, the analysis shifted to the simulation of the rear bump.

7.3.2 Rear curb impact

The loading conditions for the rear impact are shown in Figure 83. Loading conditions are equivalent to the front curb impact analysis, except that the 10000N load is now applied to the rear of the chassis while the fixed constrain is applied to the front part of the chassis.

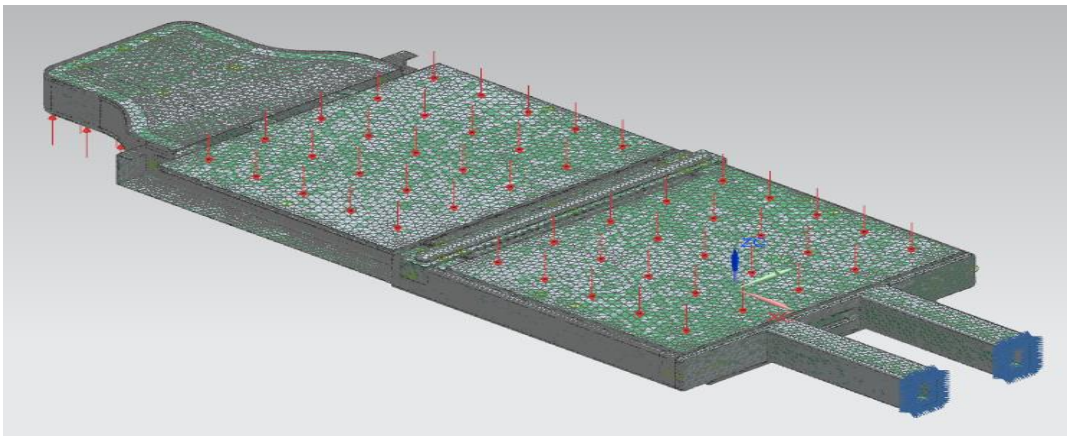

Figure 83. Front bump load condition scheme

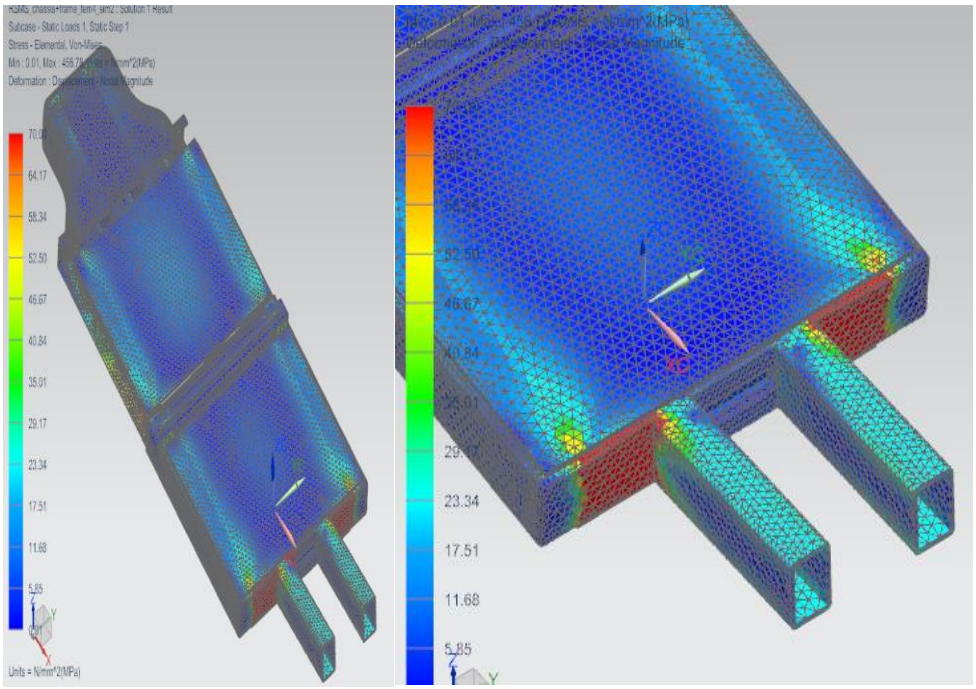

Figure 84. Stress results

TABLE VIII: STRESS ANALYSIS RESULTS COMPARISON

	Max Von Mises stress (MPa)
Last analysis	90
Previous analysis	15

As discussed above, the only part of the chassis where there are failure zones is the front beam. This problem was solved by increasing the stiffness of the metal sheet at these critical zones. The thickness was increased from 20 to 50 mm and the new results for the Von Mises stresses and deflections are shown in Figures 85 and 86 respectively.

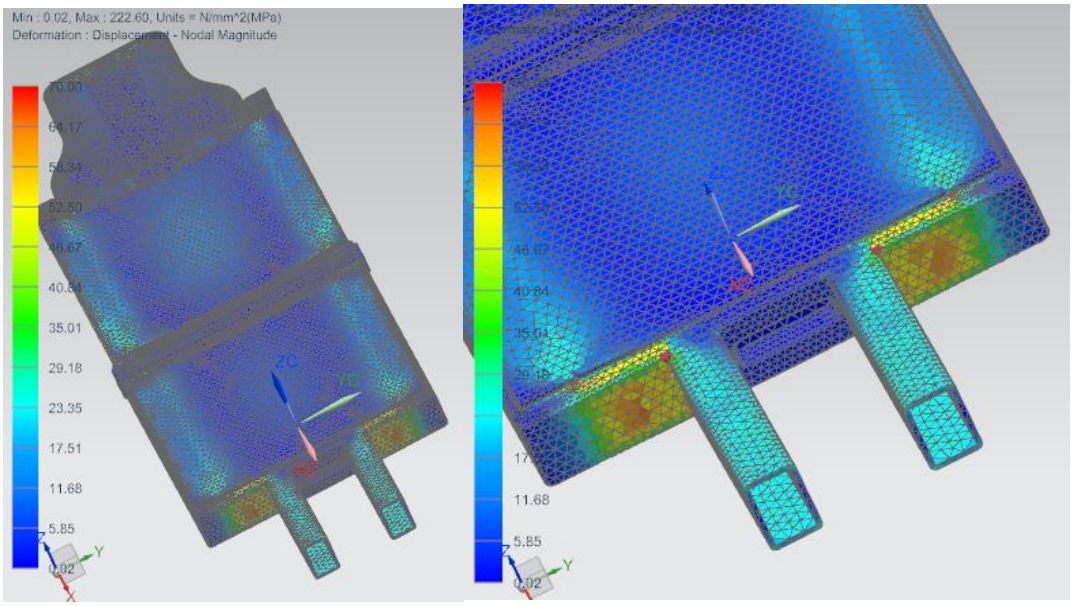

Figure 85. Stress results

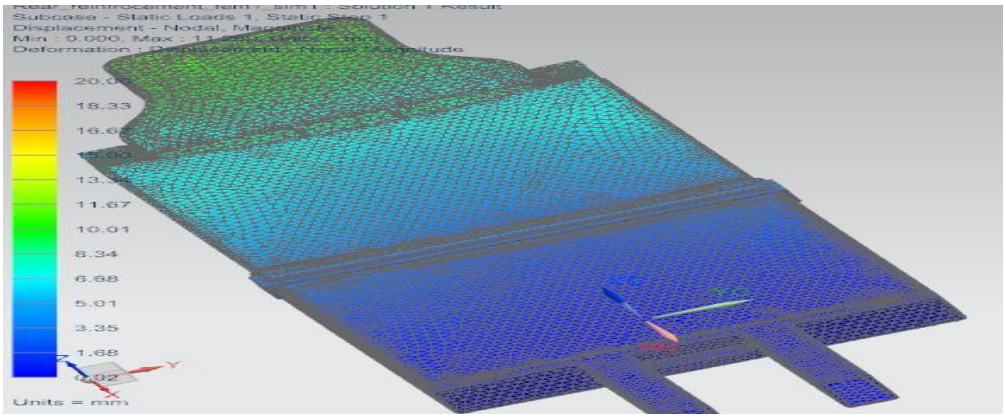

Figure 86. Displacement results

TABLE IX: STRESS ANALYSIS RESULTS COMPARISON

	Max Displacement (mm)	Max Von Mises stress (MPa)
Last analysis	30	50
Previous analysis	3	15

As seen in the last Table, both the stresses and displacements are satisfactory. The stresses are below the yield strength of 70 Mpa and the maximum displacement is 10 mm.

7.3.3 Torsion analysis

After the chassis proved to be sufficiently stiff for the two basic load conditions, two torsion analyses have been performed to test its rigidity against torsion. The hypothetical load condition is the one of the car going up on a step, with only one of the wheels on it. It is assumed, that half of the external load applied during the previous analysis (10000 N) will be applied to a wheel and all the other constraints remain the same. As said, two analysis have been conducted, one regarding the front part and the other the rear part of the chassis. In this case, since the car in only facing the obstacle with one wheel, the 5000N load will only be applied to one side of the front/rear of the chassis. Still, the load simulating the car's weight is applied and the side not receiving the external load has a fixed constrain.

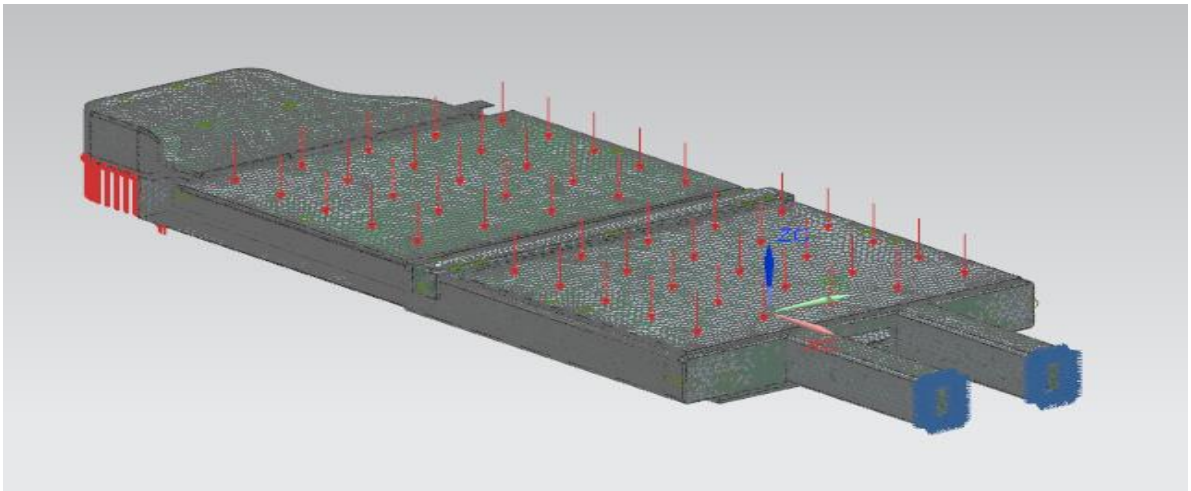

Figure 87. Load condition scheme for torsion, rear wheel

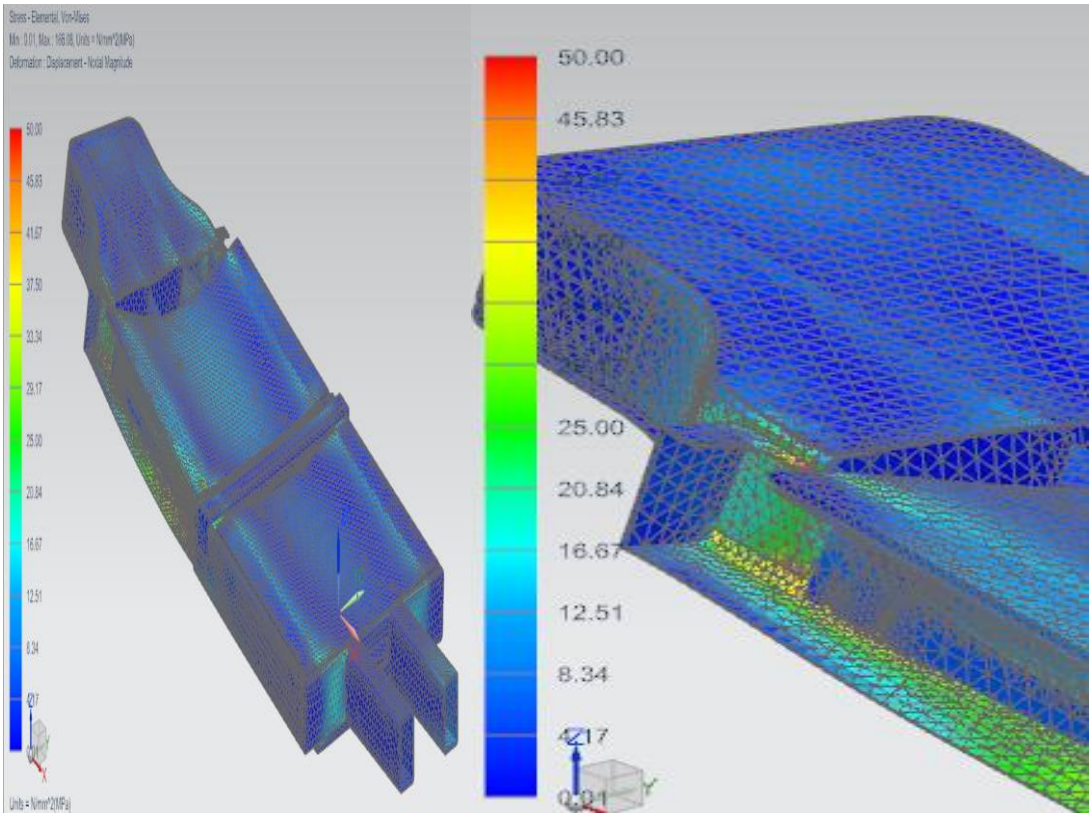

Figure 88. Rear torsion stress results

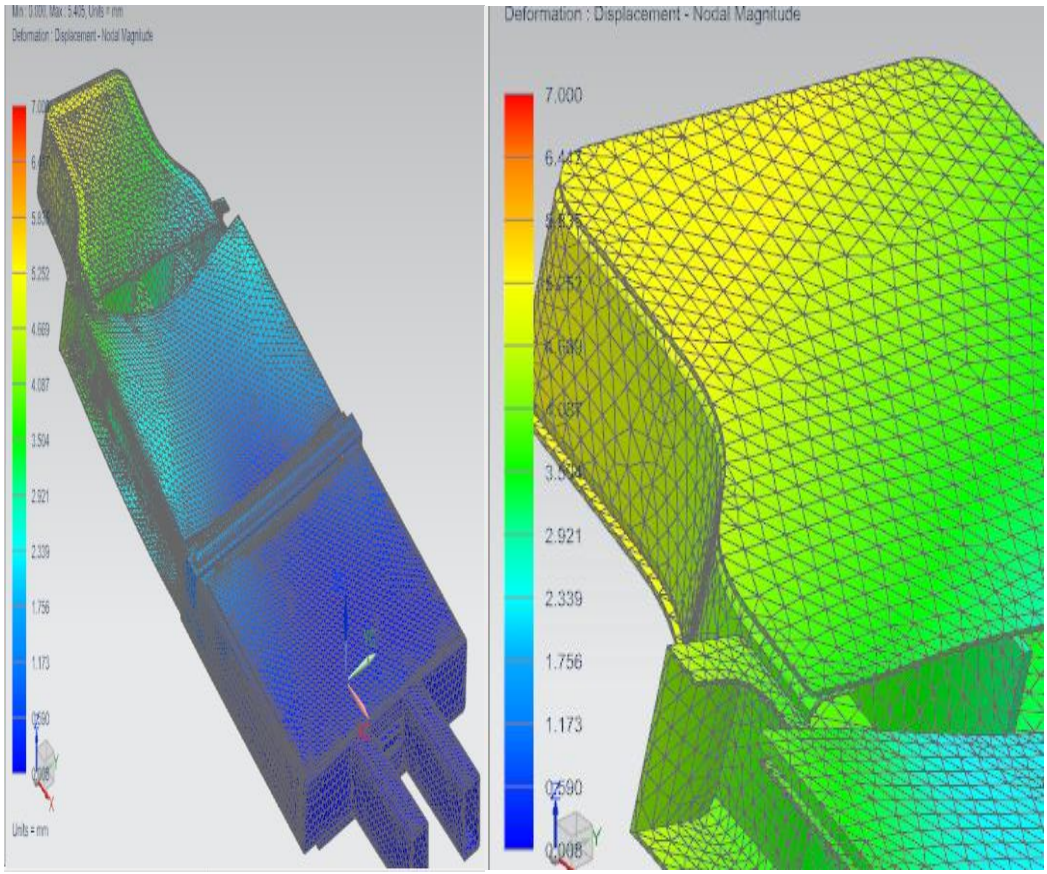

Figure 89. Rear torsion displacement results

As seen in Figures 89, the resulting Von Misses stresses do not exceed 50 MPa, while the maximum displacement is below 7 mm. Since these results are acceptable, the front torsion case was analyzed.

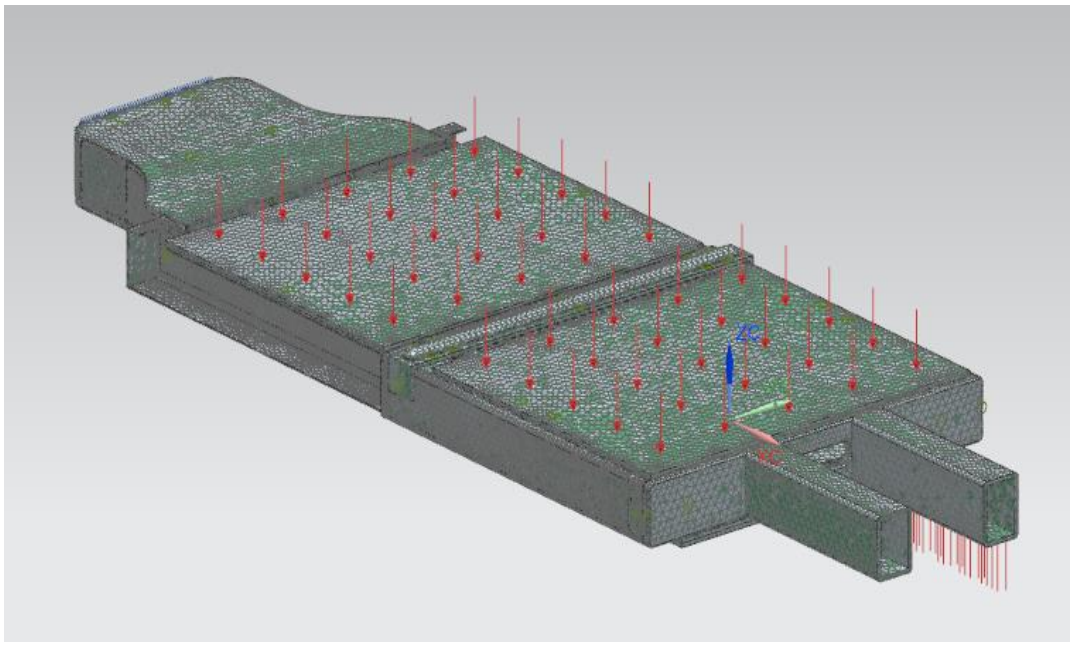

Figure 90. Load condition scheme for torsion, front wheel

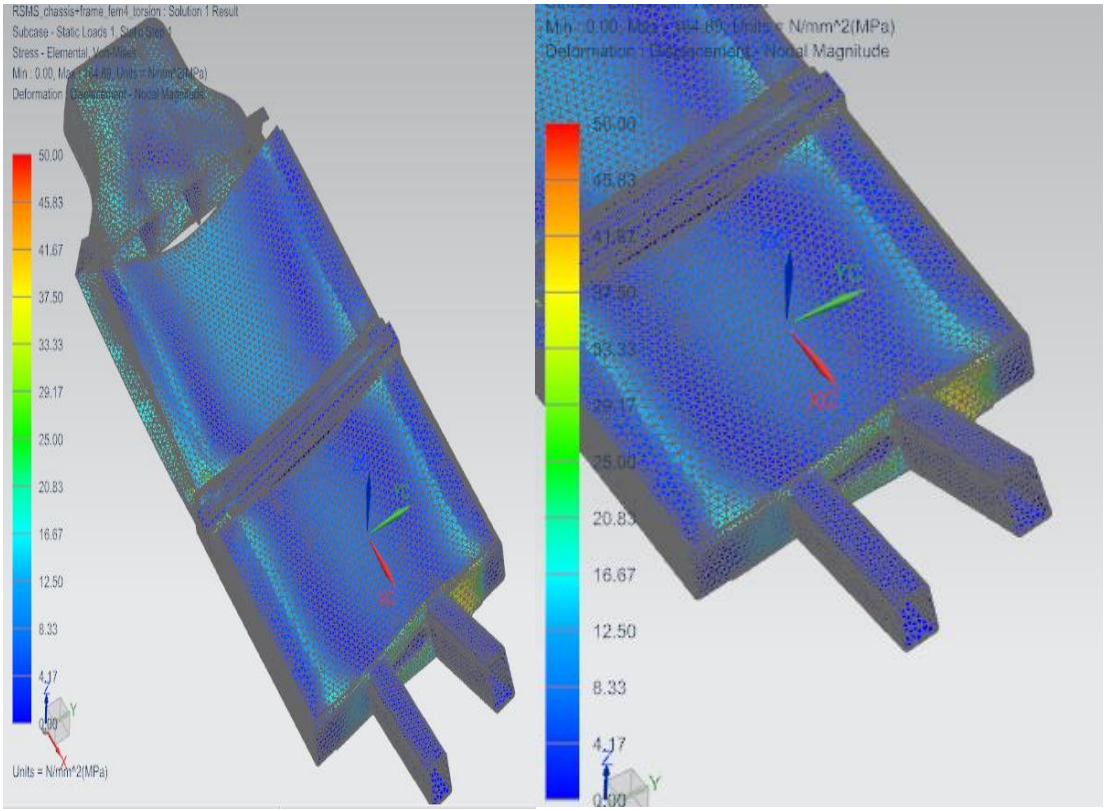

Figure 91. Front torsion stress results

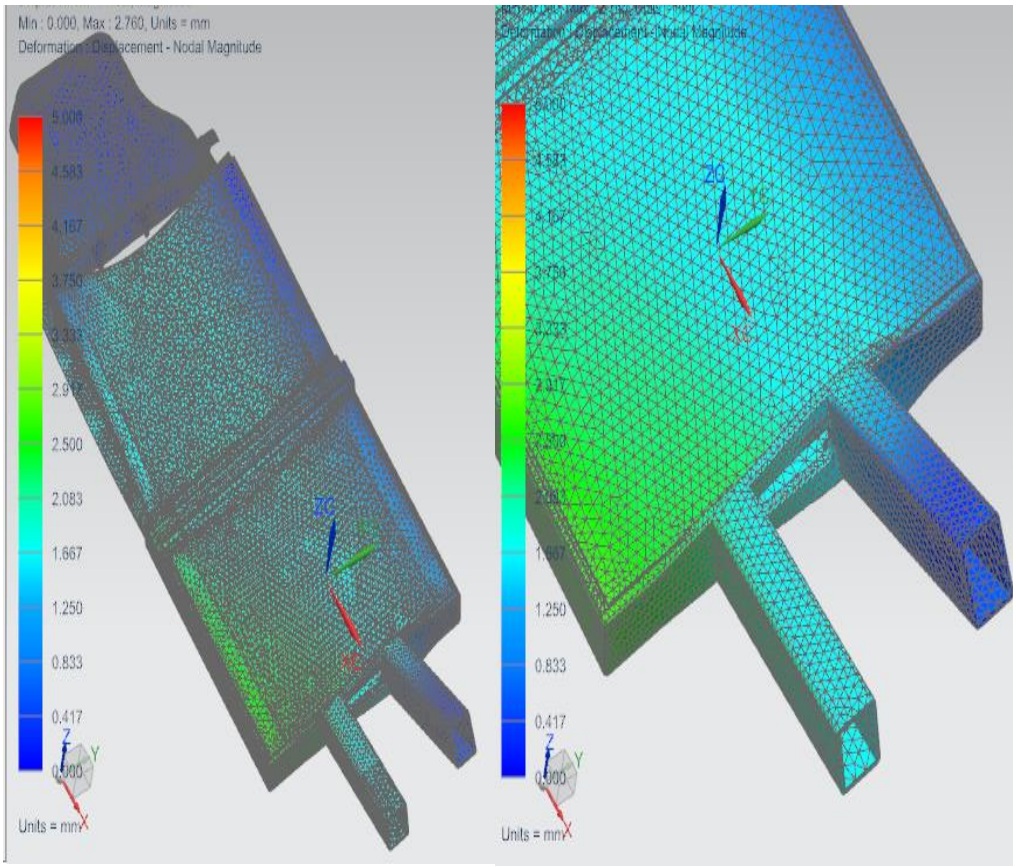

Figure 92. Front torsion displacement results

Also in this case the maximum stress is below 70 MPa (Figure 93), which means that the chassis satisfies the design criteria also in the case of torsional analysis.

As discussed above, the Von Misses stresses are below 50 MPa and the maximum displacement is below 5 mm. Therefore, it was determined that the final chassis design met all stated design criteria.

Chapter 8

CONCLUSIONS AND FUTURE WORK

In this chapter, the final configuration of the vehicle chassis is shown (figure 95), and some suggestions are made on the limitations of the performed analysis. Future work is also discussed.

Figure 95 shows a lengthenable chassis for a shared use vehicle. It has been shown how this chassis met all the designing criteria. The chassis allows the lengthening of the car, passing from 1.8 to 2.7 meters and allows it to be re-configured depending on the user's needs. Attention put on the choice of the structure's components allows the manufacturing to be very easy and cheap. Moreover, the simplicity of the structure also allows maintenance to be easy: as an example, Teflon sheets can easily be replaced since they are attached through screws. Such a chassis, allows the vehicle to address some of the problems nowadays present in the mobility field. Families using this kind of vehicles in the future, won't in fact need any more to have different cars for different needs (eg. A city car and a car for travels). Moreover, the shared use would allow the total number of cars to dramatically decrease. A single car could in fact be used by several people instead of only being used by a single owner.

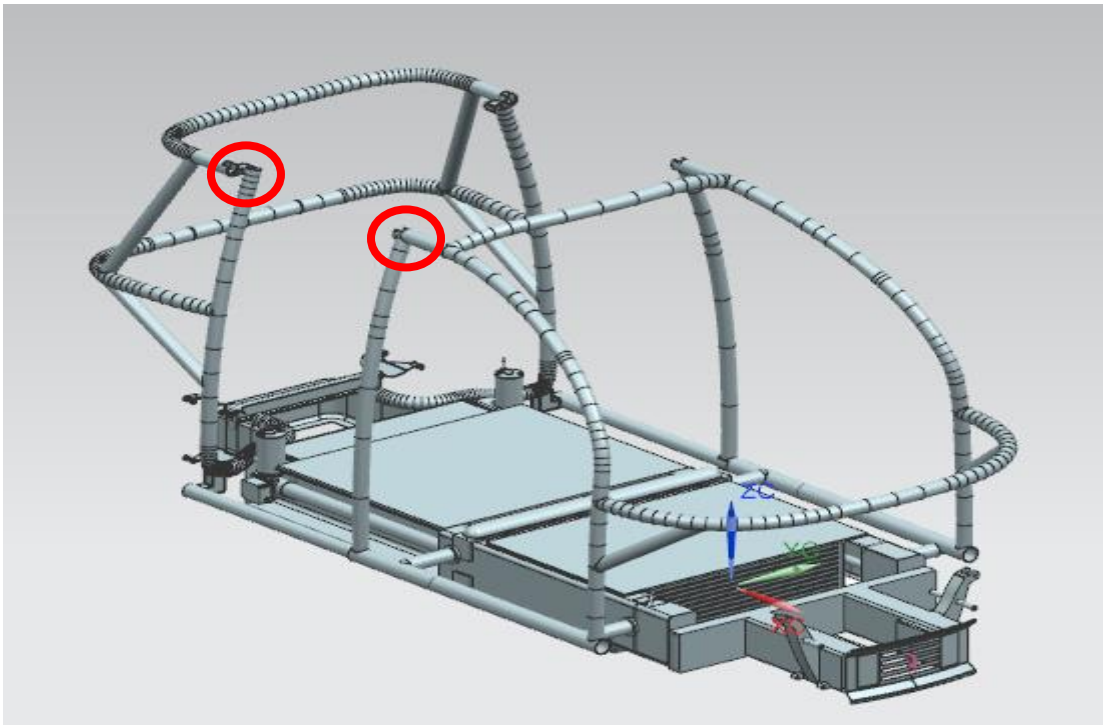

Figure 93. Complete chassis in its last version

From figure 94, it can be noticed how the upper part of the chassis has been submitted to some changes. Circular section tubes have in fact been chosen instead of rectangular ones due to the fact that they are more prone to bending manufacturing processes. From [30] and [32], it can in fact be seen that how a circular section offers less resistance to bending moments if compared to a rectangular one with comparable dimensions.

The chassis shown in figure 94 is in the open (or long) configuration, it can in fact be seen how the two red circled parts are have a gap between them, which gives space to the sub-module structure to be mounted. The two parts highlighted by red circles in figure 95 are made to come in contact when in closed (or short) configuration, and a proper and safe closing mechanism has to be designed to maintain the two parts firmly in contact. This first design aspect, is hence something a research design could focus on in the future.

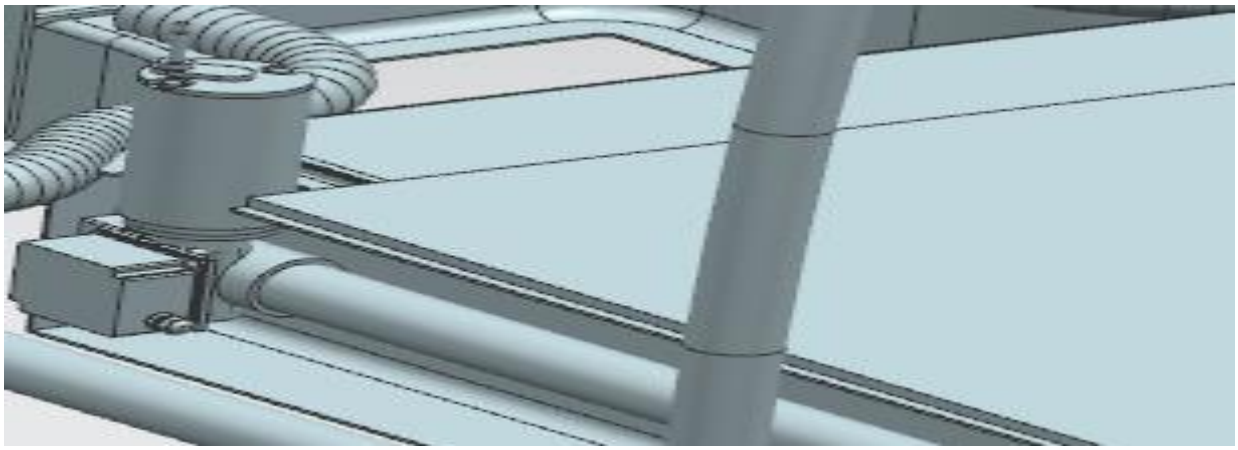

Figure 94. Actuator detail

When the user wants to change the length of the car, two actuators are activated and the closing mechanism will open to allow the movement. Actuators are placed inside the “c” shape of the male, on both sides of the chassis (see figures 94). A proper dimensioning is also required for the system to guarantee sufficient power as well as a sufficiently high number of service hours before replacement is needed. Also, analysis regarding the required power could be performed during such a study.

The front beam has been updated through the addition of a component, shown in Figure 98, allowing protection of the important parts of the vehicle (such as brakes and wheels) in the event of a front impact. The aim of this component would then be the one of absorbing the energy coming from the impact by deforming and preventing deformation to happen in the just mentioned important components. Impact should in fact taken into account during the design of a car’s chassis, and this is an important aspect which has not been taken under consideration during the performed analysis. Future work includes the simulation of a car

crash in the frontal, lateral and rear directions to develop a proper safety structure against impacts. The suggested analysis should not only aim at protecting the vital parts of the car, but of course also the driver and passenger. Joints allowing mounting of wheels and brakes are also present in this assembly.

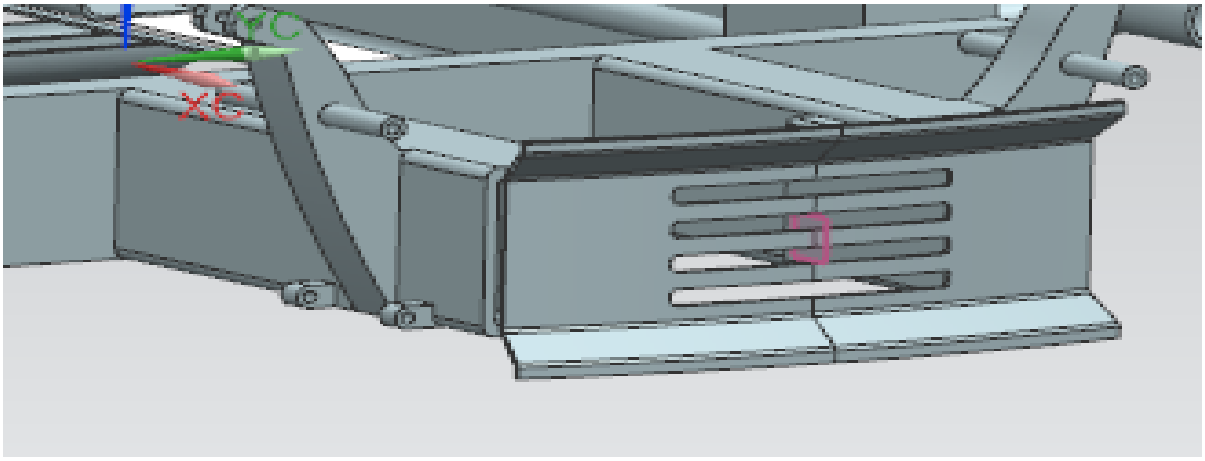

Figure 95. Front protection

Figure 96 shows the brackets to attach both the wheels and the braking system. These components have been modeled as an example, and also attention should be payed to a proper dimensioning of them.

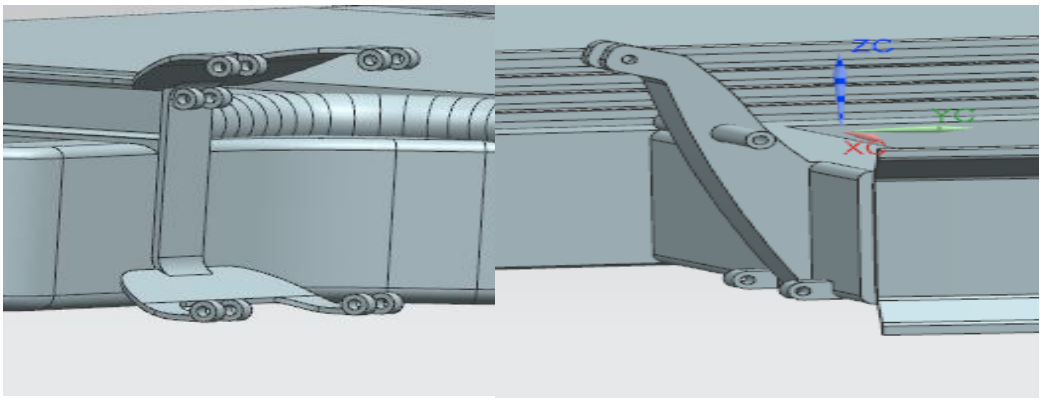

Figure 96. Wheels and brakes joint. Front joint on the left and rear joint on the right

APPENDIX

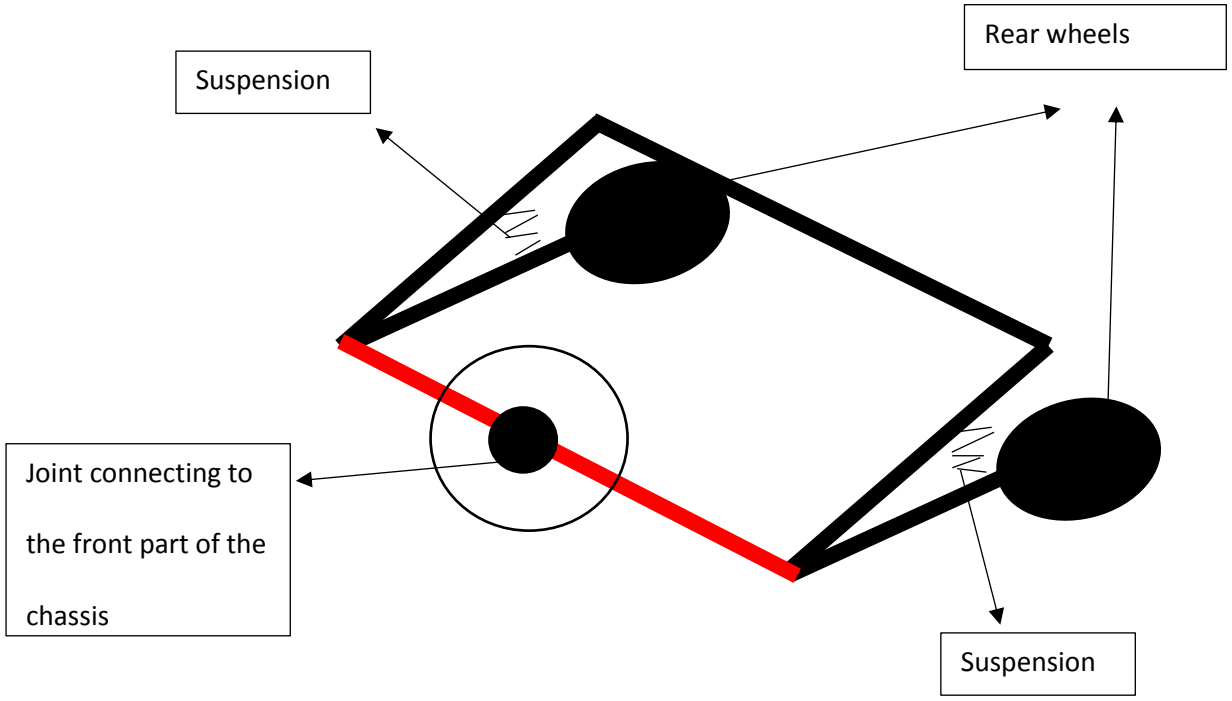
Rear wheels
Suspension
Joint connecting to the front part of the chassis
Suspension

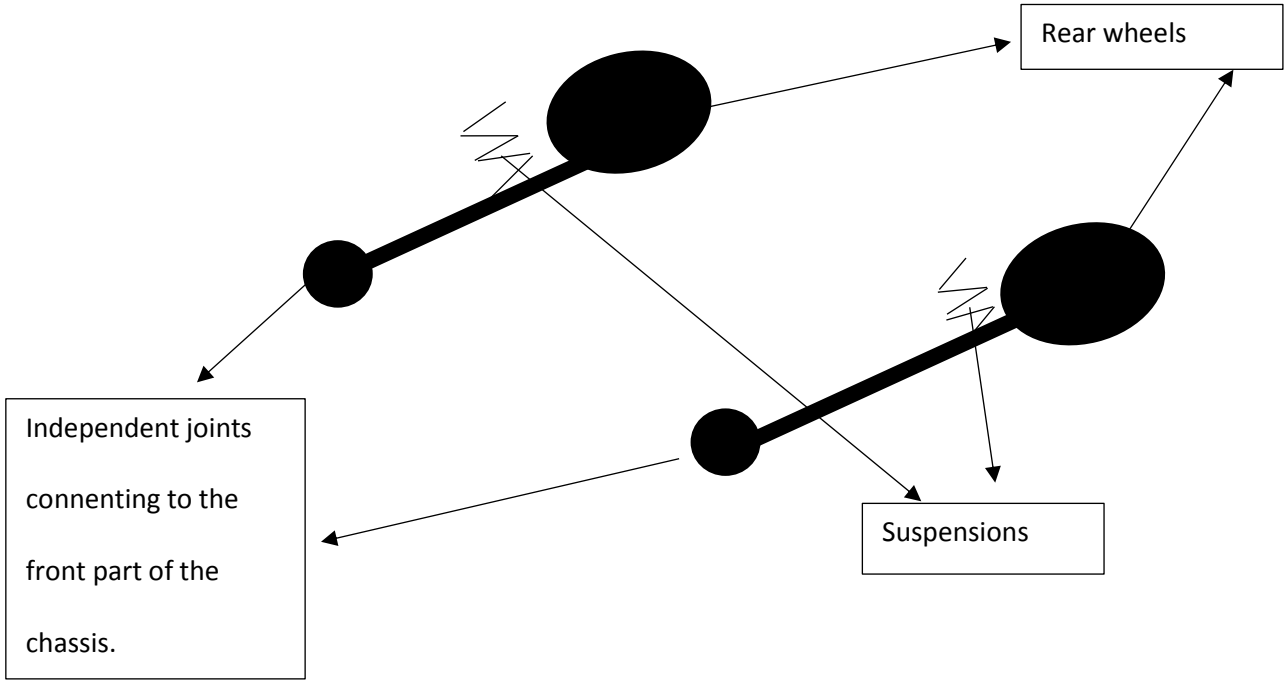
Rear wheels
Independent joints connenting to the front part of the chassis.
Suspensions

CITED LITERATURE

1. PACE institution: Global collaboration project. Retrieved September 1, 2015, from http://pacepartners.org.

2. World Bank: Cebu Bus Rapid Transit (BRT) project. Retrieved September 11, 2015, from http://www.worldbank.org.

3. Ericson: Networked city index. Retrieved September 11, 2015, from http://www.ericsson.com

4. Slobodan, M.: Urban transport projects: patterns and trends in lending, 1999-2009, Retrieved October 1, 2015, from http://www.sitesources.worldbank.org

5. Valero, J.: Viegas: We will move differently in the future. Retrieved October 3, 2015, from http://www.euractiv.com

6. Hibler, M.: Taking control of air pollution in Mexico City, Retrieved October 10, 2015, from http://www.idrc.ca

7. www.theaa.com: Euro emission standards, Retrieved October 17, 2015, from http://www.theaa.com

8. Bhattacharya, B: Urbanization, urban sustainability and the future of the cities, concept publishing company, 2010.

9. Nissan: Nissan becomes the first company to sell 100% electric cars in Mexico city, Retrieved October 23, 2015, from http://nissannews.com

10. www.nyc.com: Mayor De Blasio commits to 80 percent reduction of greenhouse gas emissions by 2050, starting with sweeping green buildings plan, Retrieved November 1, 2015, from http://www.nyc.com.

11. nydailynews: Ford focus electric gets $4000 price out, still prices than fully loaded gas model, Retrieved November 12, 2015, from http://www.dailynews.com

12. www.threehugger.com: All new chevy Volt gest $1175 price cut, now $26495 after federal tax credit, Retrieved December 3, 2015 from http://www.threehugger.com

13. Brown, C.: CarSharing: State of the market and growth potential, Retrieved December 1, 2015, from http://www.autorentalnews.com

CITED LITERATURE (continued)

14. OSVehicle: OSVehicle's mission is to democratize mobility by enabling businesses and startups to design, prototype and build custom electric vehicles and transportation systems, Retrieved December 3, 2015, from http://www.OSVehicle.com

15. www.tuvie.com: Futuristic TET city car by Chao Gao, Retrieved December 3, 2015, from http://www.tuvie.com

16. www.averageheight.co: Average male height by country, Retrieved December 15, 2015, from http://averageheight.co

17. The city of New York: PlaNYC. Retrieved November 15, 2015 from http://www.nyc.gov

18. Allport, R., Brown, R., Glaister, S., Travers, T.: Success and failure in urban transport infrastructure projects, Retrieved October 2, 2015 from http://www.workspace.imperial.ac.uk

19. www.hypertextbook.com: Coefficients of friction for Teflon, Retrieved November 18, 2015 from http://www.hypertextbook.com

20. Scolari, P.: Motor vehicles and their evolution Vol.2, Politecnico di Torino - Ingegneria dell'autoveicolo, Ninth edition, September 2008

21. www.telegraph.co.uk: What is a Segway?, Retrieved December 7, 2015 from http://www.telegraph.co.uk

22. Aird, F.: The race car chassis, Motorbooks interntional, 1997

23. Gadagottu, I., Gadagottu, M.: Structural analysis of heavy vehicle chassis using honey comb structure, International Journal of mechanical Engineering and Robotics research, ISSN 2278 – 0149 Vol. 4, No. 1, January 2015

24. Tresca, R.V.: On Saint Venant's Principle, Retrieved December 18, 2015, from http://projecteuclid.org

25. Azom: AISI 1020 low carbon/low tensile steel, Retrieved December 9, 2015 from http://www.azom.com

26. Boston University: Mechanics of materials: Bending – Normal stresses, Retrieved December 9 from http://www.bu.edu

CITED LITERATURE (continued)

27. ocw.nthu.edu.tw: Stresses in beam (basic topics), Retrieved December 9, 2015, from http://ocw.nthu.edu.tw

28. www.ewp.rpi.edu: Stress concentration, Retrieved December 14, 2015, from http://www.ewp.rpi.edu

29. www.edmundus.com: 2015 Smart ForTwo: features and specs, Retrieved January 5, 2016 from http://www.edmunds.com/

30. www.engineering.com: Moments of inertia, retrieved February 9, 2016 from http://www.engineering.com

31. www.fratellipelandi.it: Travi, retrieved February 9, 2016 from http://www.fratellipelandi.it

32. Dahlgren, J.: Structural engineering: why is an I shaped beam the way it is?, Retrieved March 1, 2016 from http://www.quora.com

33. www.mathalino.com: Stress-strain curve, retrieved January 6, 2015 from http://www.mathalino.com

34. www.virginia.edu: Dislocations and strengthening mechanisms, Retrieved January 6, 2015 from http://www.virginia.edu

35. Consteel: Catalogue, Retrieved December 3rd, 2015 from http://www.consteel.com.sg

36. www.ideaprototipi.it: Prototyping, Retrieved January 8, 2015 from http://www.ideaprototipi.it

37. www.recombu.com: MonoEV, Retrieved December 10th, 2015 from https://www.recombu.com

VITA

NAME	Eduardo Terzidis
EDUCATION	Laurea di I Livello in Ingegneria Meccanica, Politecnico di Torino, 2014.
	Laurea specialistica in Mechanical Engineering, Politecnico di Torino, 2016.
	Master of Science in Mechanical Engineering, University of Illinois at Chicago, 2016.
LANGUAGE SKILLS	
Italian	Native speaker
English	Full working proficiency
	2015 – IELTS 7.5
WORKING EXPERIENCE AND PROJECTS	
March 2016 – July 2016	Internship at Enevete, Airborne Wind Energy
August 2015 – December 2015	UIC Morotorsport Formula SAE member
2014 – 2016	Politecnico di Torino PACE RSMS team member
2011 – 2014	Politecnico di Torino PACE PAMD team member
January 2014 – March 2014	Internship at Danisi Engineering, Automotive and manufacturing